Calcium-Aluminum-rich Inclusions

&

Chondrules

Guy Libourel

CRPG-CNRS, Nancy, France

UNIVERSITÉ DE LORRAINE

cnrs INSU Institut national des sciences de l'Univers

CRPG

Constituents of primitive meteorites

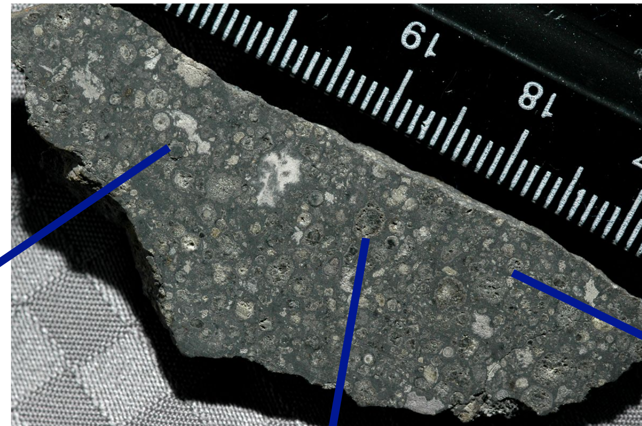

Allende CV3

(Mexico, fall, February 8, 1969)

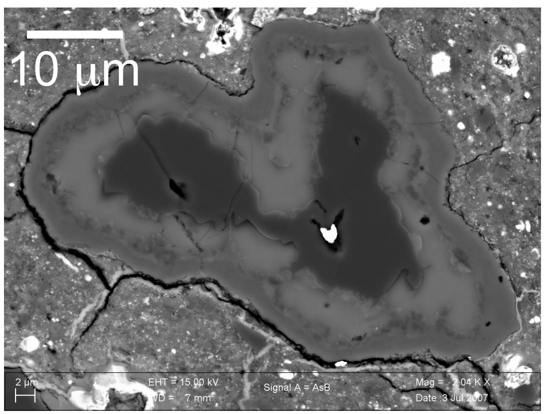

Ca - Al-rich inclusions (CAI)
(10 µm - 2 cm)

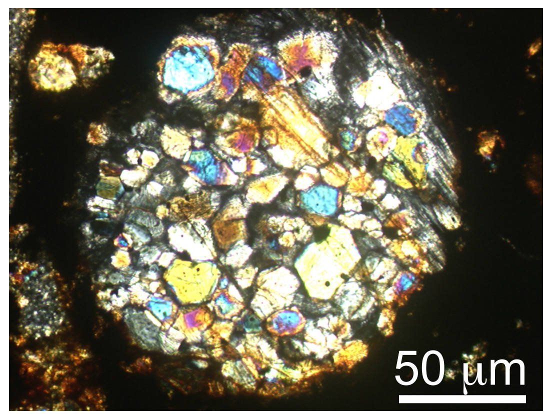

Chondrules
(10 µm - 0.2 cm)

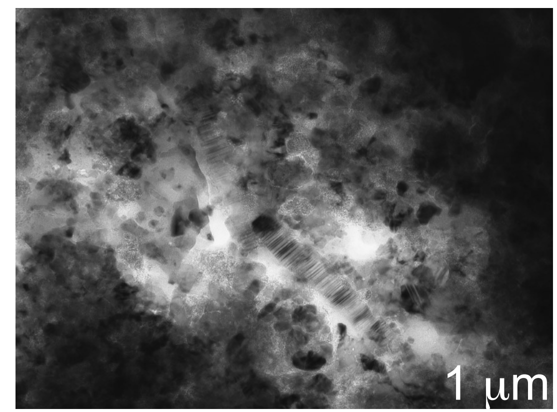

Matrix
(nm - 10s µm)

Oldest solids
in the solar system (t=0)
4,567 MA

20-80 % by volume of primitive meteorites (chondrites)

Constituents of primitive meteorites

- Chronology & isotope chemistry
- Mineralogy & petrology
- Chemistry
- Thermodynamic
- Experiments

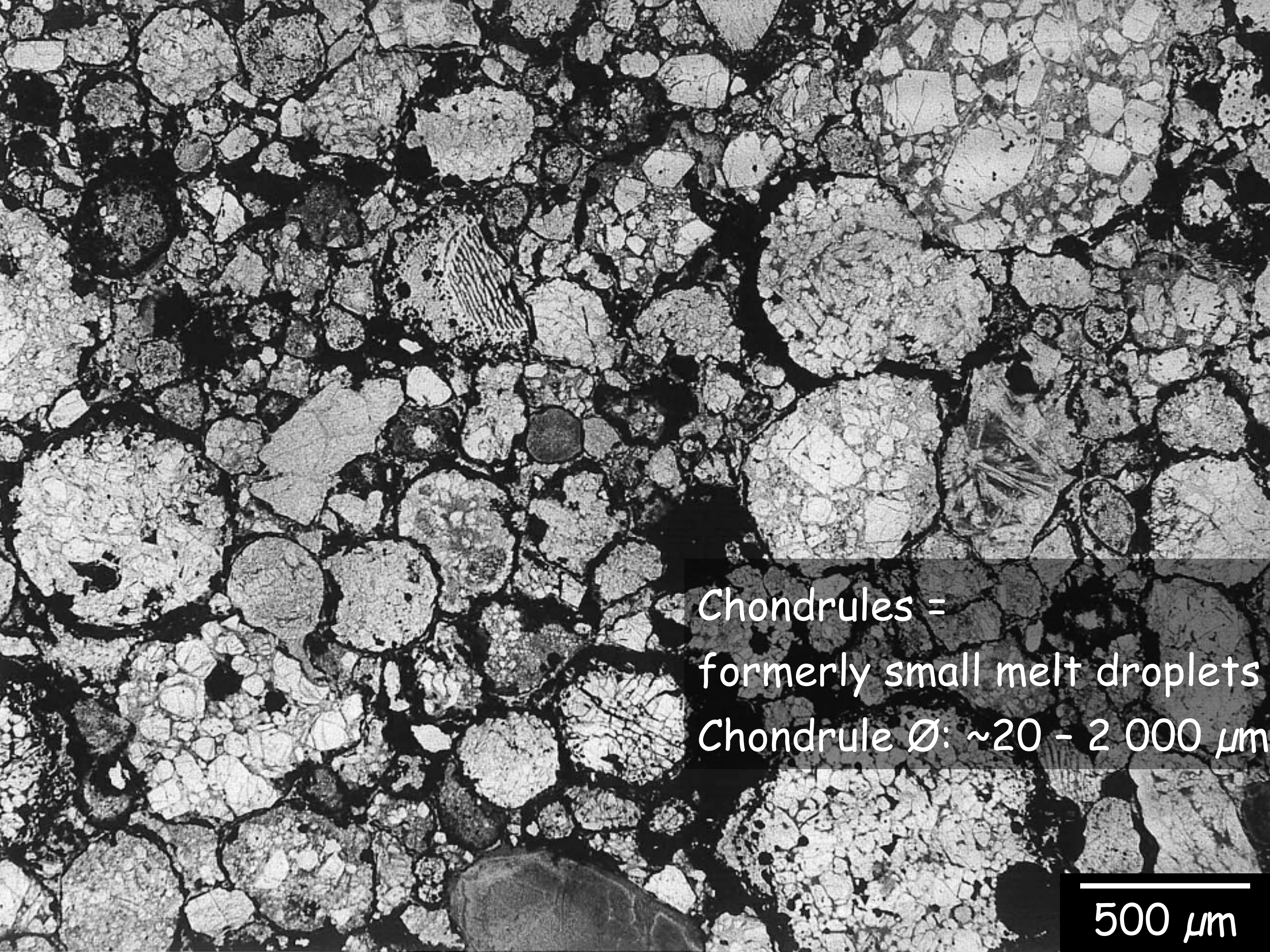
Chondrules =
formerly small melt droplets
Chondrule Ø: ~20 – 2 000 µm
500 µm

Chondrules = millimeter-sized silicate igneous droplets

Chondrules = up to 80% of the chondritic meteorites

Mass of chondrules in the asteroid belt today ≈ 2×10^{24} g ≈ $2 \times 10^{-4}\ M_{\oplus}$

Chondrules = formed only millions of years after the oldest solids formed in the solar nebula

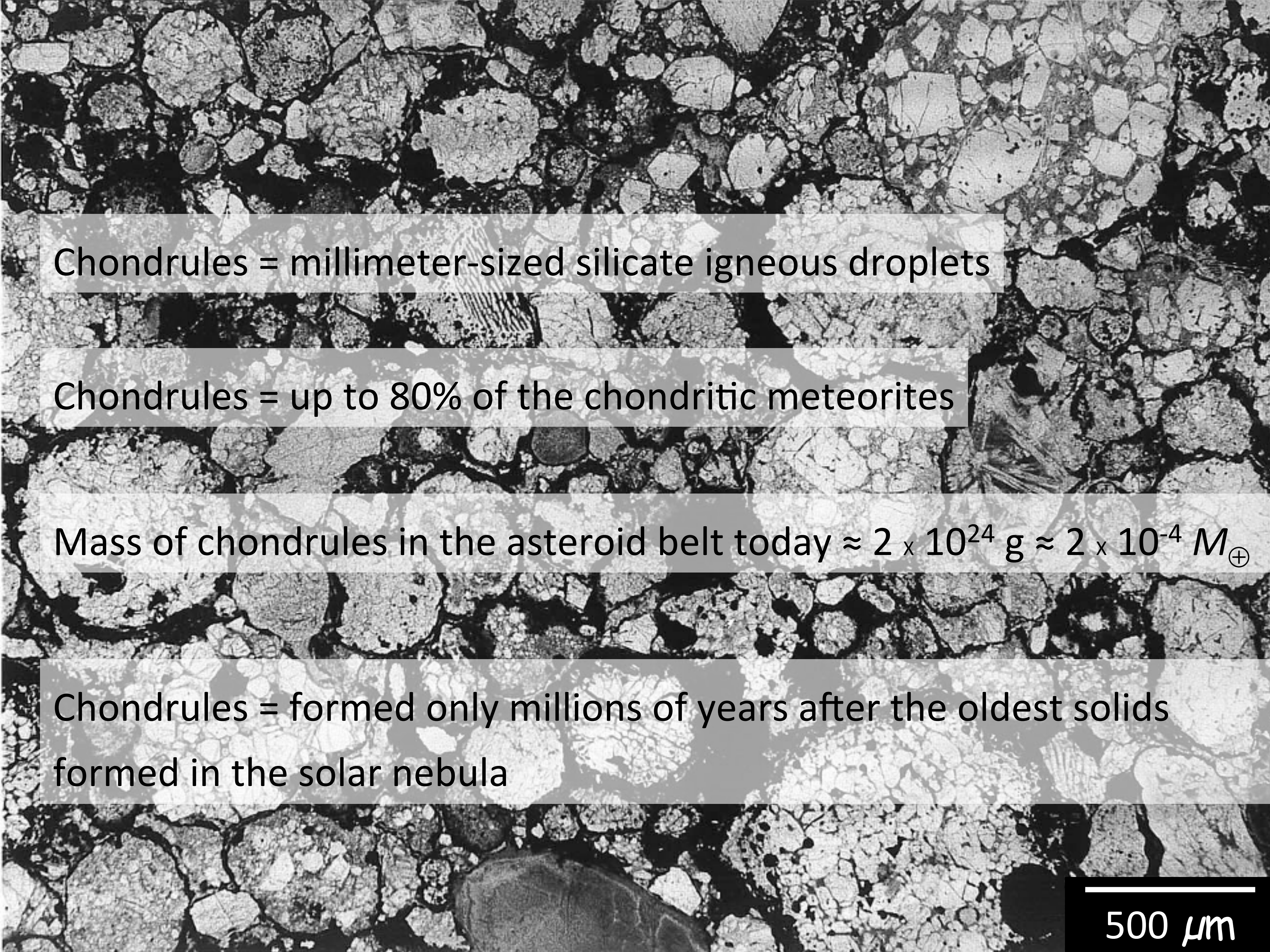

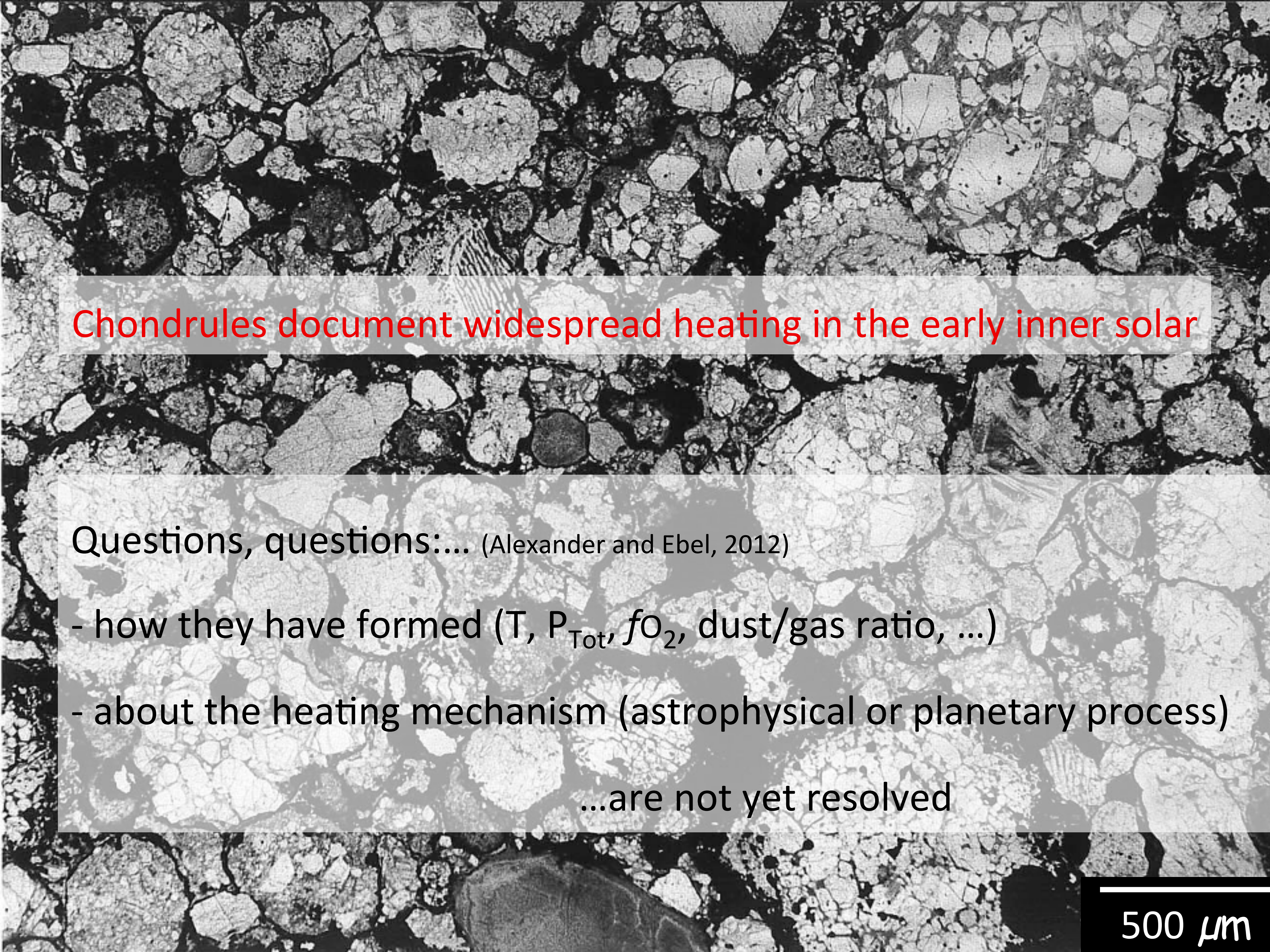

Chondrules document widespread heating in the early inner solar

Questions, questions:… (Alexander and Ebel, 2012)

- how they have formed (T, P_{Tot}, fO_2, dust/gas ratio, …)
- about the heating mechanism (astrophysical or planetary process)

…are not yet resolved

Diversity of chondrule textures & chemistry

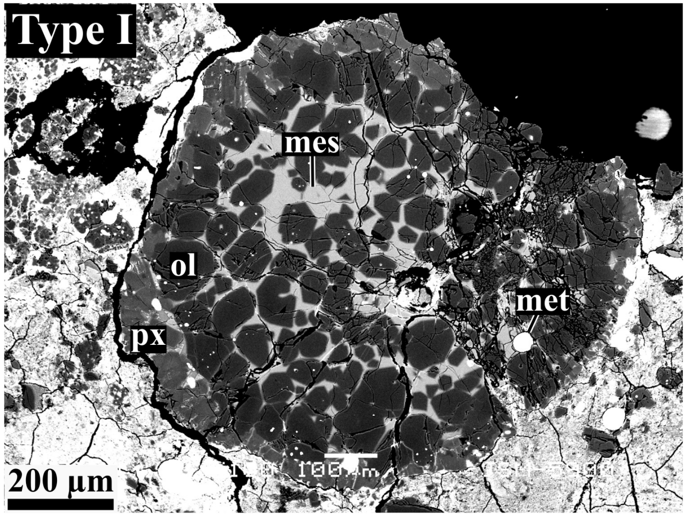

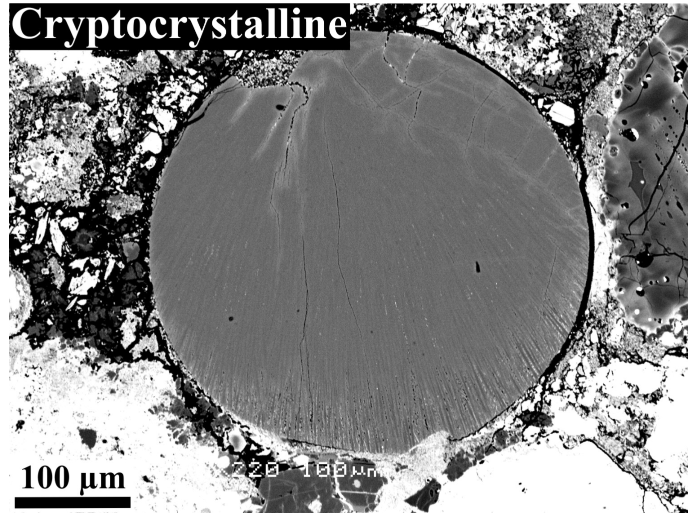

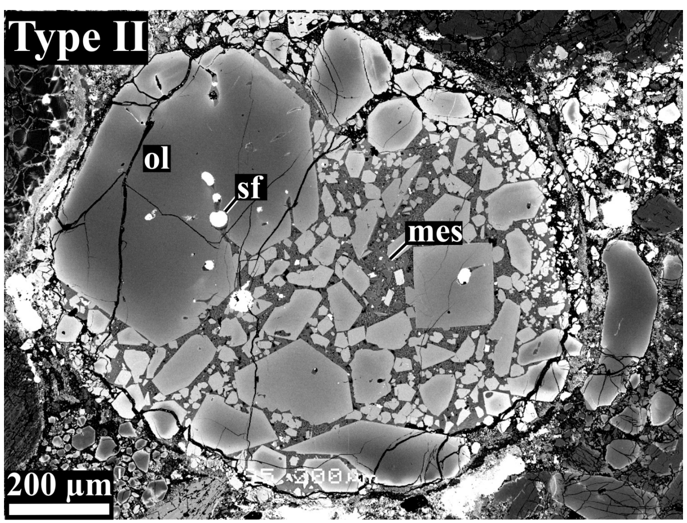

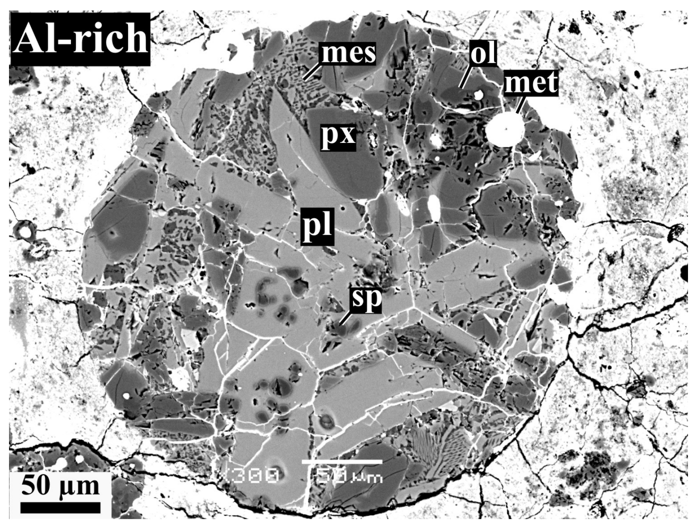

- -large variations in sizes, textures, mineralogy, chemistry
- -porphyritic & nonporphyritic
- -olivine-rich & pyroxene-rich
- -FeO-poor (Type I) FeO-rich (Type II), Al-rich

Dynamic crystallization (cooling rate) experiments

porphyritic

nonporphyritic

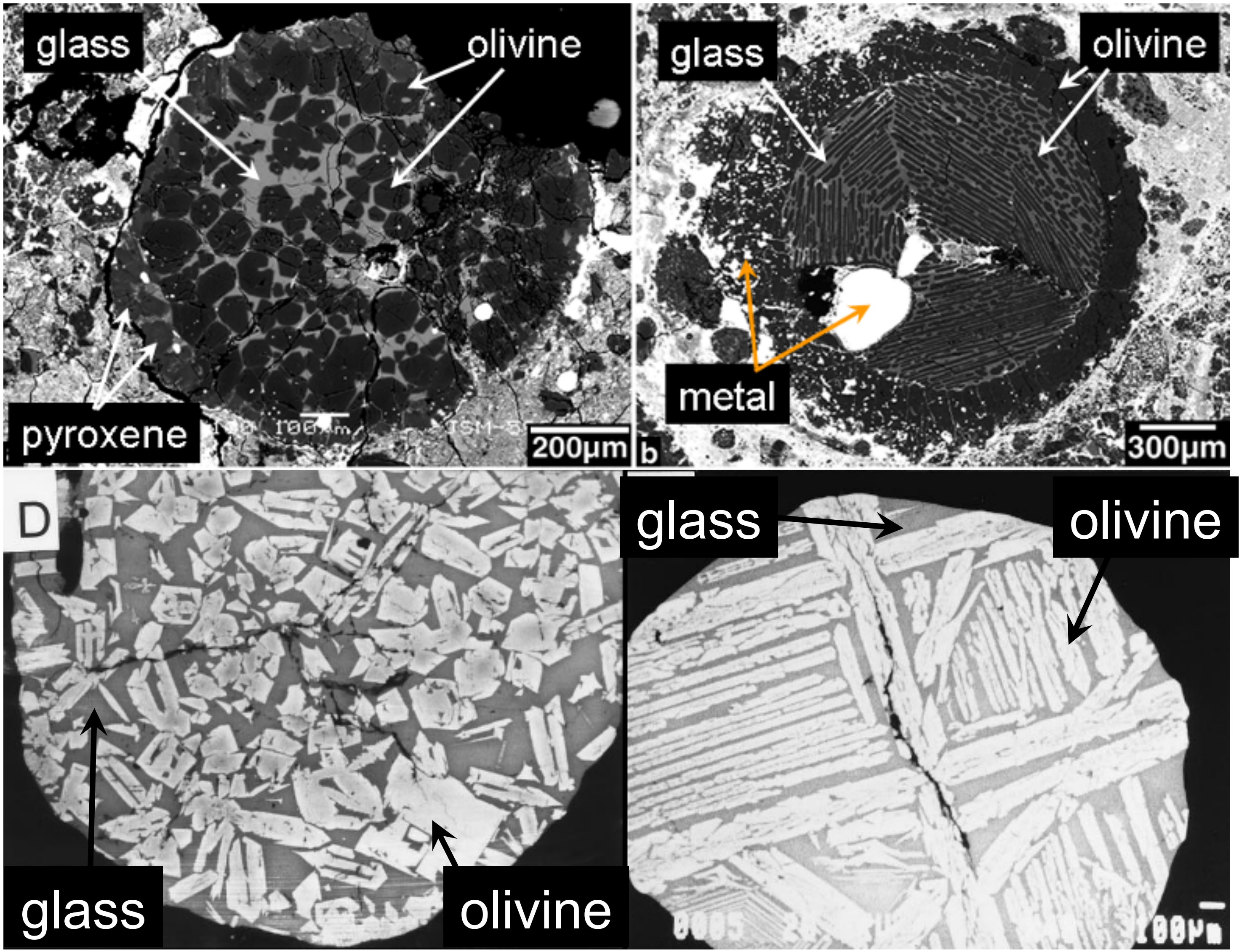

Connolly *et al.* 1998

Chondrule formation process

Conditions of fash-melting of dust precursors

Pressure	*10^{-3} - 10^{-6} bar*
Temperature	*1400 - 1750°C*
Cooling rate	*10 - 1000°C.hr^{-1}*
time	*min to hours*

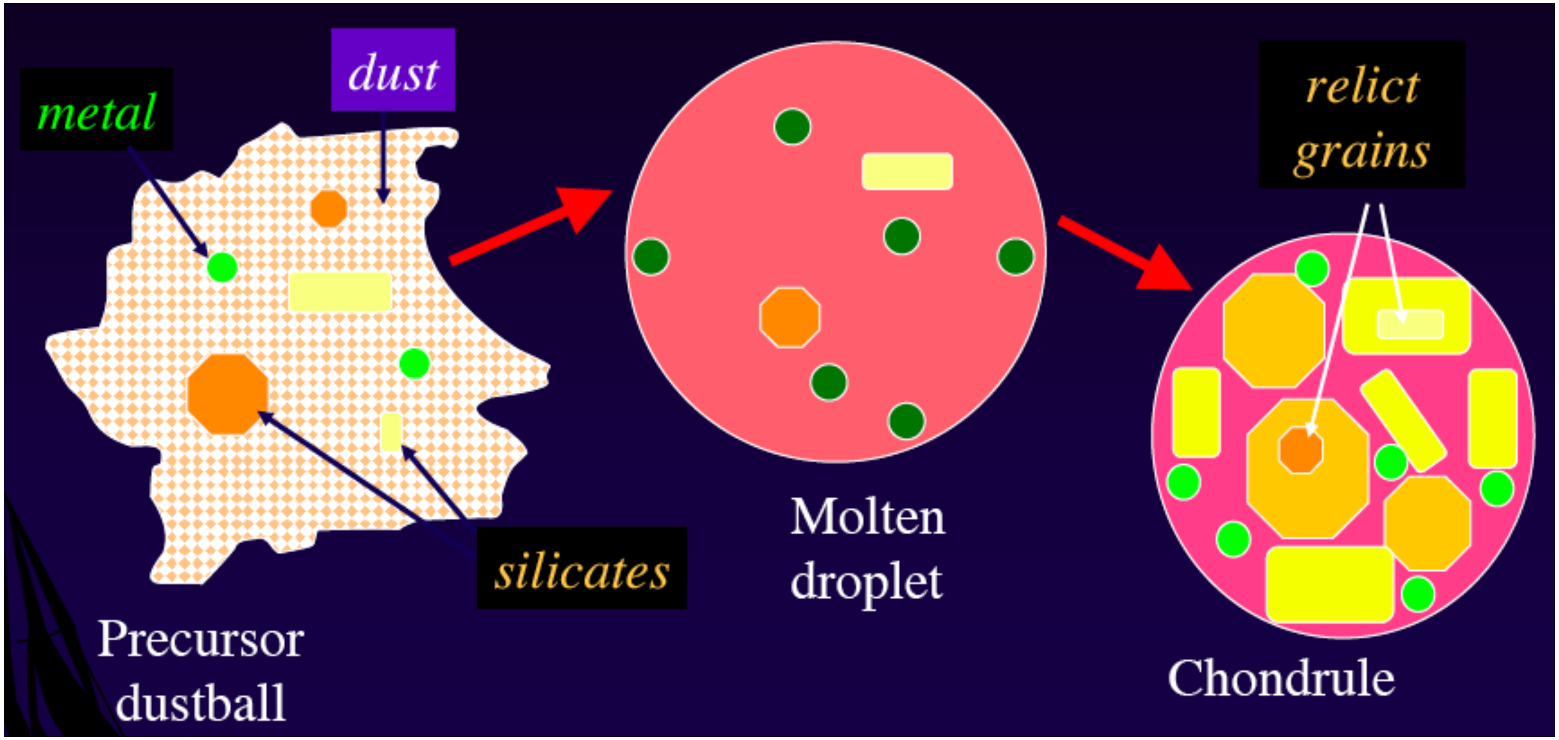

Jones et al., 2005

Chondrules form by brief heating events

Chondrule formation process

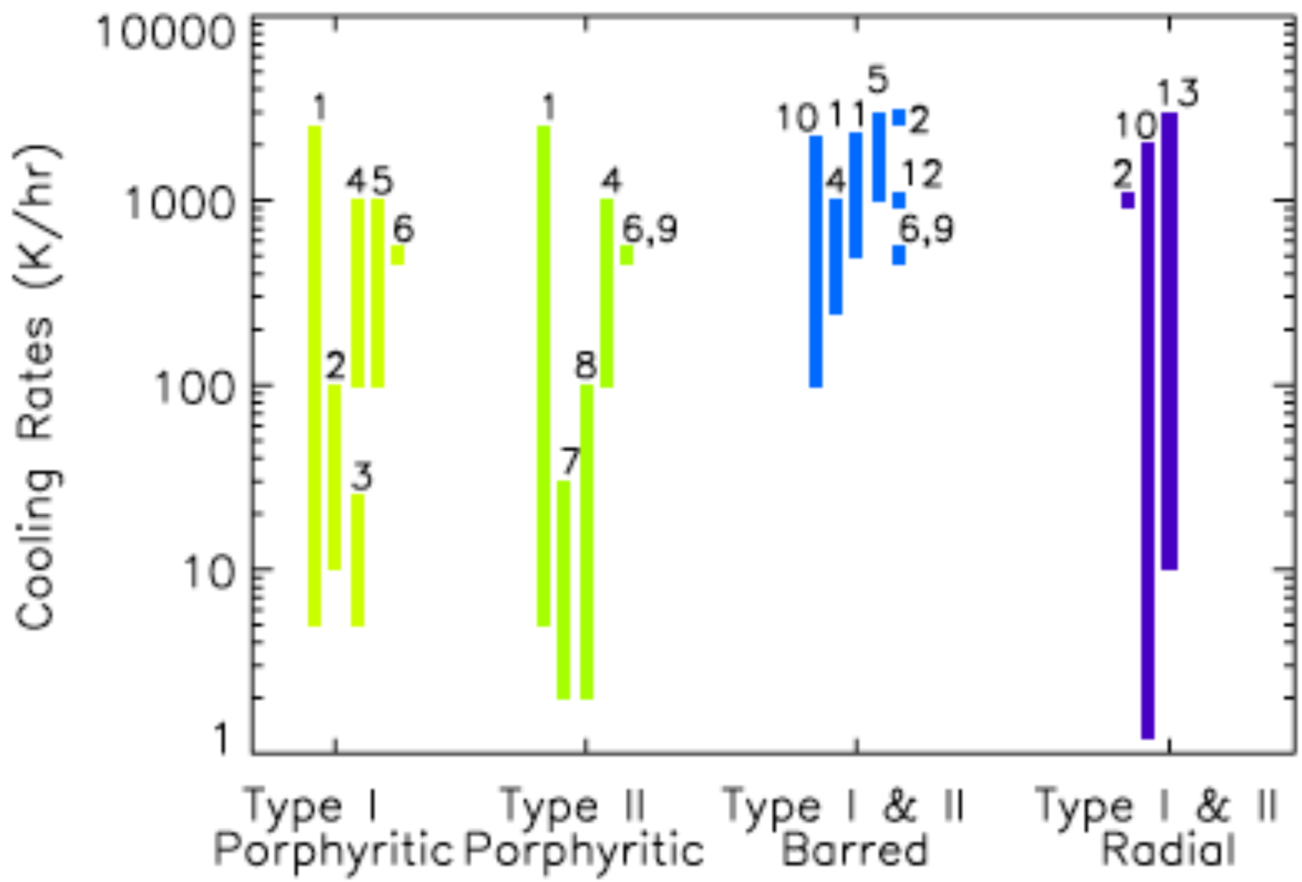

(Desch et al., 2011)

Chondrule formation process

Table 2. Constraints on chondrule thermal histories.

Constraint	X-wind	Lightning	Bow shocks	GI shocks
Ambient T < 650 K	X	✓	✓	✓
Heating duration < 10 min[a]	X	✓	✓	?
Peak $T \geq 2000$ K	X	?	✓	✓
Cooling rate from peak $\sim 10^3$–10^4 K h^{-1} [a]	X	?	✓	✓
Crystallization cooling rate ~ 10–10^3 K h^{-1} (porphyritic)	✓	X	?	✓
Crystallization cooling rate $\sim 10^2$–10^3 K h^{-1} (barred)	X	X	?	✓
Cooling rate correlates with chondrule density	X	X	?	✓

(Desch et al., 2011)

Chondrule formation process

How Shock Waves Melt

Shock waves heat up chondrules in three ways:

- Gas-drag friction
- Thermal exchange with hot gas
- Thermal radiation from dust, chondrules

(Hood &Horanyi 1993; Ruzmaikina & Ip 1994; Desch & Connolly 2002)

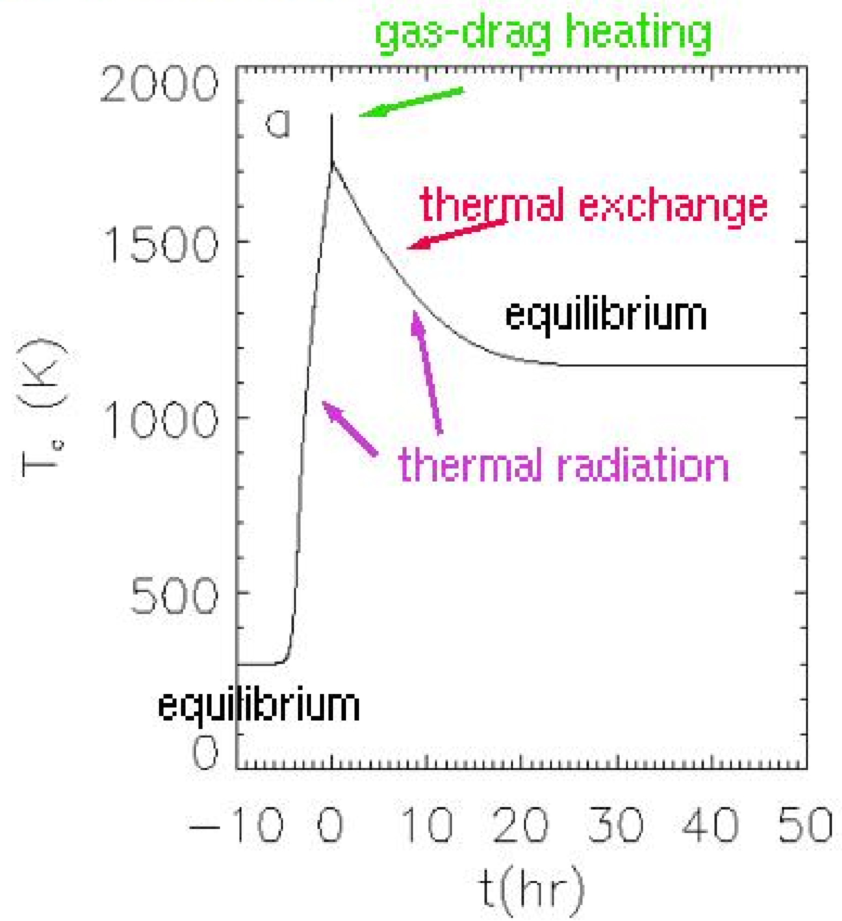

Chondrule formation process

Porphyritic chondrule thermal histories

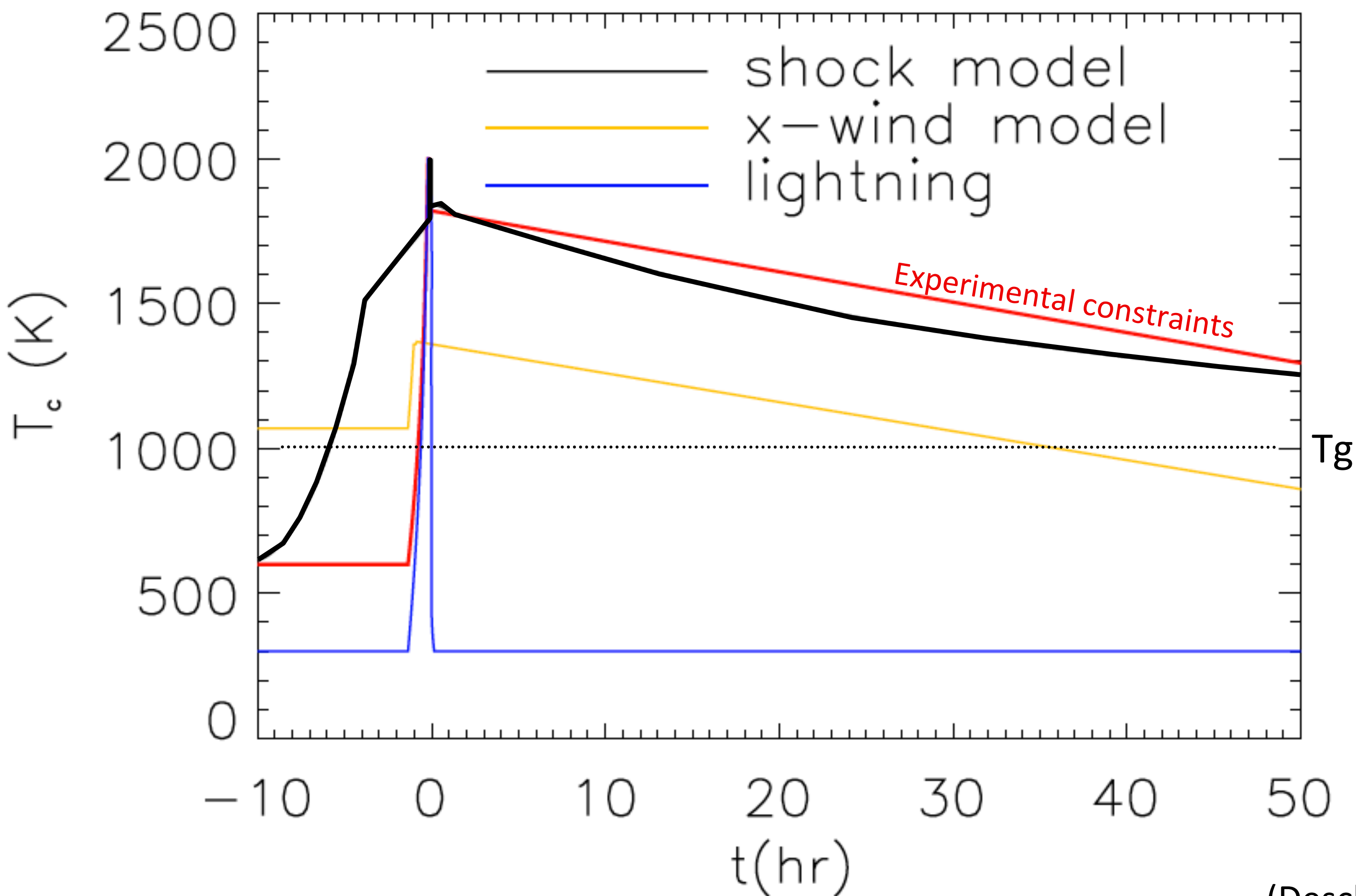

- Crystallization cooling rate

  $10\text{-}10^3$ $K.h^{-1}$

- Time at high temperature

  > 50 - 100 h

Chondrule formation: Quicker and faster?

(Desch et al., 2011)

Chondrule formation process

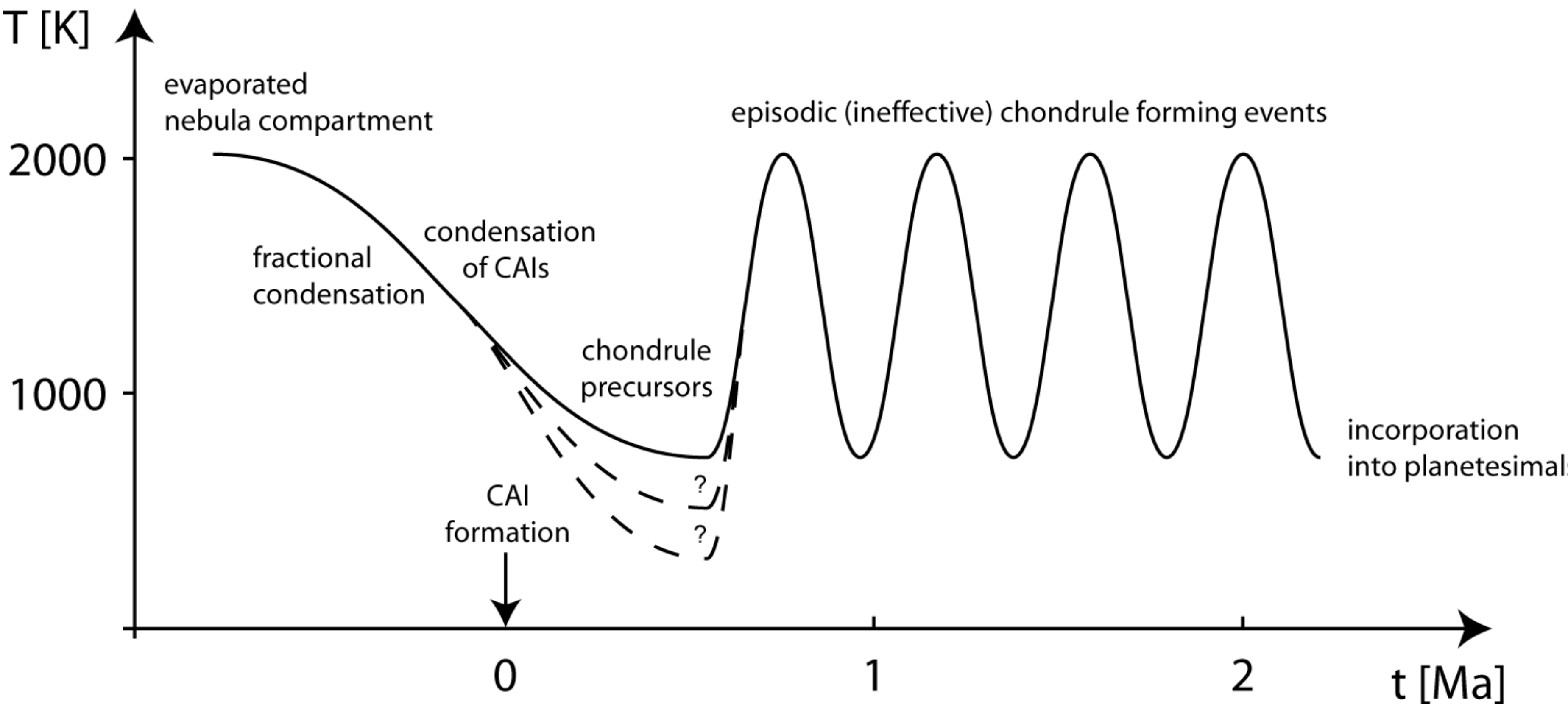

Schematic model of the formation of solid matter in the early solar system

Chondrule formation process

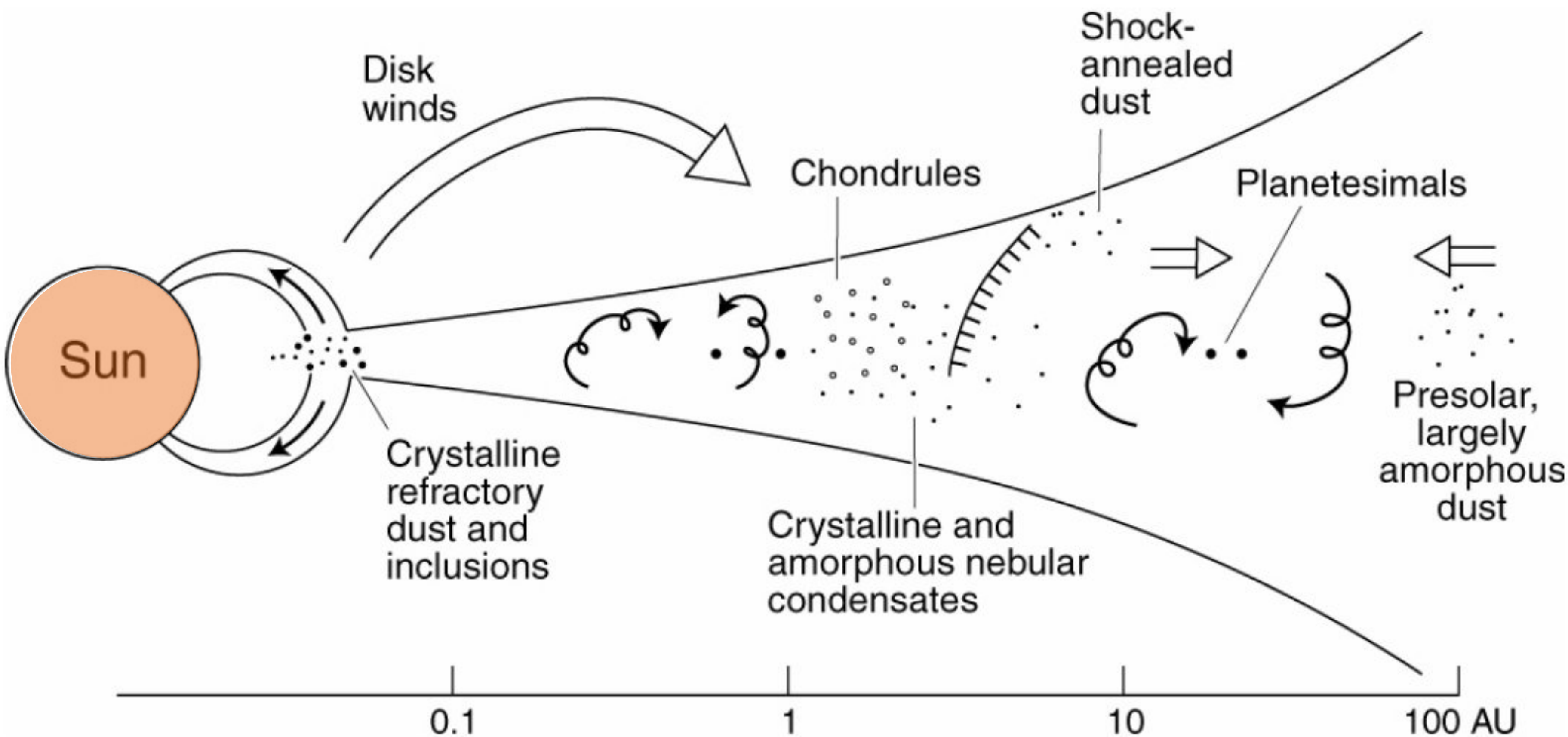

(Scott and Krot, 2005)

Constraints on the protoplanetary disk evolution

Diversity of chondrule textures & chemistry

Type I porphyritic chondrules

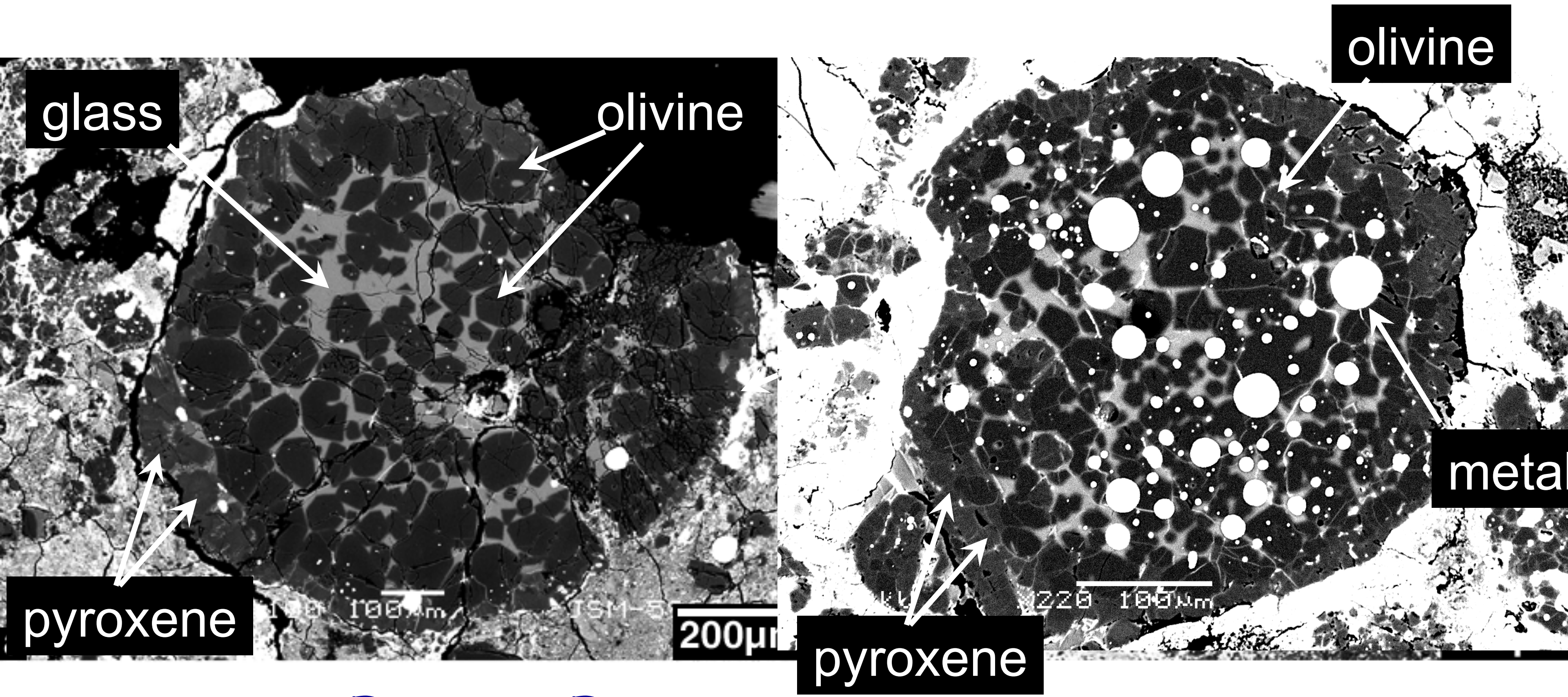

$Fo_{99.8-95}$; $Fs_{>95}$

$Fo_{99.8-95,}$; $FeNi_{5-10}$

Diversity of chondrule textures & chemistry

Type II Porphyritic olivine chondrules

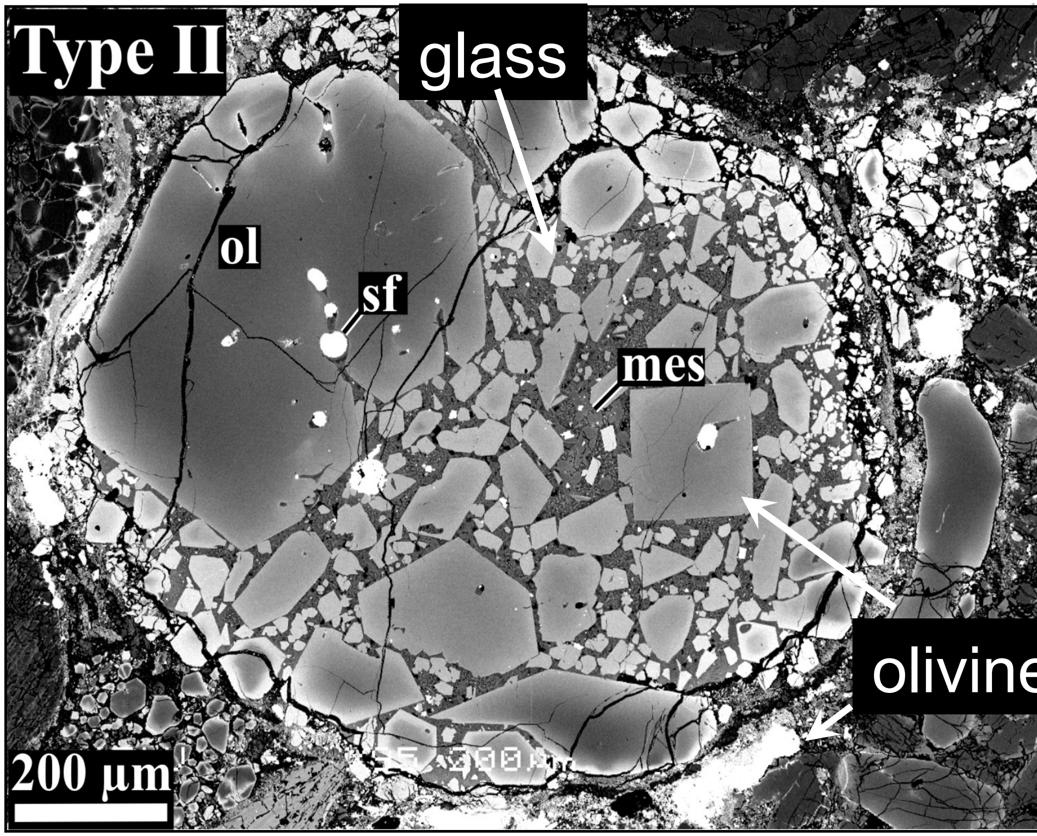

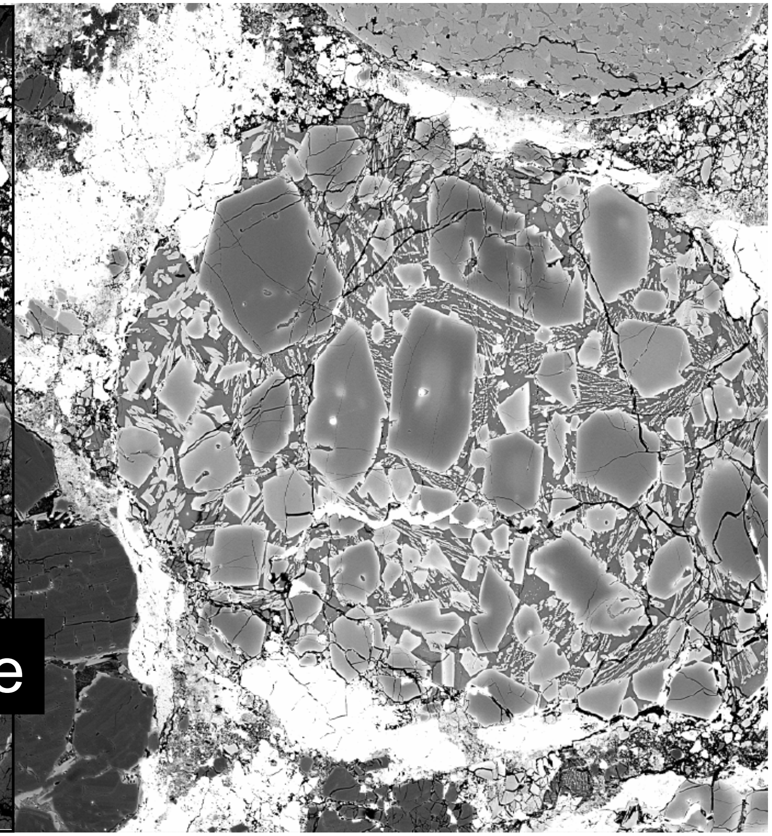

$Fo_{90\text{-}55}$

Chondrule formation process

Closed system

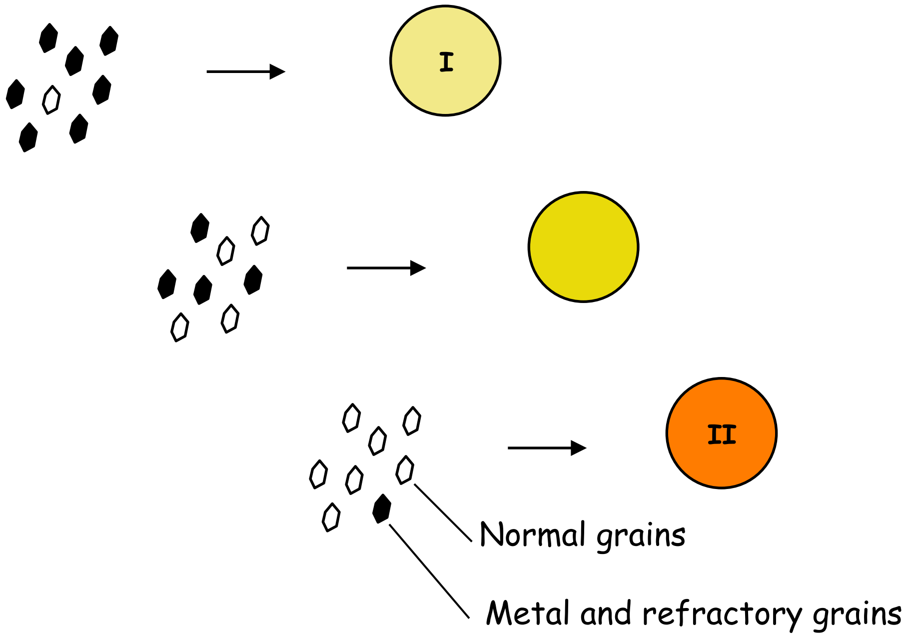

(Gooding et al., 1983; Grossman, 1988; Hewins, 1991; Jones, 1994, Alexander et al. 2008 ...)

Information on precursors

Chondrule formation process

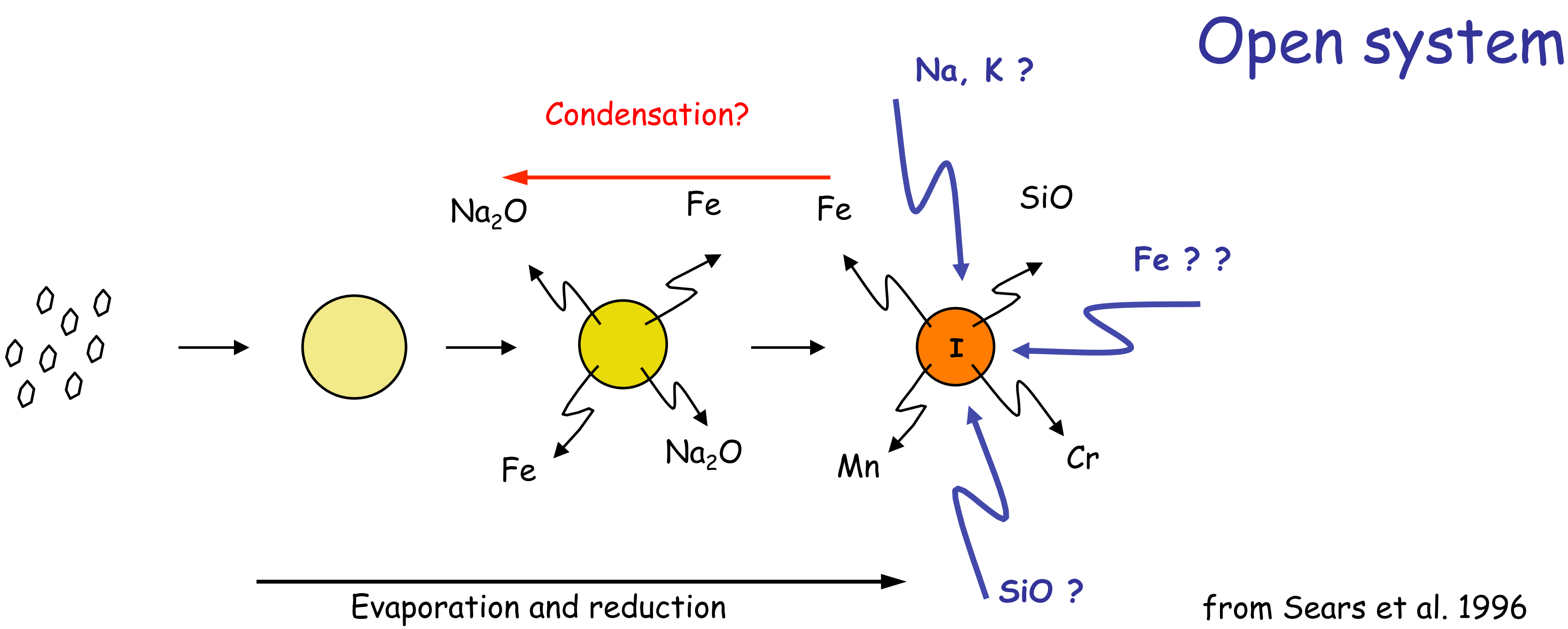

(Lewis et al., 1993, Georges et al., 2000, Matsunami et al., 1993, Alexander, 1996, Tissandier et al., 2002, Krot et al., 2005, Libourel et al. 2007 ...)

Information on the protoplanetary disk conditions

Chondrule formation process

Type I chondrules are complex objects composed of:

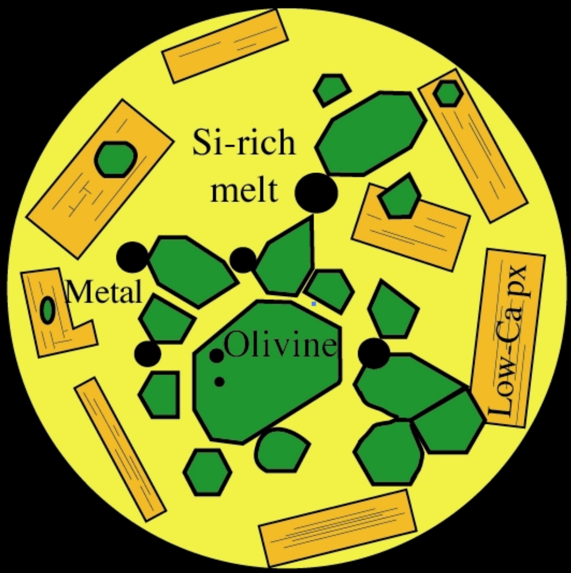

– fragments of differentiated planetesimals

Mg-rich olivine ± Fe,Ni-metal ± Ca-Al-rich glass

<u>and</u>

– an igneous component "equilibrated" with the gaseous environment

Si-Na rich glass ± low-Ca pyroxene ± high-Ca pyroxene ± silica phase.

Impacts on planetesimals with a vapor plume

Plan

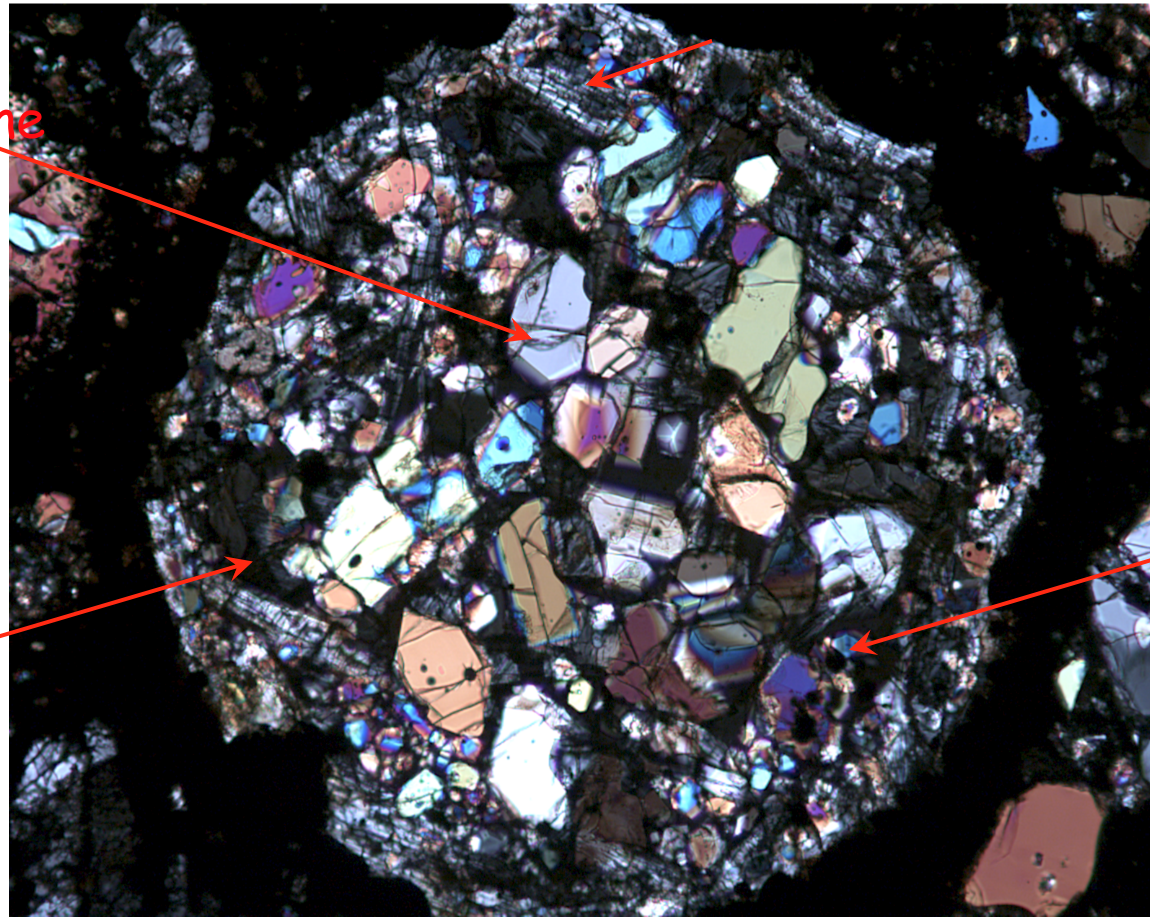

- *Evidence for interaction with gas phase*
- *Mg-rich olivines from differentiated planetesimals?*
- *Constraints on the formation of chondrules*

Type I FeO-poor chondrules in Semarkona (PO, POP, PP)

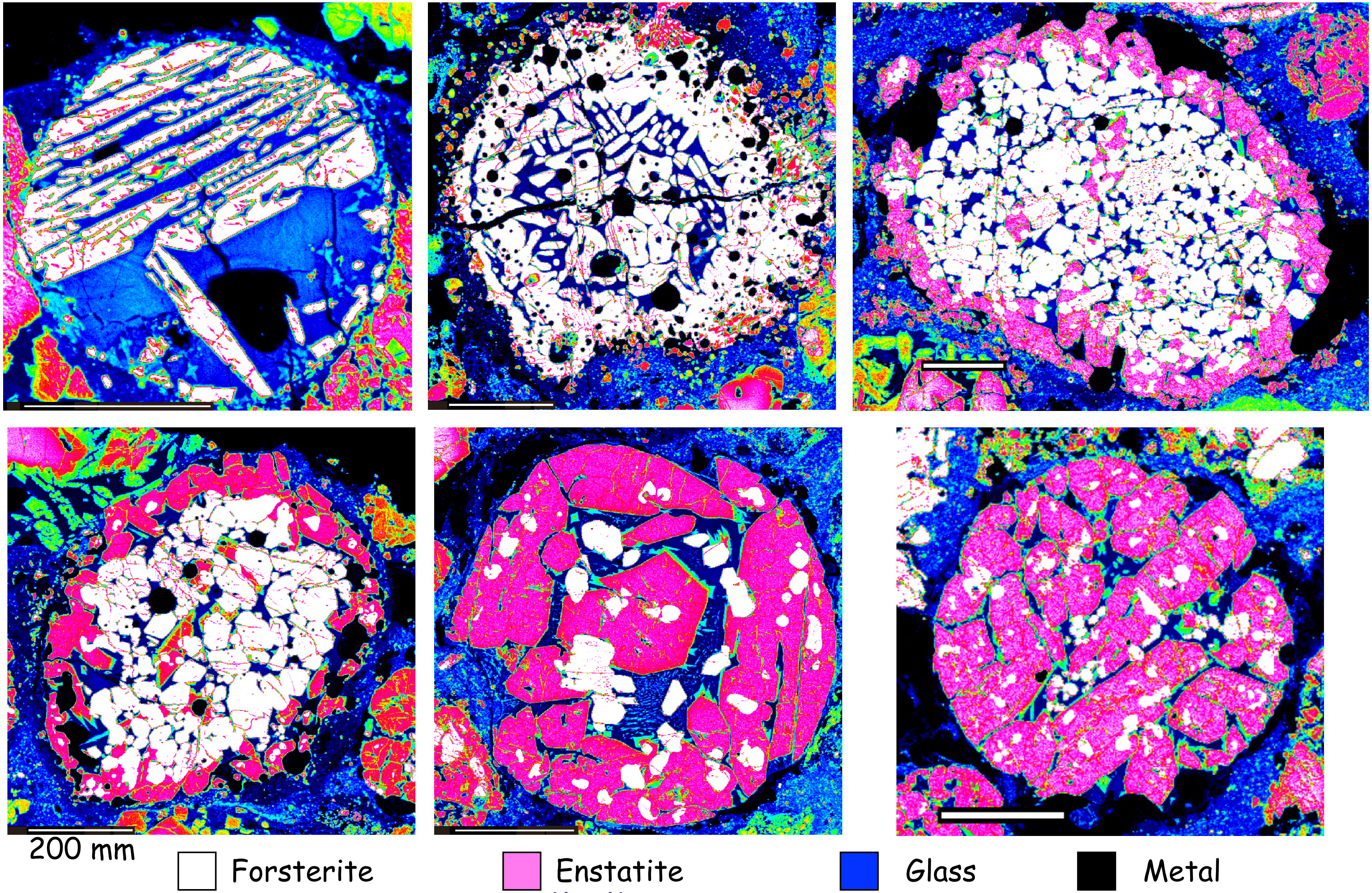

Grossman et al. 2000

Texture

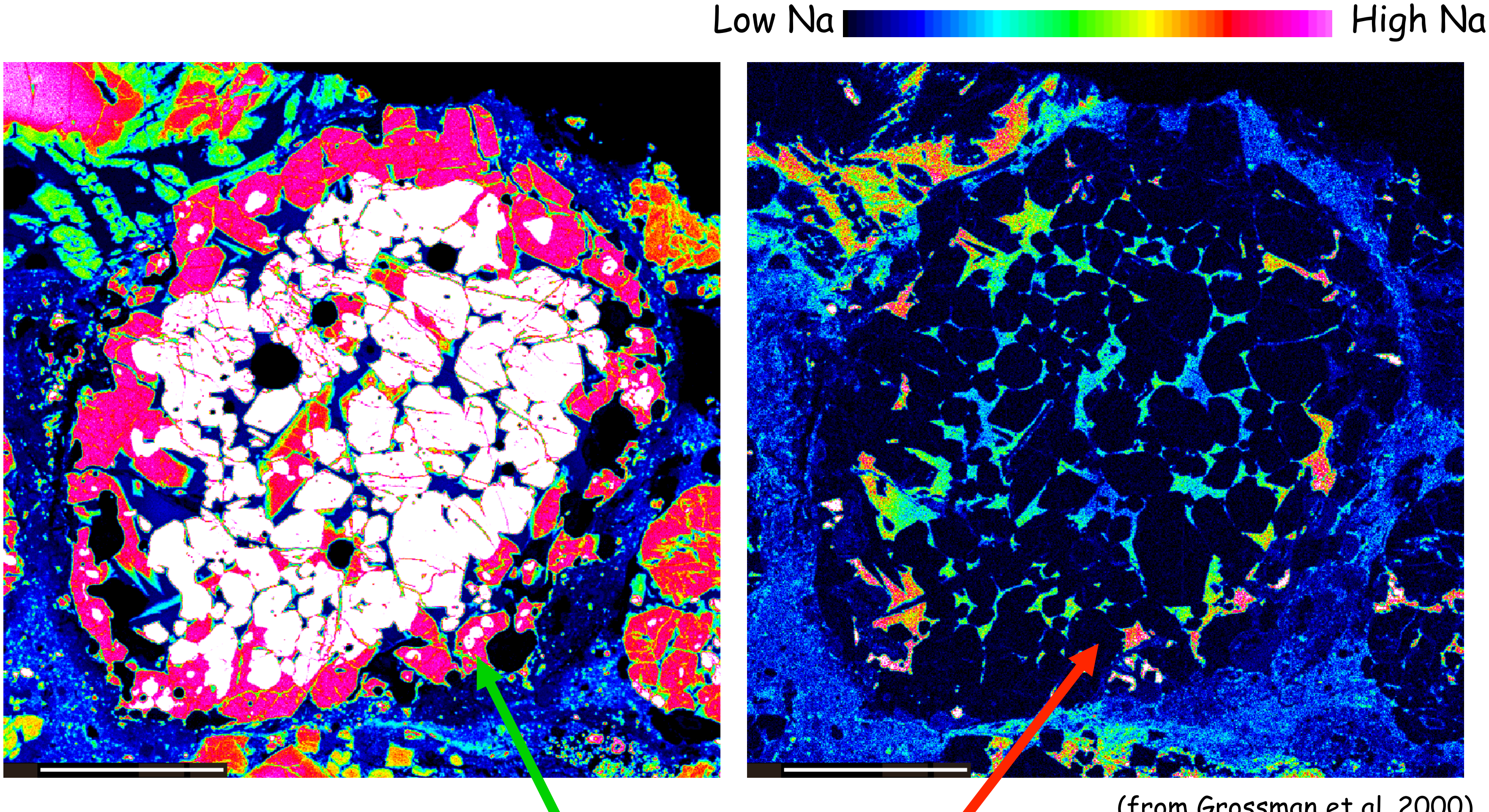

(from Grossman et al. 2000)

Pyroxene-rich (high-Si) zone ≈ Alkali-rich zone

Increasing a_{SiO2} from core to rim in the mesostase.

Gas - melt interaction experiments : Nebulotron

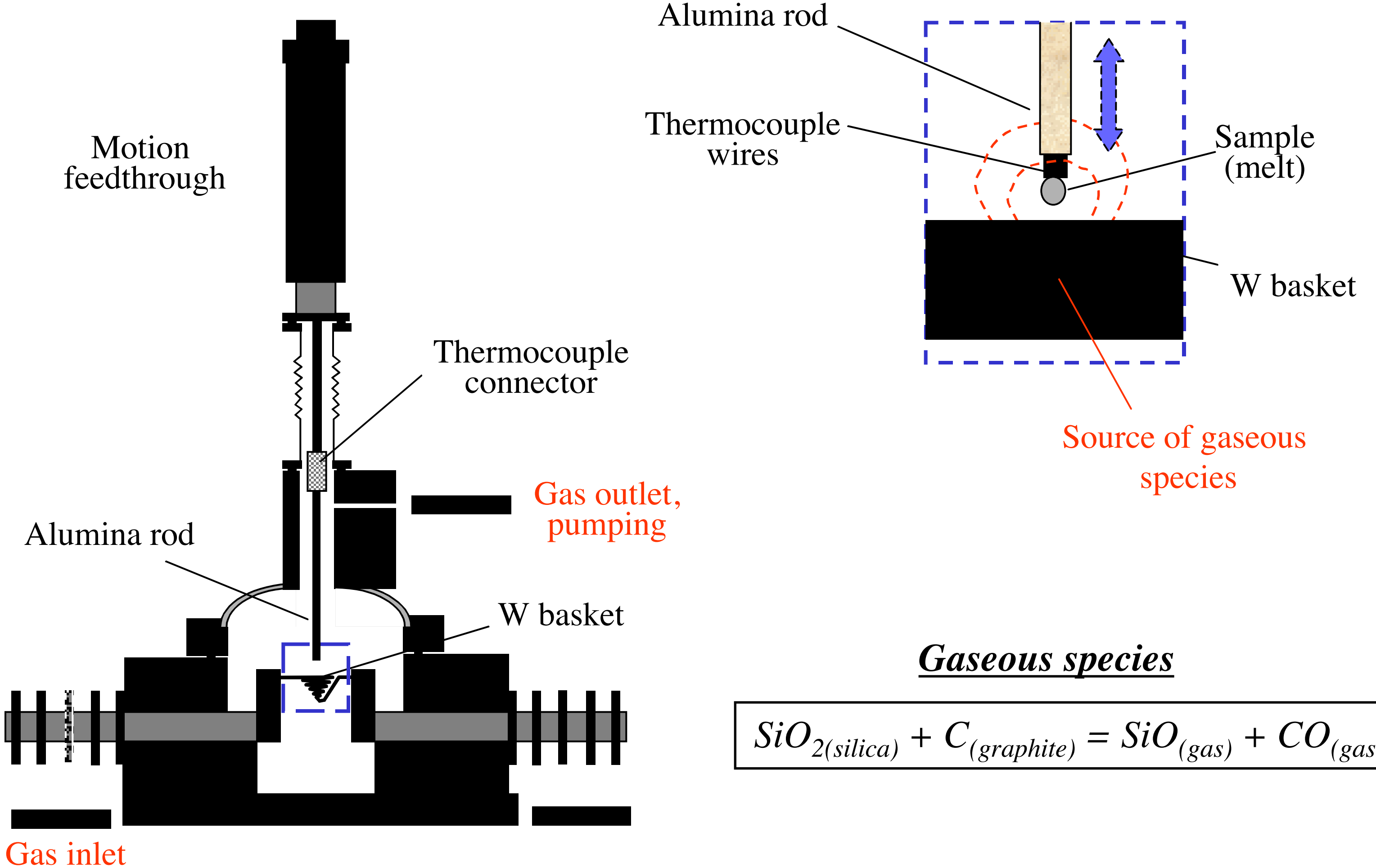

Gaseous species

$$SiO_{2(silica)} + C_{(graphite)} = SiO_{(gas)} + CO_{(gas)}$$

Tissandier et al., 2002

SiO gas - melt interaction

$SiO_{(gas)} + 1/2\ O_{2(gas)} = SiO_{2(melt)}$

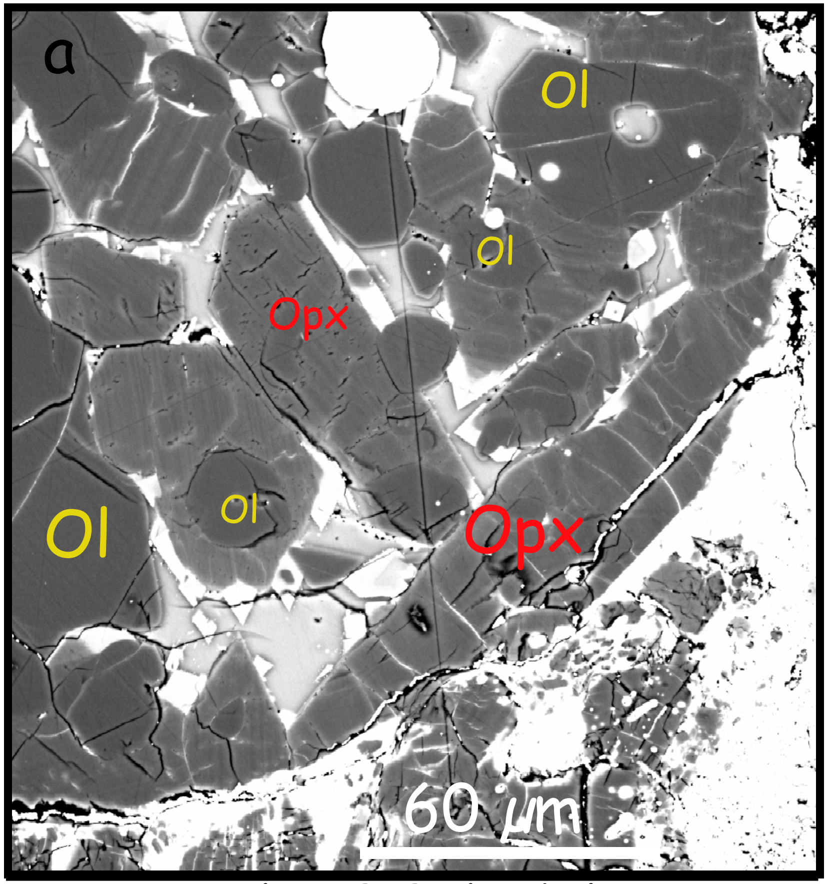

Semarkona POP Chondrule

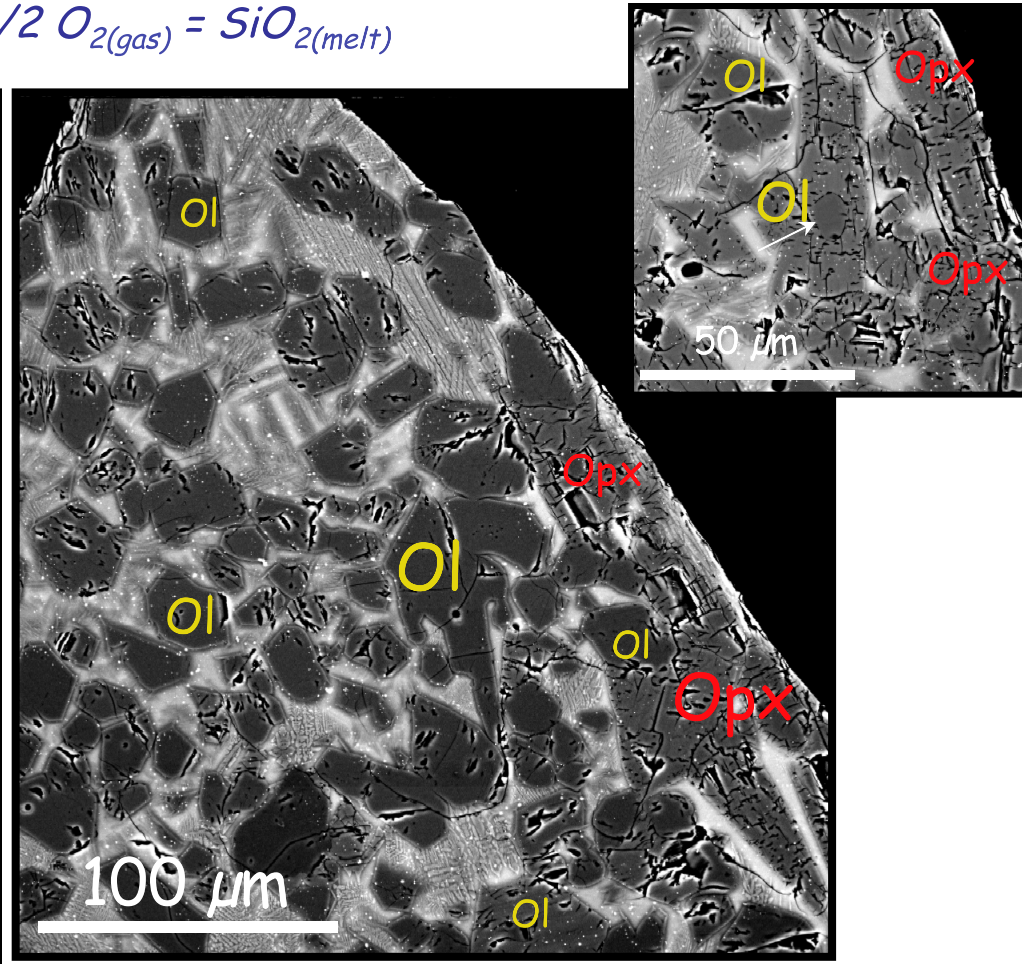

SiMS3-9, 300 s à 1451°C, $P_{SiO(g)}$

Mineralogical zonation similar to chondrules

Direct $SiO_{(gas)}$ <u>condensation</u> into chondrule melts

SiO evaporation-condensation experiments

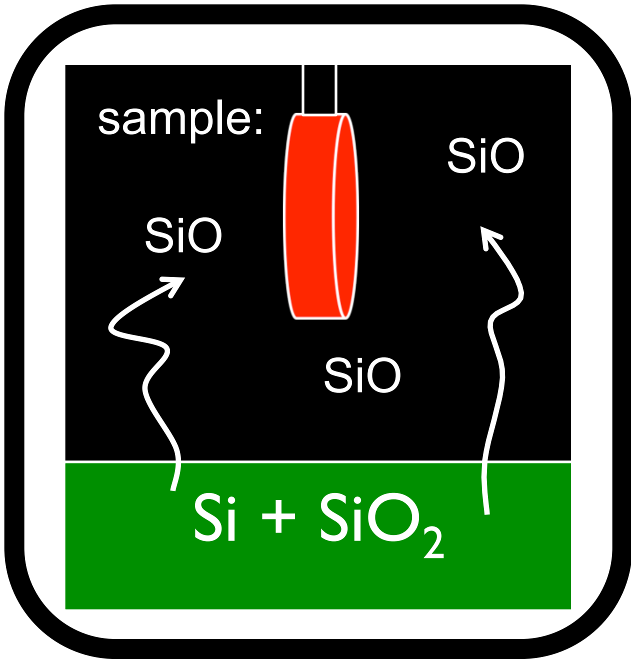

source + sample in closed crucible

Source (evaporation):

$$Si^{(source)} + SiO_2^{(source)} \leftrightarrow 2\ SiO^{(gas)}$$

Sample (condensation):

$$SiO^{(gas)} + 1/2\ O_2 \leftrightarrow SiO_2^{(sample)}$$

$$= \ (P_{SiO}) \cdot (P_{O2})^{1/2} \ / \ (K_{eq(T,P)} \cdot \gamma_{SiO2}^{(sample)})$$

SiO gas - solid interaction

Production of SiO(g)

- T_{exp} = 1723 K = 1450°C:
- using "amorphous" SiO powder: $Si_{(s)} + SiO_{2\,(s)} \rightleftharpoons 2\,SiO_{(g)}$

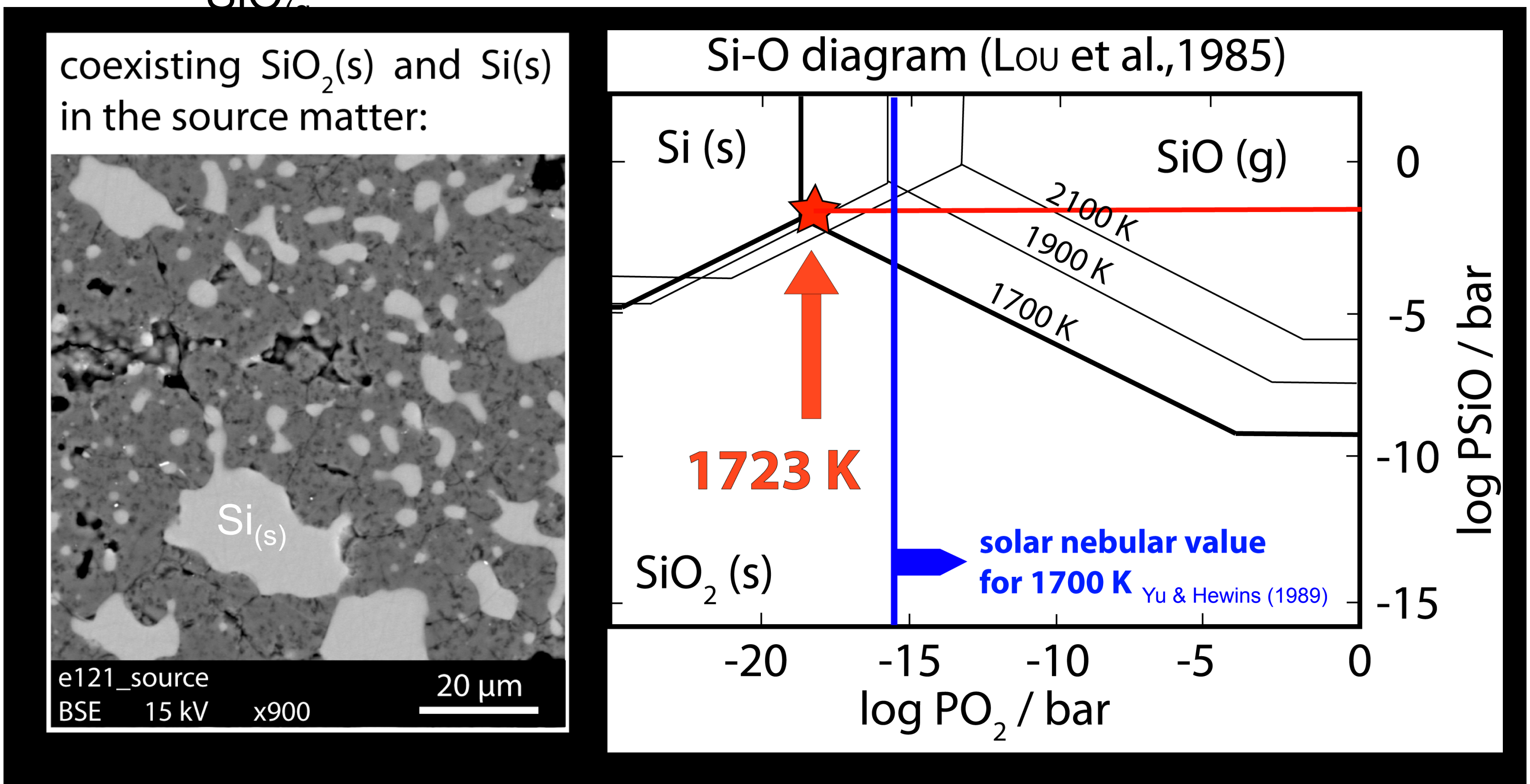

Results: © pure forsterite monocrystallin samples

- in all monocrystal experiments formation of an enstatite rim
- En thickness 10-30 µm
- all samples have Si-rich melt with 70-98 wt.% SiO_2

30 minutes

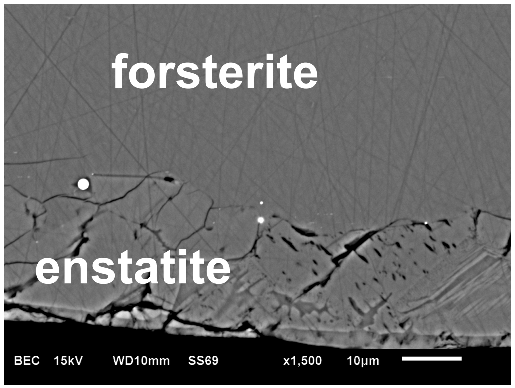

bar=10µm

60 minutes

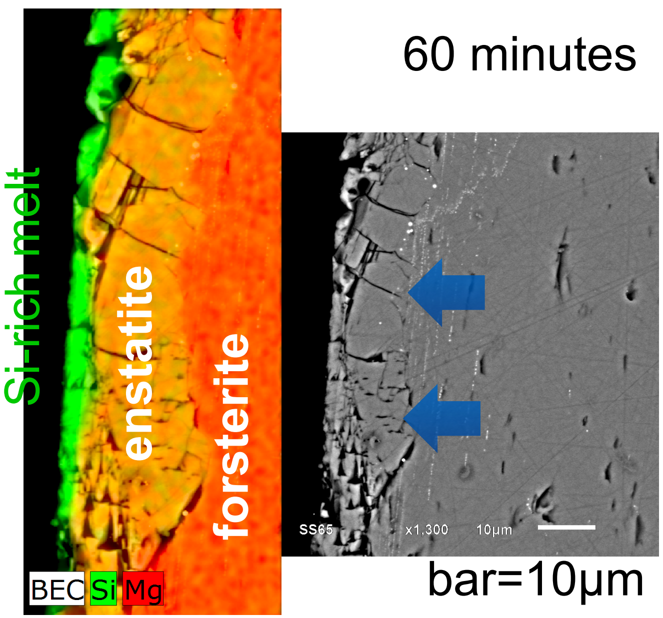

bar=10µm

120 minutes

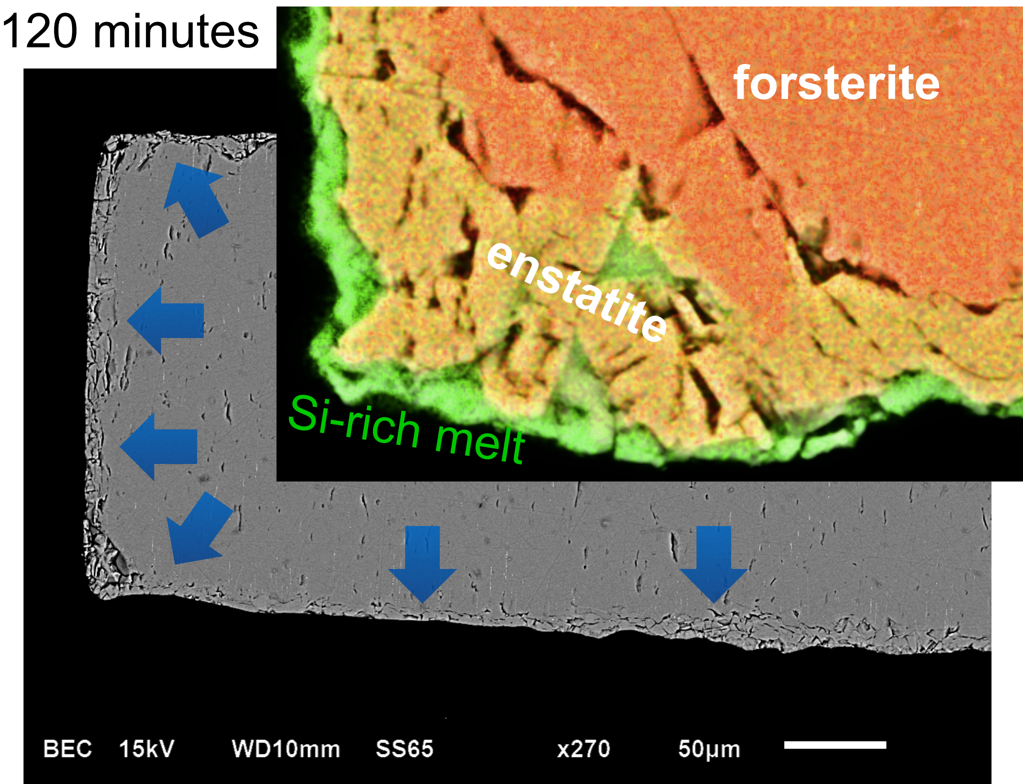

Application to chondrules and refractory forsterite

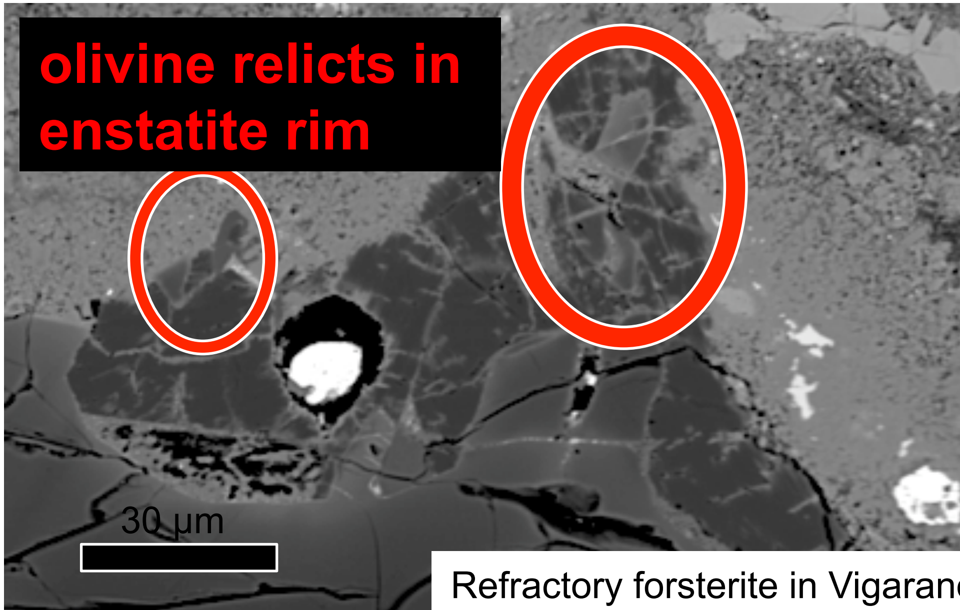

Refractory forsterite in Vigarano

Enstatite replaces olivine!
(enstatite is not condensed)

120 minutes

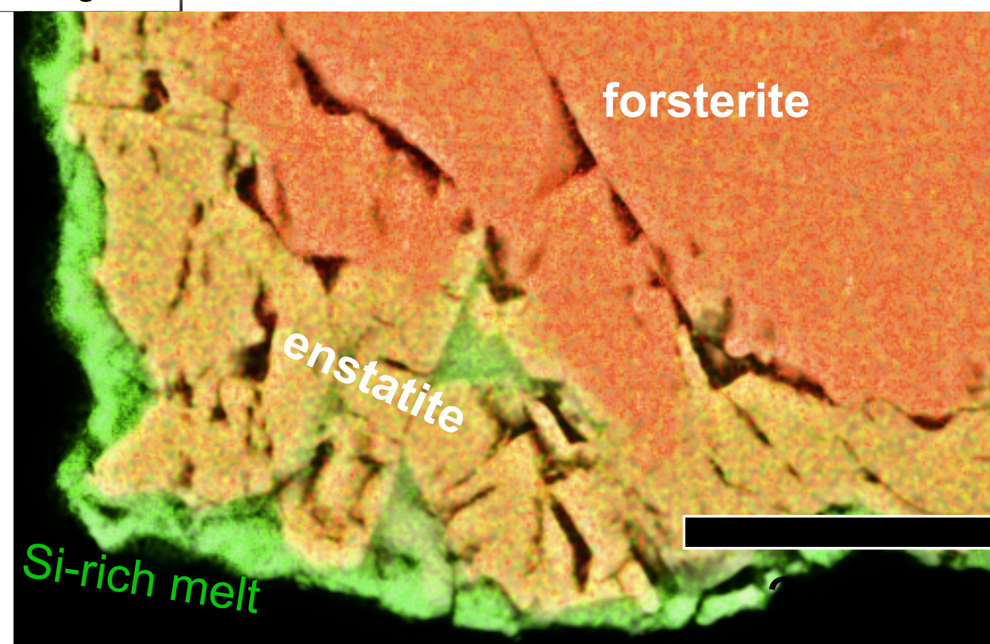

Chondrule formation process

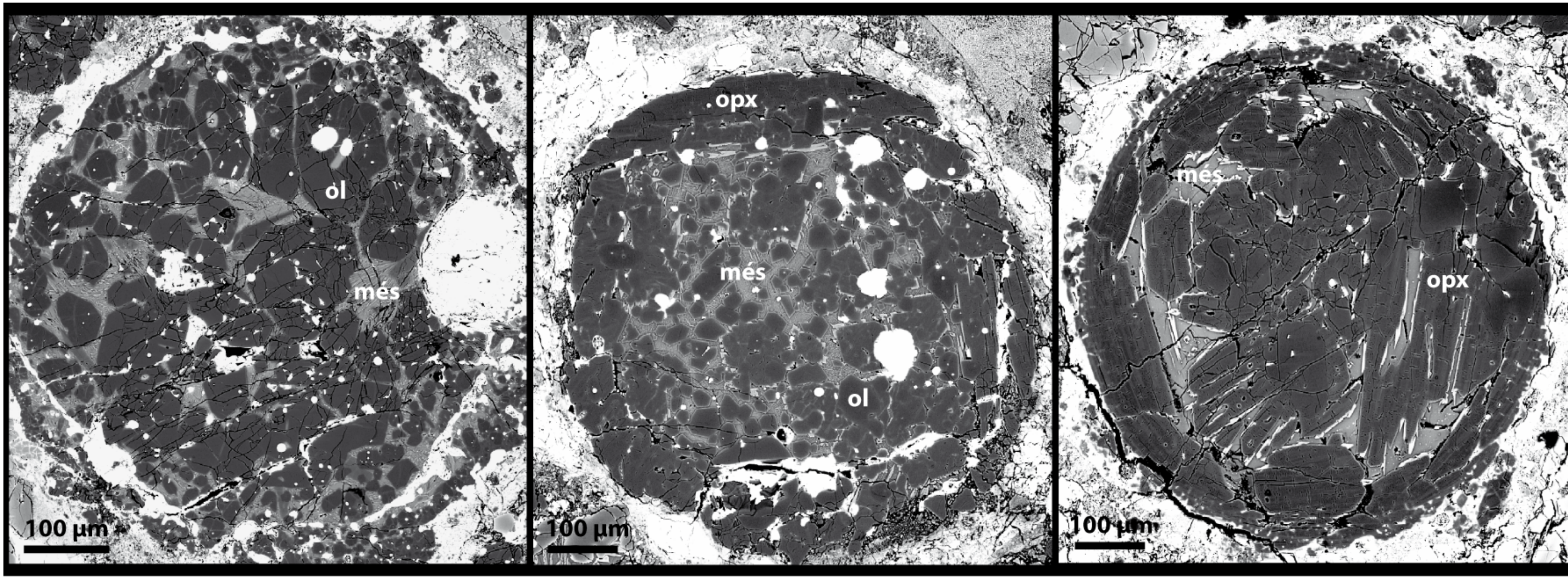

Sem-Ch2	Sem-Ch8	Sem-Ch10
type I PO	type I POP	type I PP
(SiO_2 = 54,44%; Na_2O = 1,31%; K_2O = 0,07%)	(SiO_2 = 61,47%; Na_2O = 5,16%; K_2O = 0,59%)	(SiO_2 = 65,58%; Na_2O = 6,19%; K_2O = 0,59%)

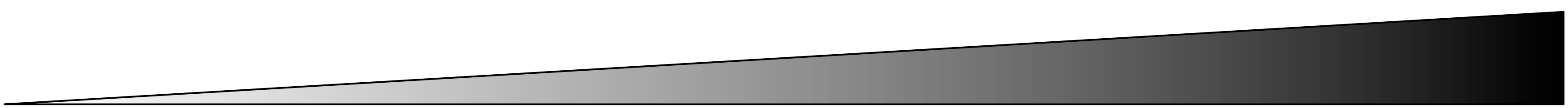

- **$SiO_{(g)}$ [$Na_{(g)}$, $K_{(g)}$]** **+**

Gas-melt interactions

(e.g. Tissandier et al., 2002; Krot et al., 2004; Libourel et al., 2003, 2006; Chaussidon et al. 2008)

Plan

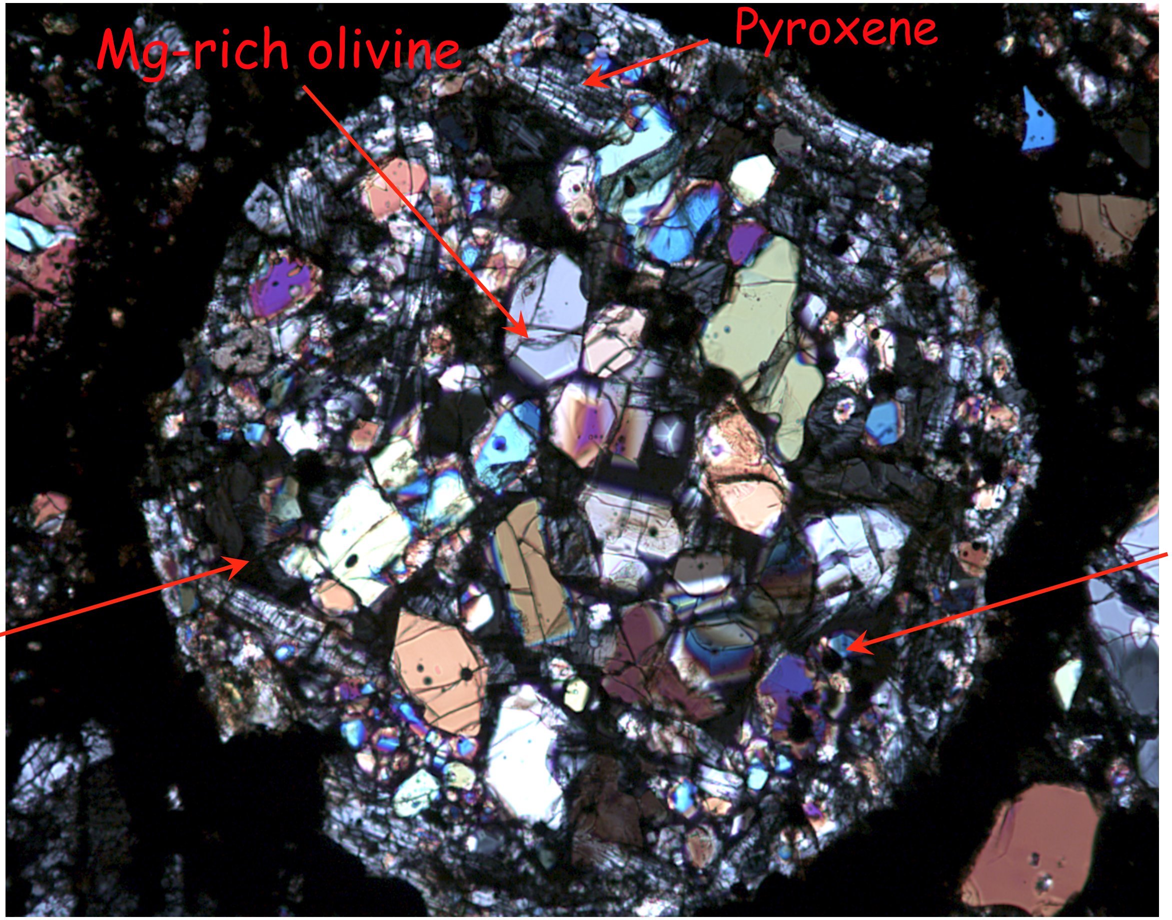

- *Evidence for interaction with gas phase*
- *Mg-rich olivines from differentiated planetesimals?*
- *Constraints on the formation of chondrules*

Chondrule #2 Vigarano (PO)

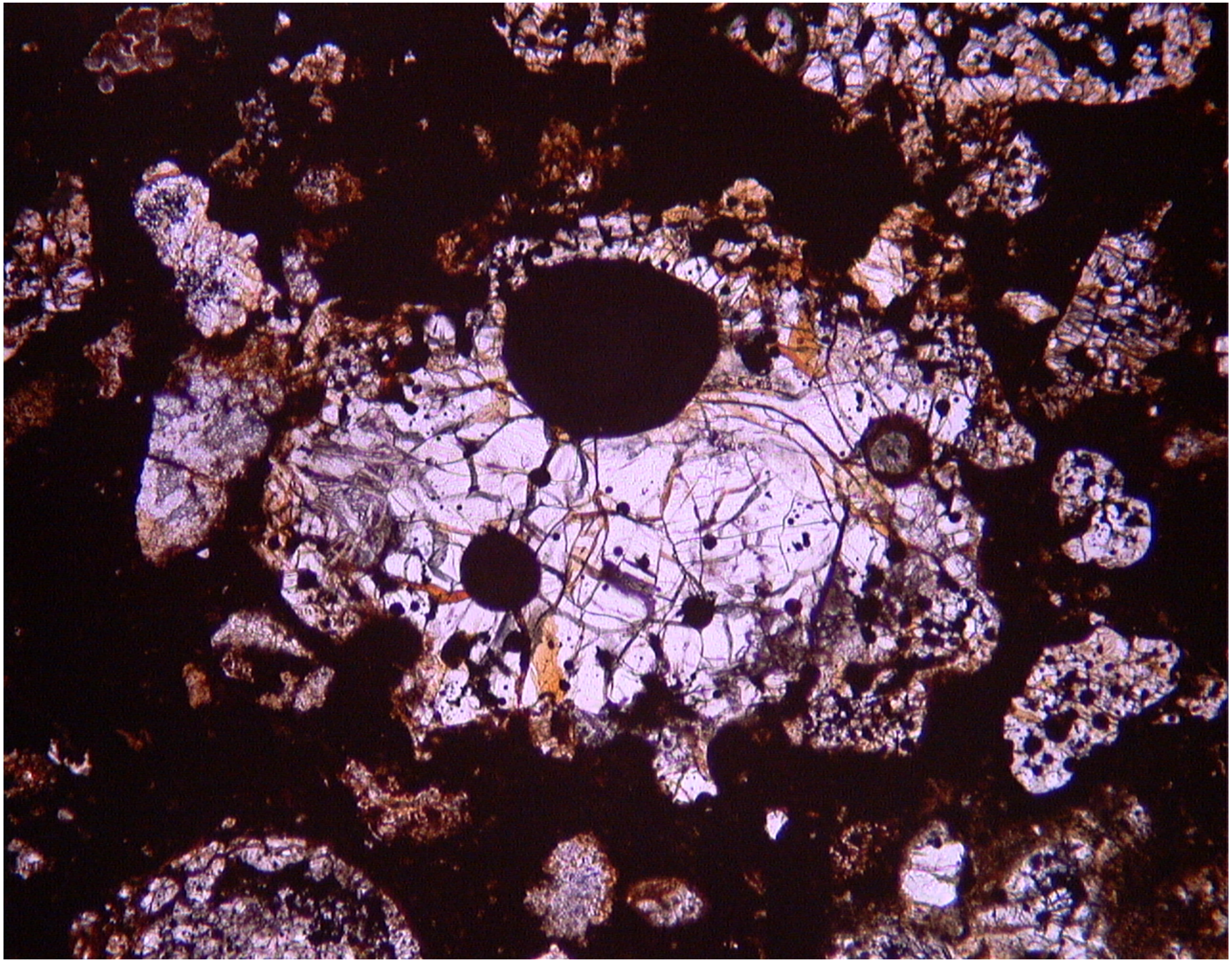

Transmitted light

Libourel & Krot, 2007

Chondrule #2 Vigarano

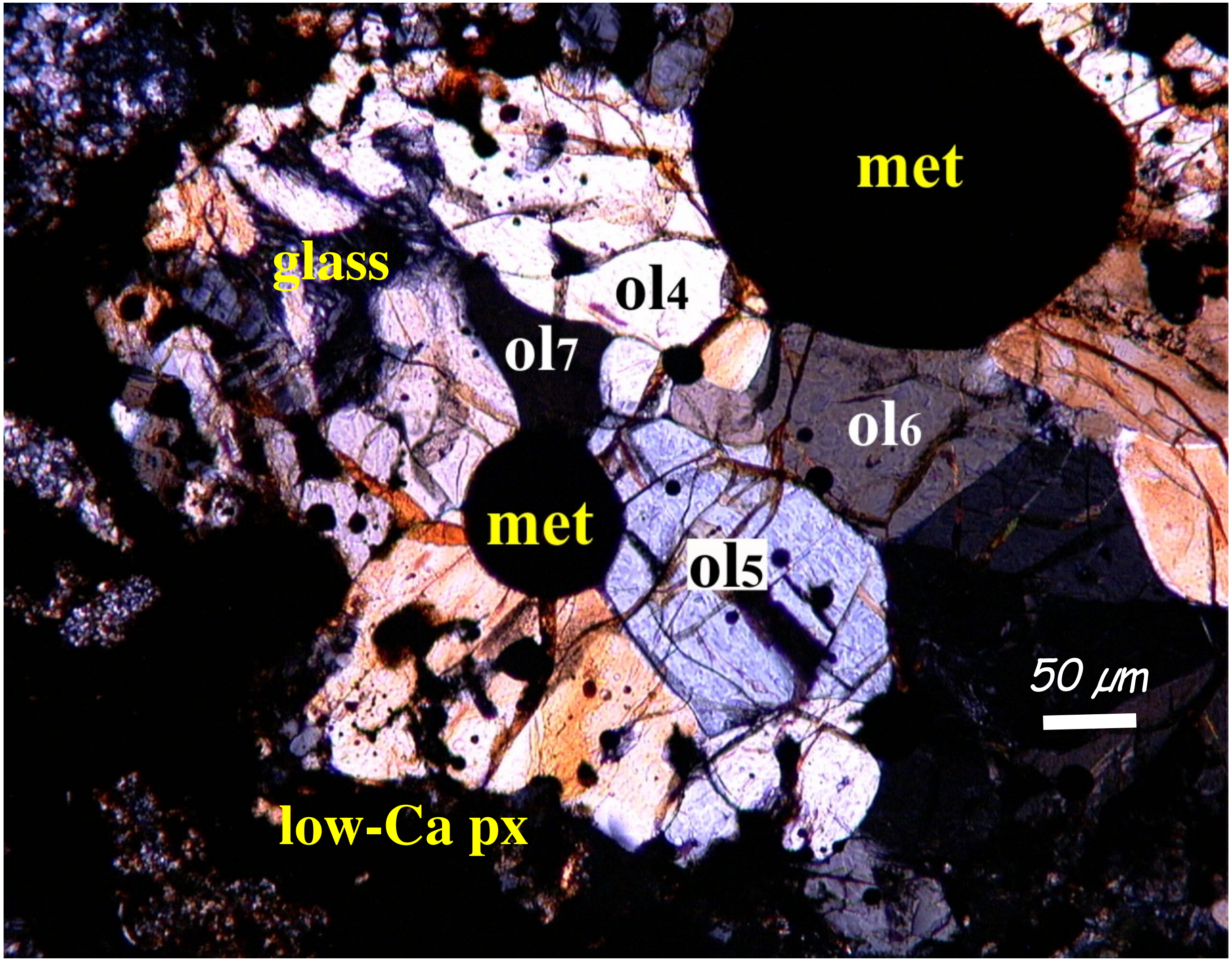

Chondrule #2 Vigarano (PO)

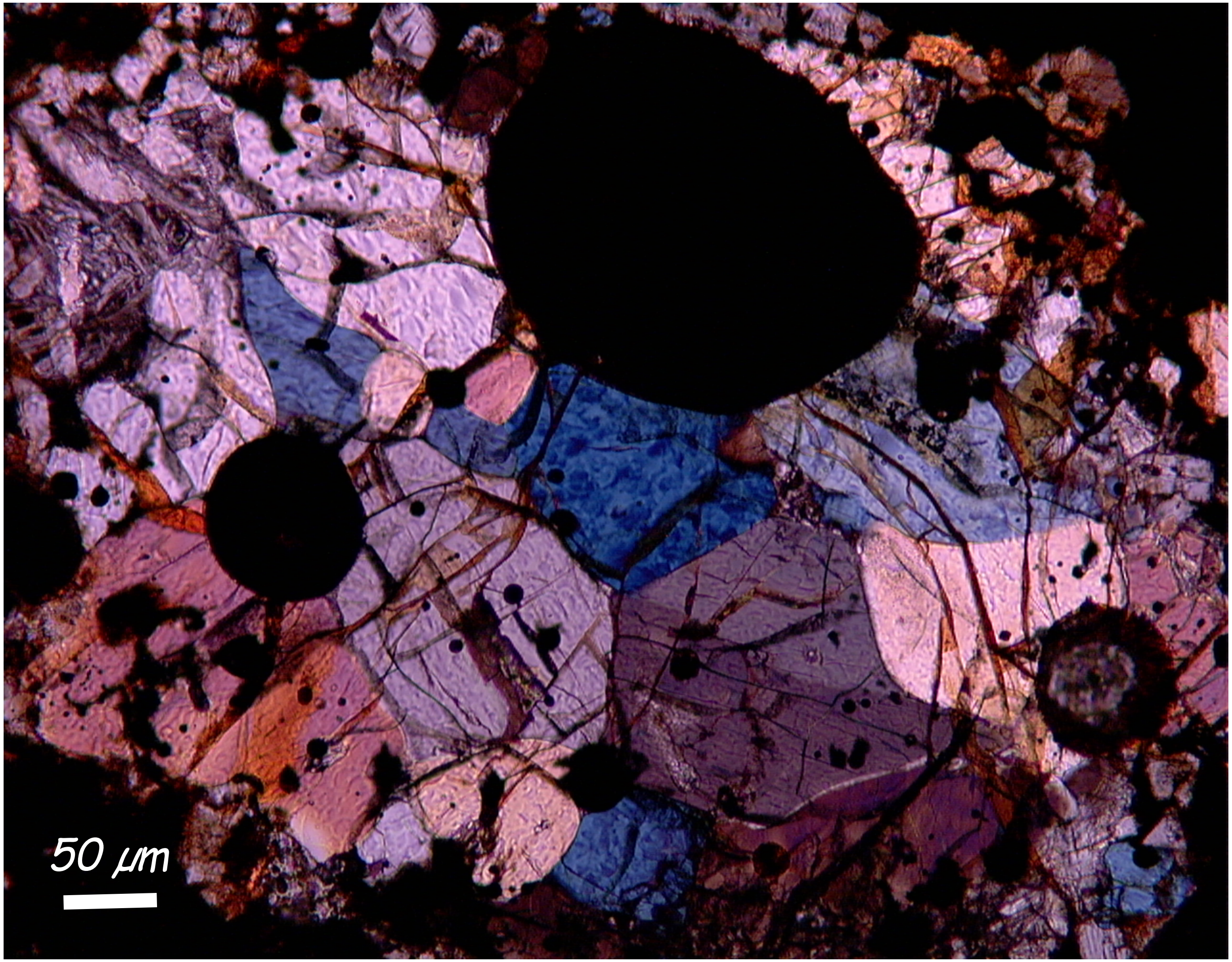

<ol-ol-ol> triple junctions

Triple junctions indicate equilibrium textures

Earth mantle peridotite

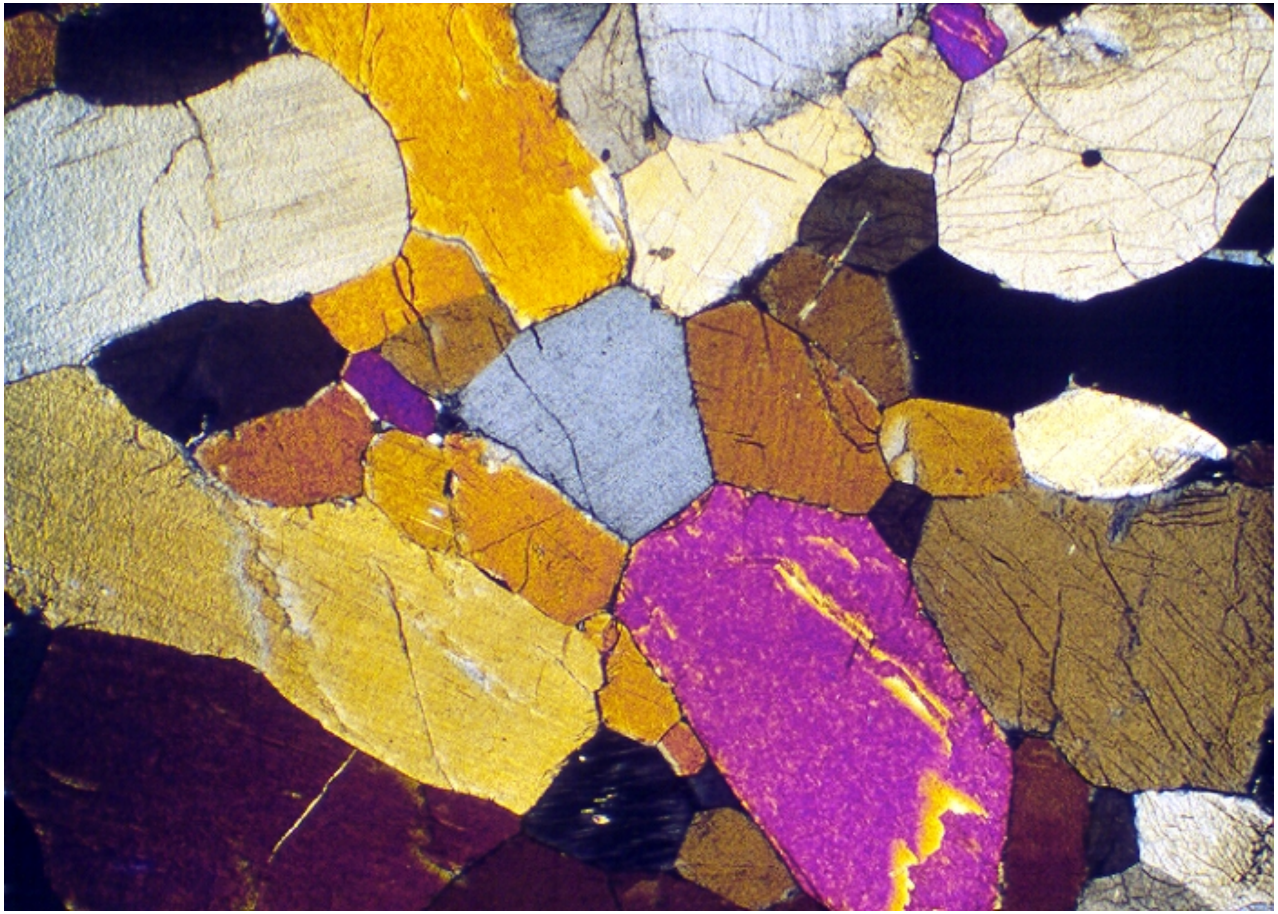

Such textures (sintering and annealing) <u>can not be</u> produced by crystallization from chondrule melts but could have been achieved on <u>differentiated parent bodies</u>.

Crystal growth: ostwald ripening

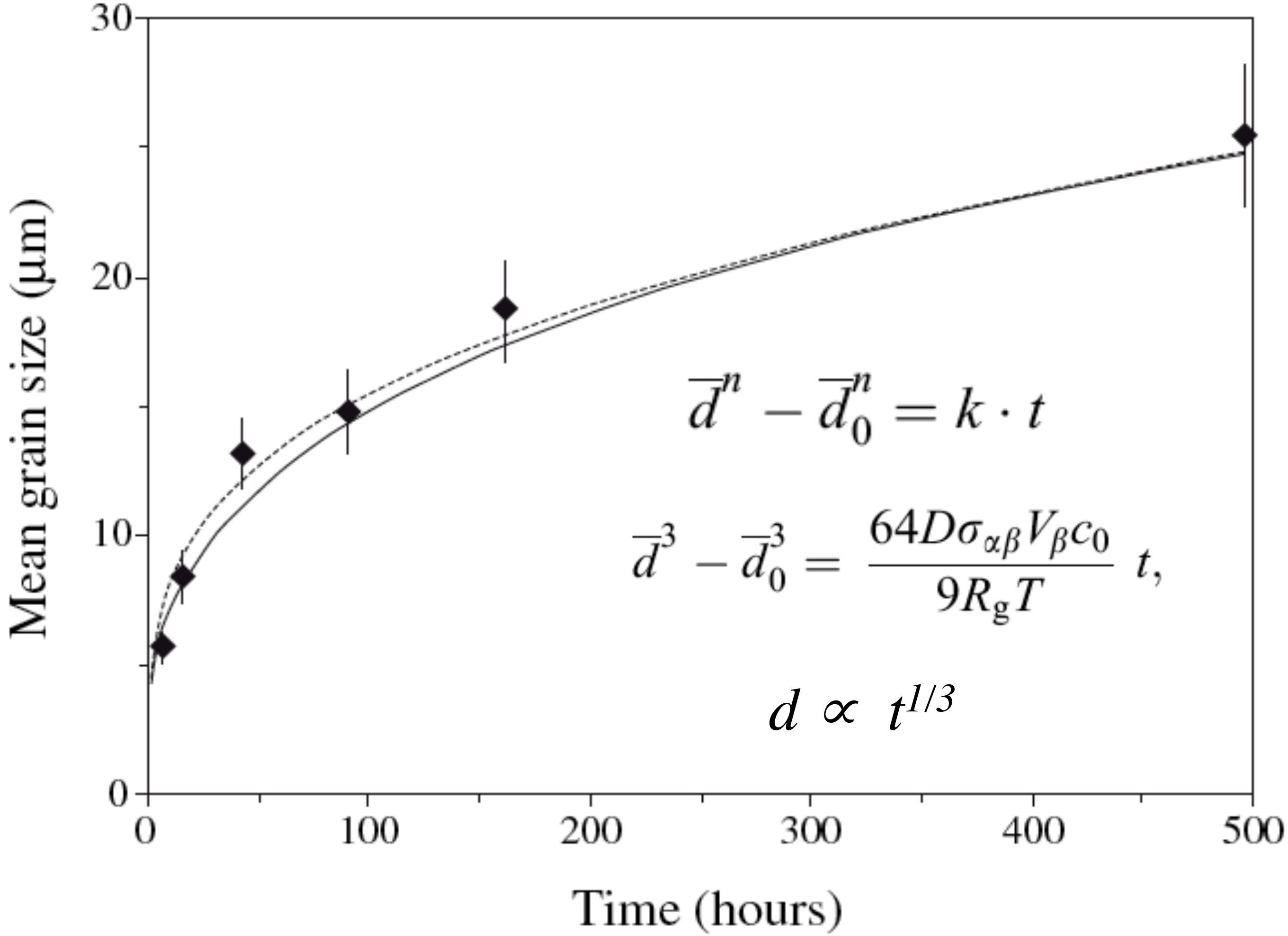

Cabanne et al. 2005; Faul & Scott, 2006

Ostwald ripening

$$\bar{d}^3 = 36.1\ t + 13.4$$

Duration (Years)	Mean grain size (μm)
	Olivine[a]
1	68 ± 10
10	147 ± 21
1,000	680 ± 100
10^5	3160 ± 460

Cabanne et al. 2005; Faul & Scott, 2006

Chondrule #3 Vigarano (POP)

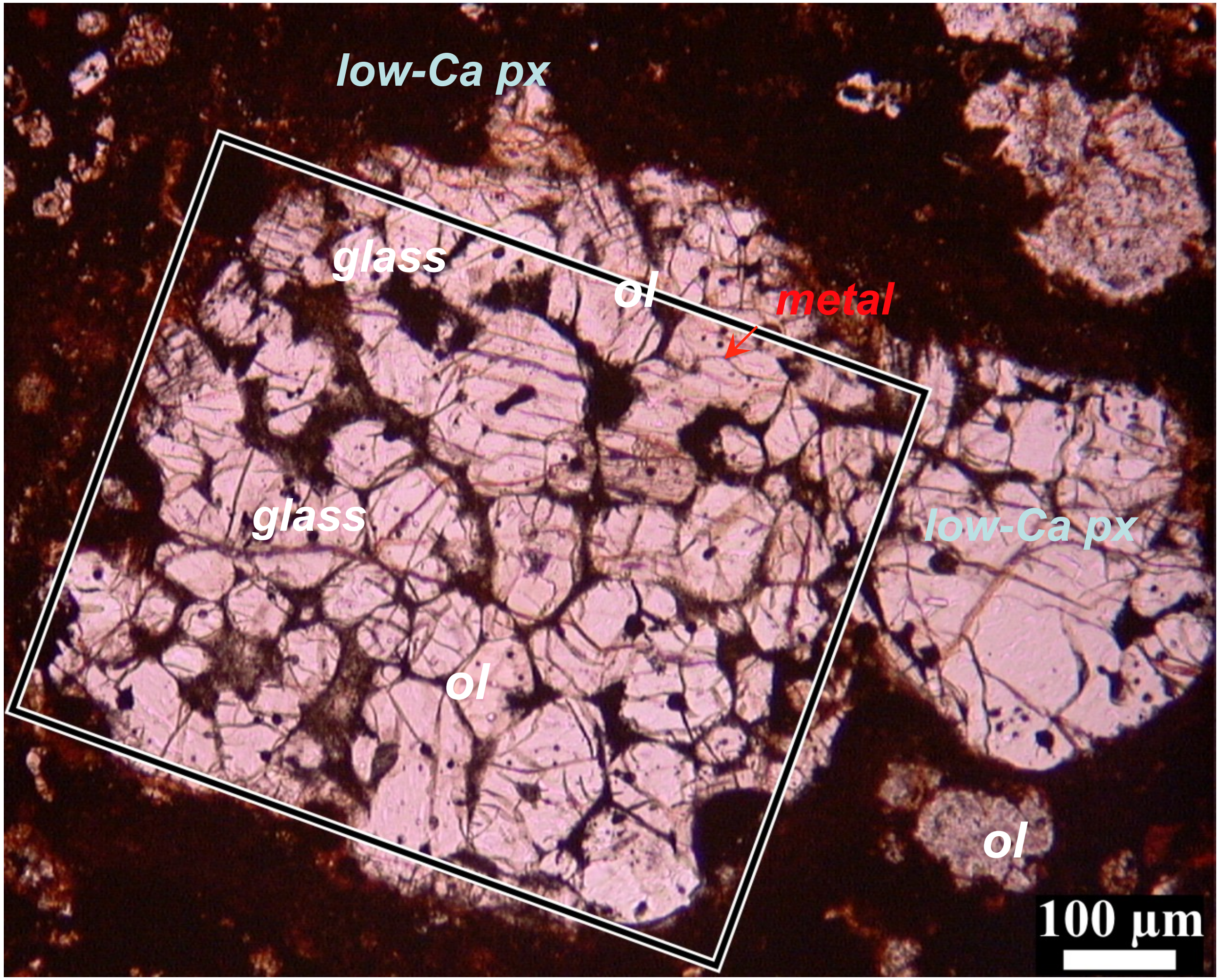

Transmitted light

Chondrule #3 Vigarano (POP)

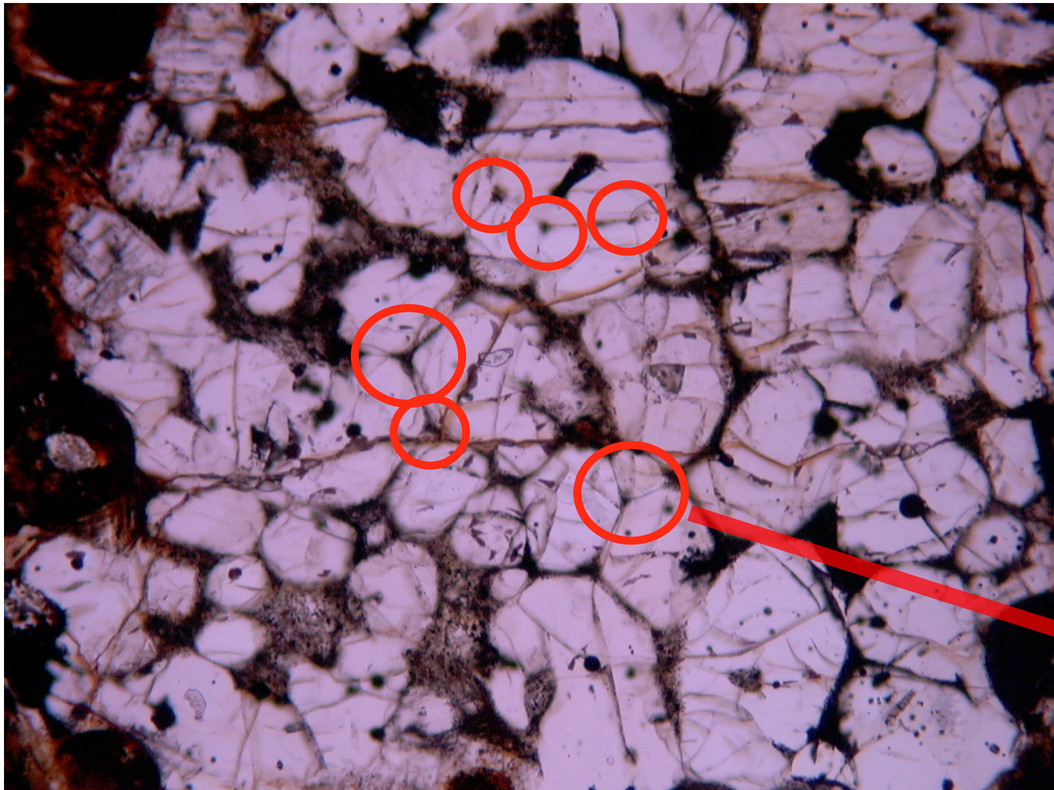

Olivines with triple junctions.

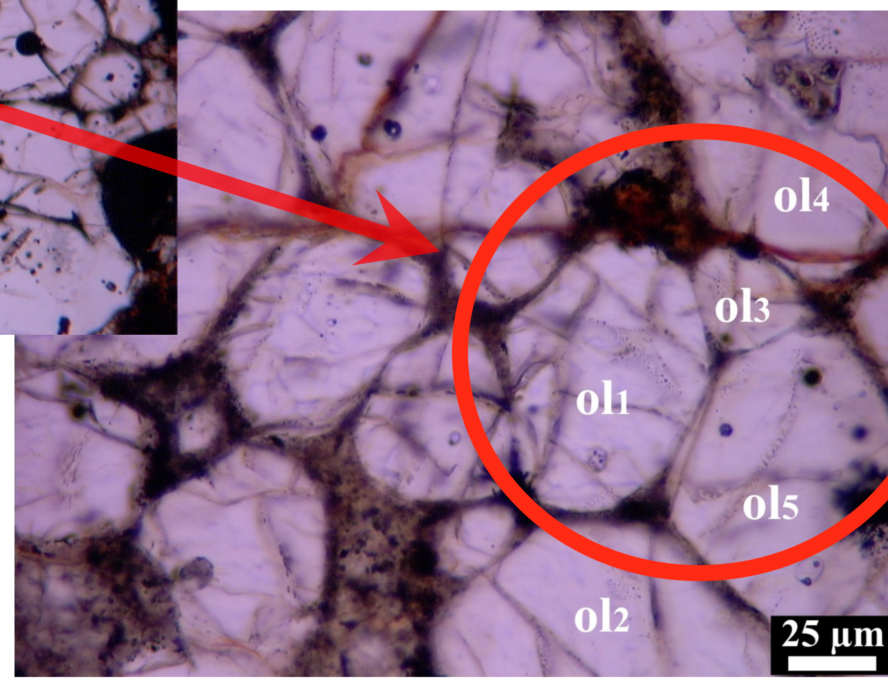

Olivine grains separated by glass have rounded outlines and embayments, indicating dissolution.

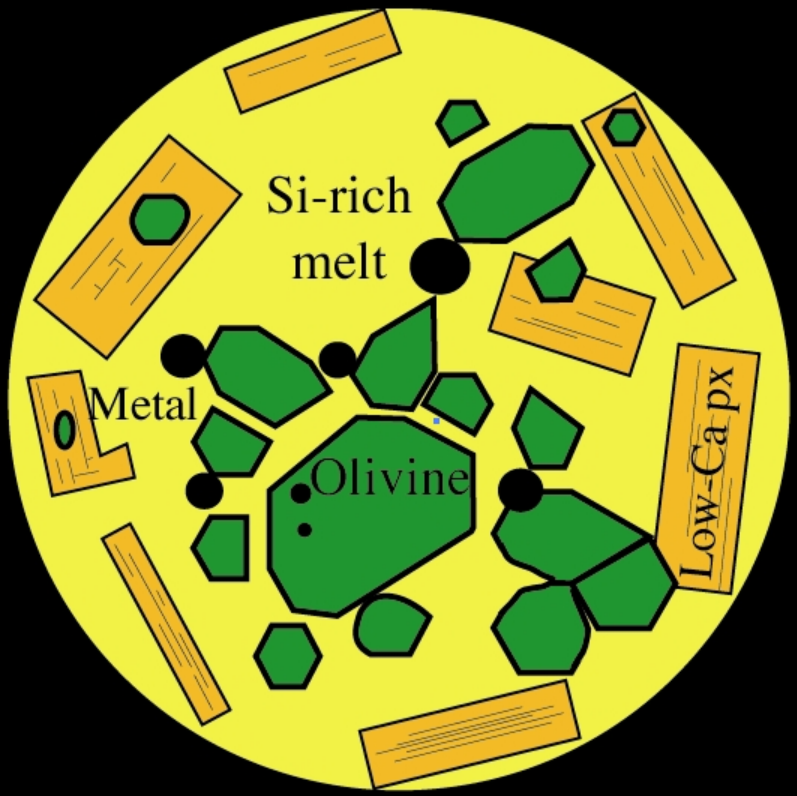

Si-rich
melt
Metal
Olivine
Low-Ca px

Magnesian chondrule formation

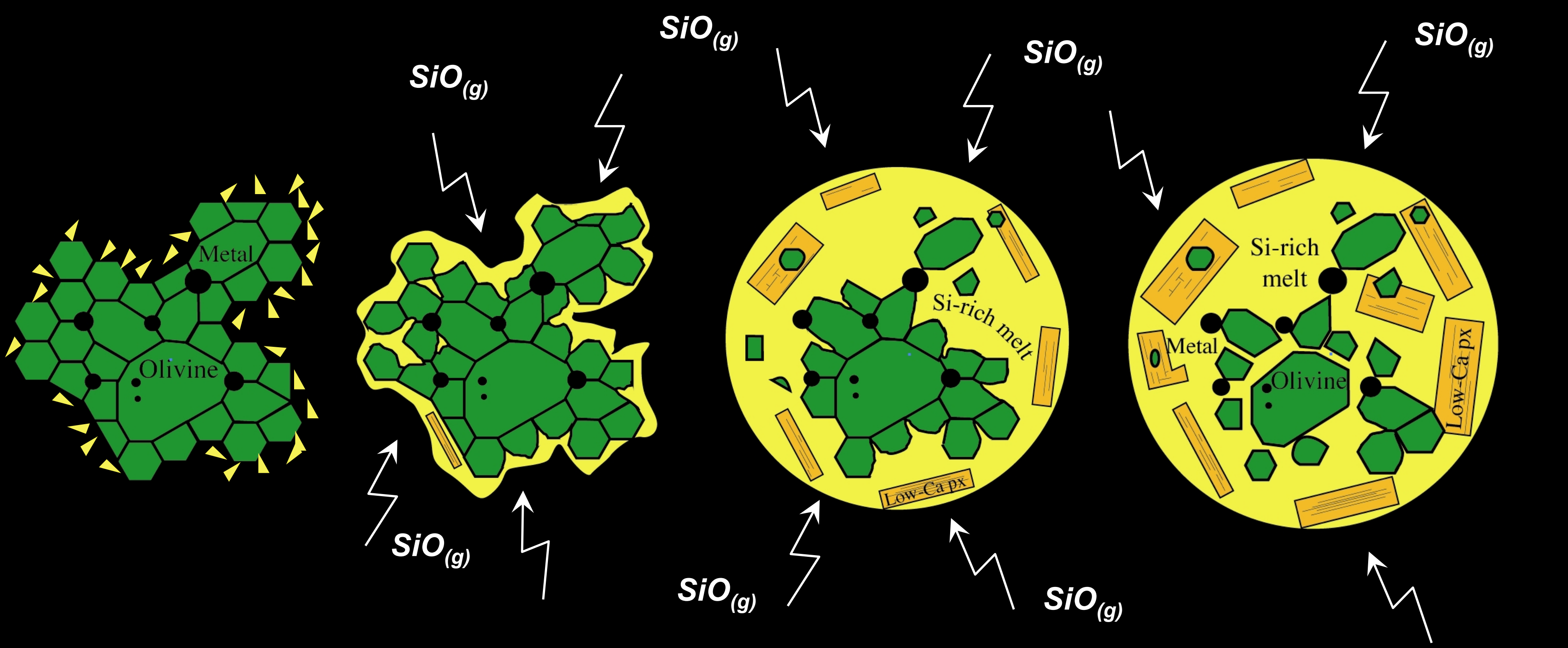

$$aSiO_{2(melt)} = XSiO_{2(melt)} \cdot \gamma SiO_{2(melt)} = PSiO_{(gas)} \cdot K[T] \cdot (fO_2)^{1/2}$$

$$Mg_2SiO_{4(olivine)} + SiO_{2(melt)} = Mg_2Si_2O_{6(low\text{-}Ca}$$

Terrestrial analogy

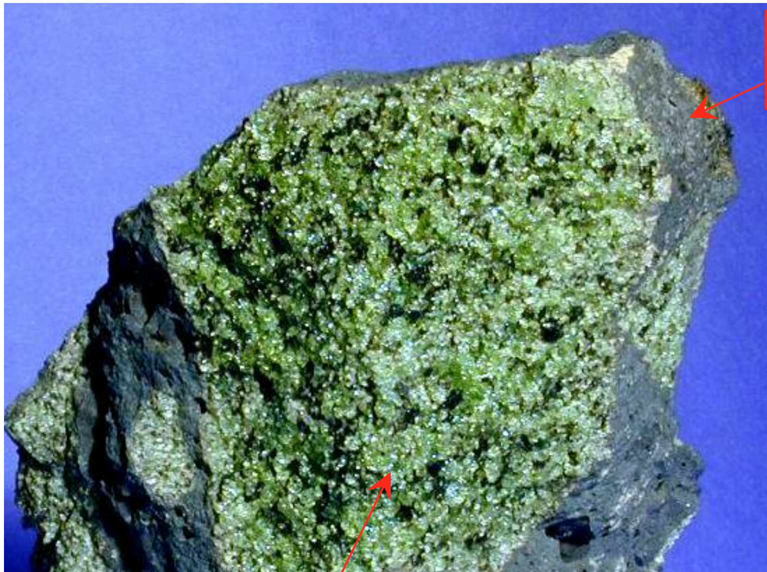

basalt = liquid

xenolith = mantle

Mg-rich olivines in chondrules:

- xenocrysts (isolated grains)
- xenoliths (fragment)

San Carlos, AZ/ USA

Two very different predictions for the distribution of Δ^{17}O values of Mg-rich olivines depending on their origin

Nebular origin

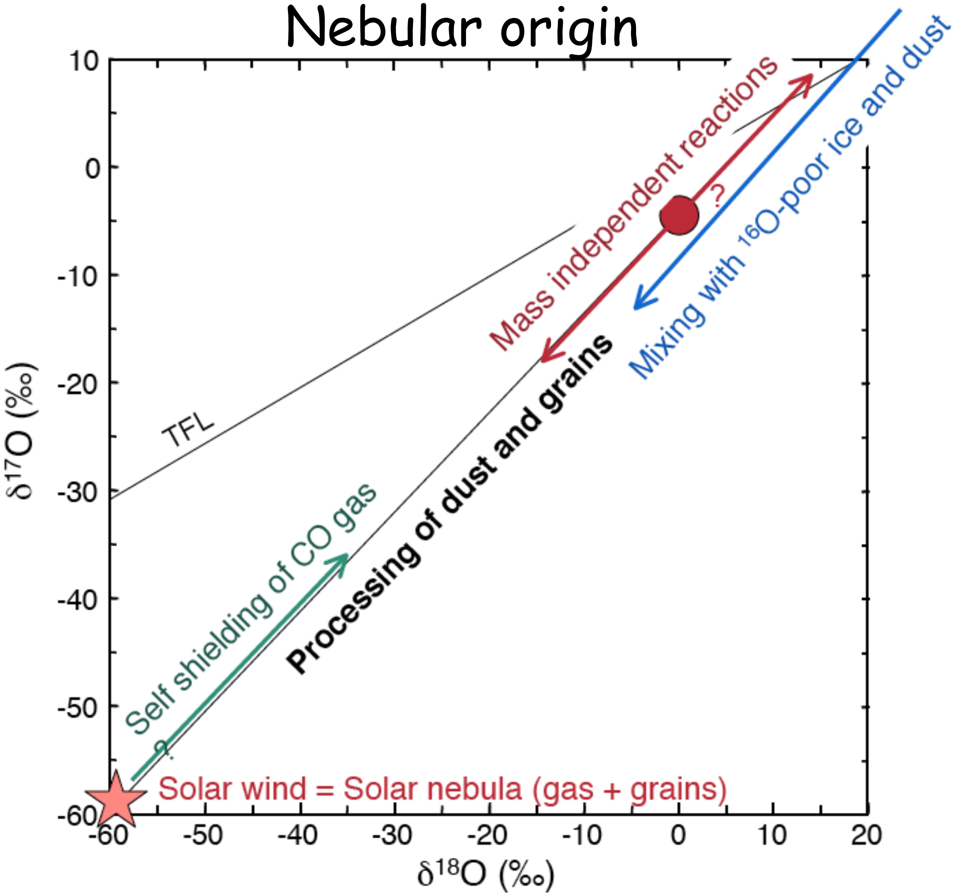

≈ Continuum of Δ^{17}O values

Planetary origin

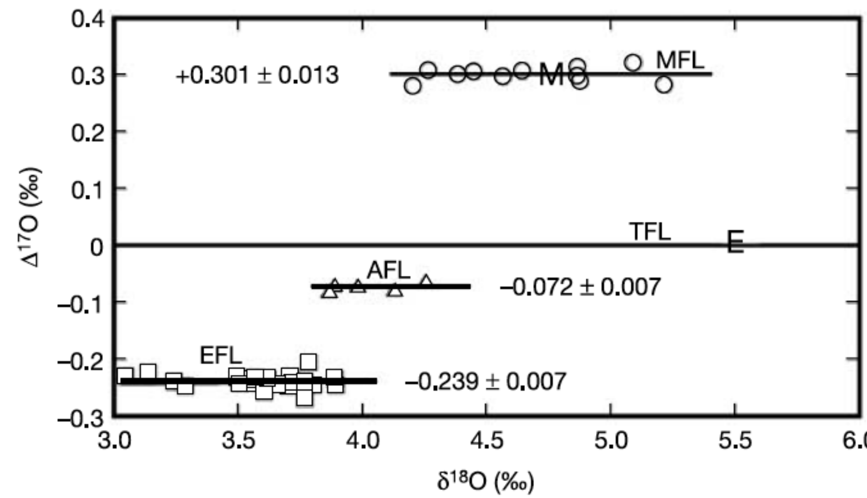

Greenwood et al., 2005

Several distinct Δ^{17}O values

Mg-rich olivines aggregates: Oxygen isotopic compositions

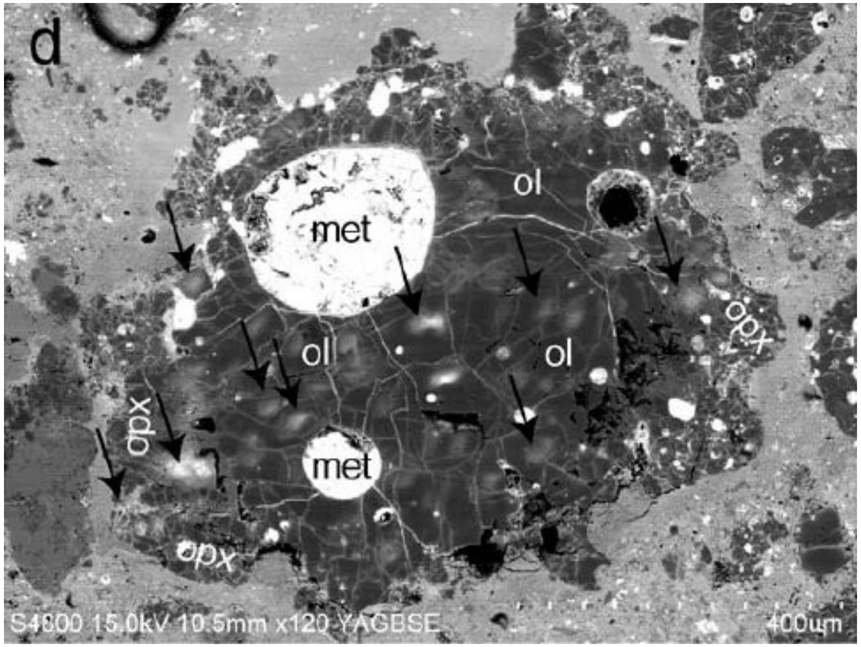

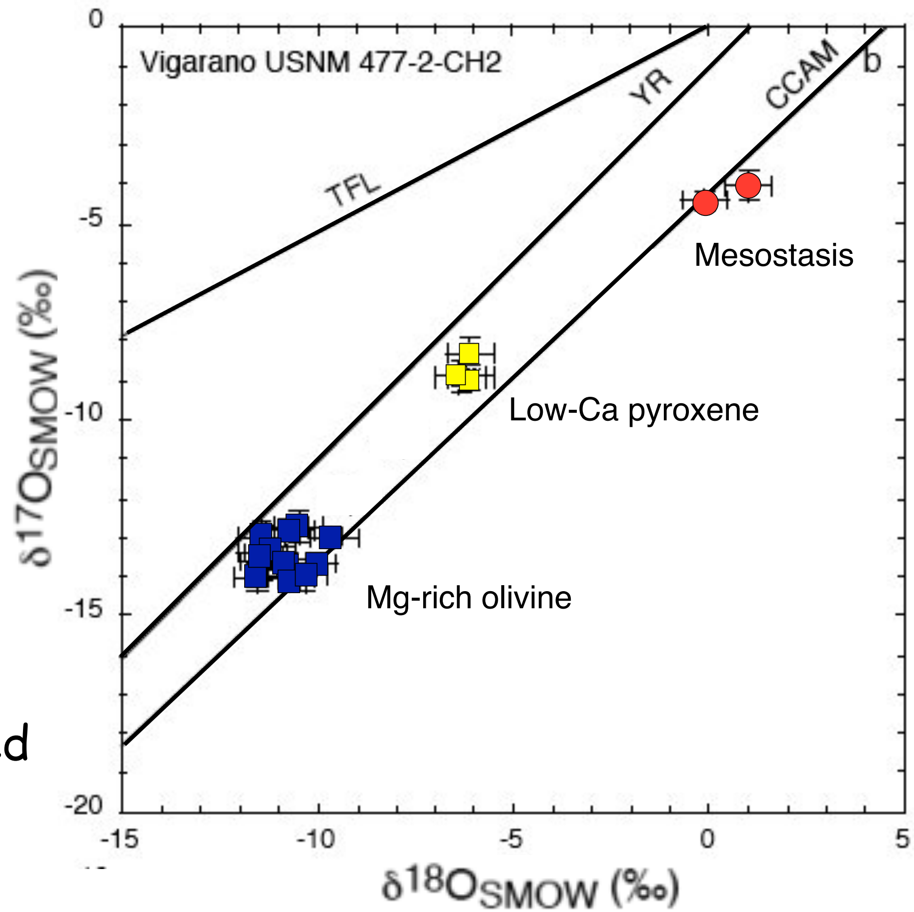

Mg-rich olivines within coarse-grained aggregates are in isotopic disequilibrium with pyroxene and mesostasis.

Chaussidon et al., 2008

Mg-rich olivines preserved their pristine oxygen isotopic composition even if they underwent partial dissolution (consistent with oxygen diffusion).

Mg-rich olivines in type I chondrules of Semarkona LL3.0

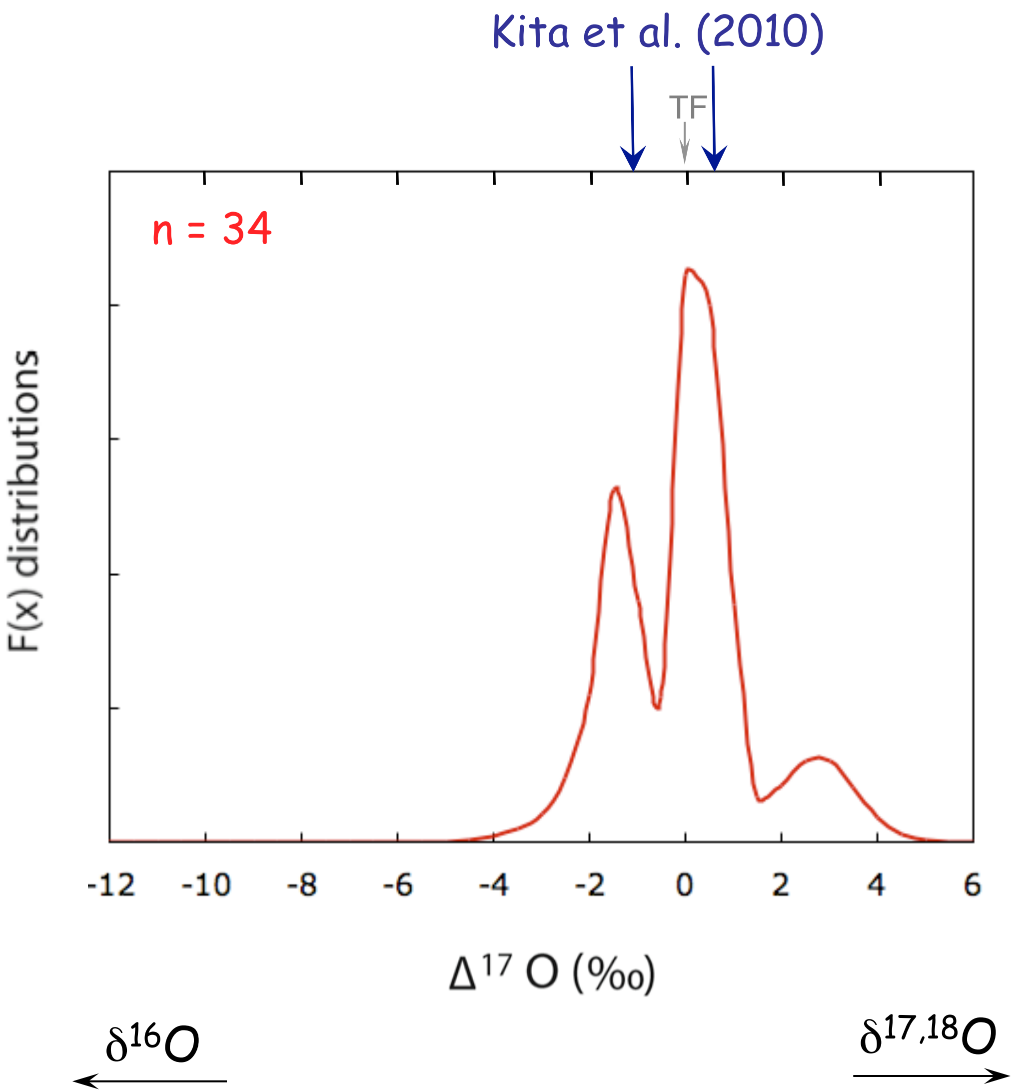

- No continuum of $\Delta^{17}O$ values
- 3 discrete $\Delta^{17}O$ (± 0.5‰) modes
- 2 modes are consistent with Kita et al. 2010.

Mg-rich olivines in type I chondrules

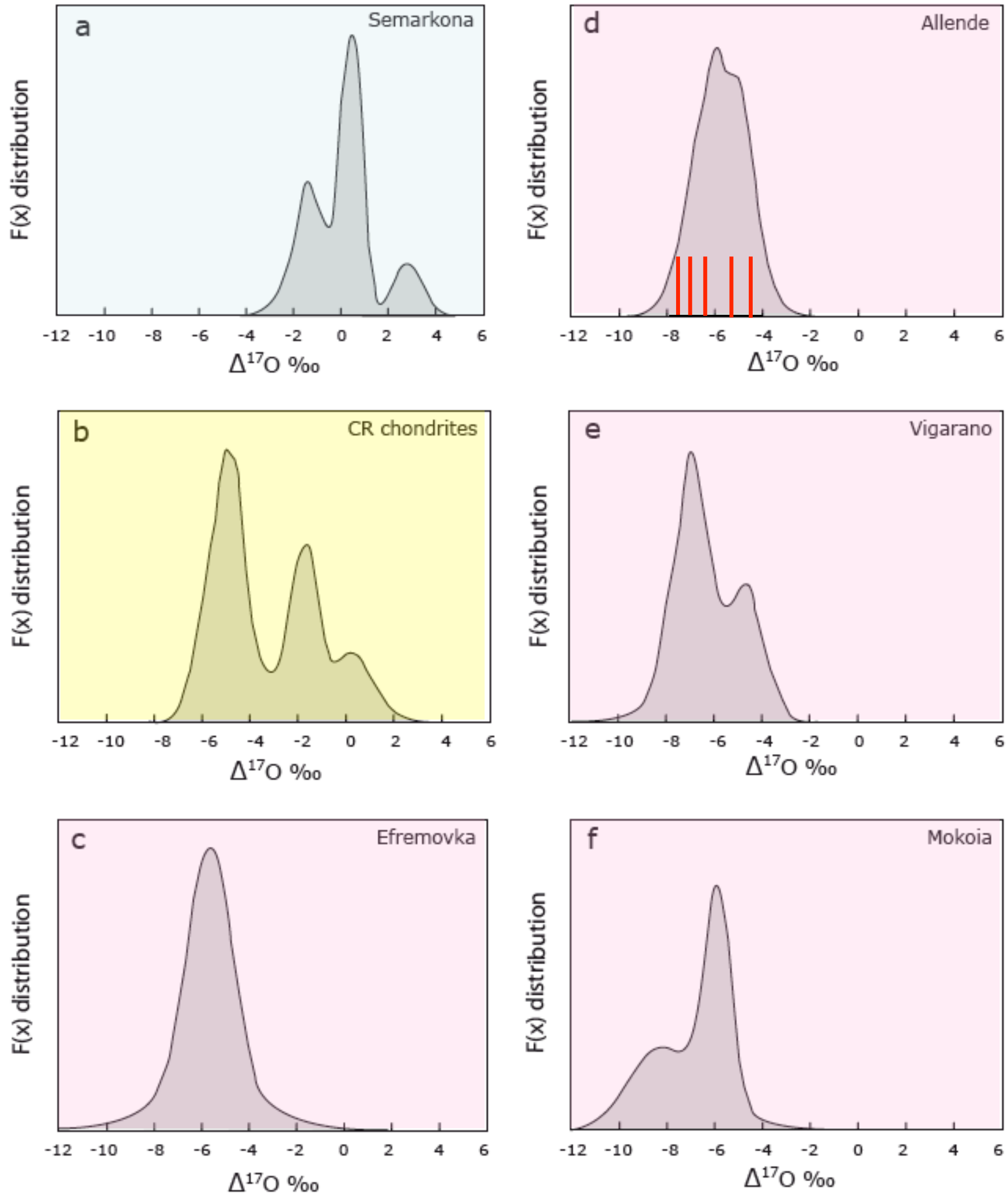

OC | CV

CR | CV

CV | CV

Chaussidon et al. MetSoc 2010

Mg-rich olivines in type I chondrules

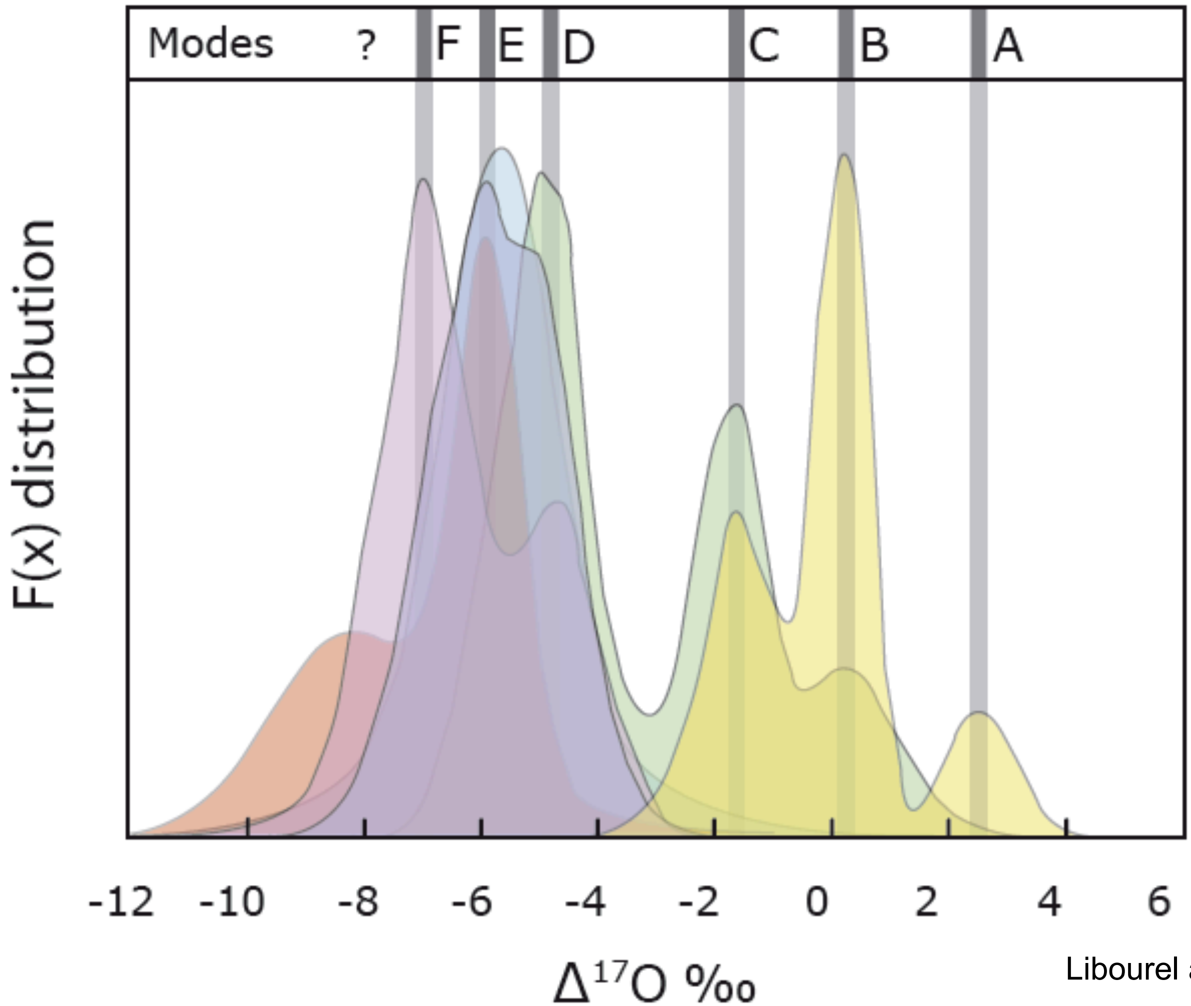

Libourel and Chaussidon, 2011

Mg-rich olivines originating from the disruption of the mantles of differentiated planetesimals

Mg-rich olivines in type I chondrules

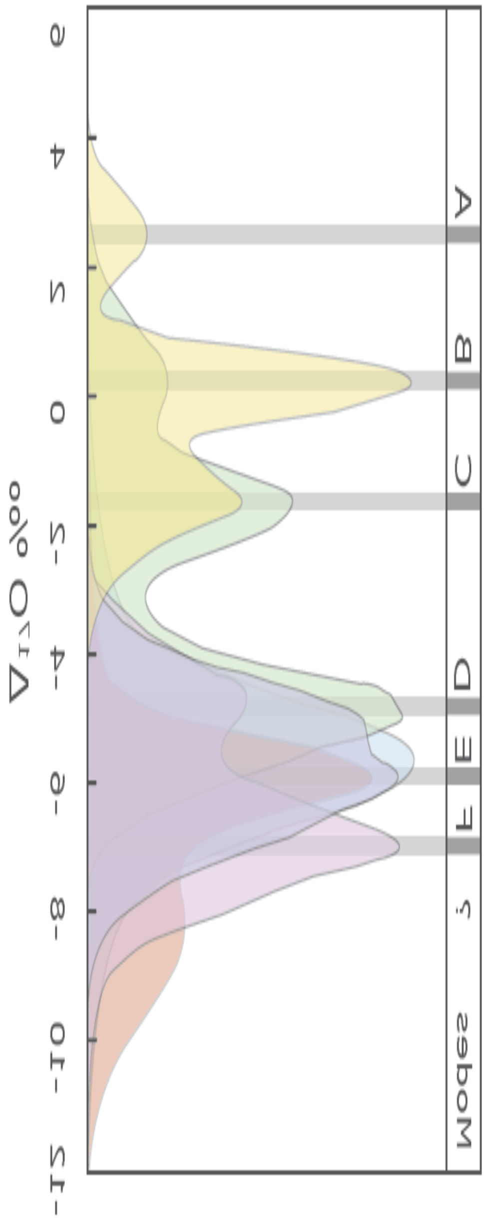

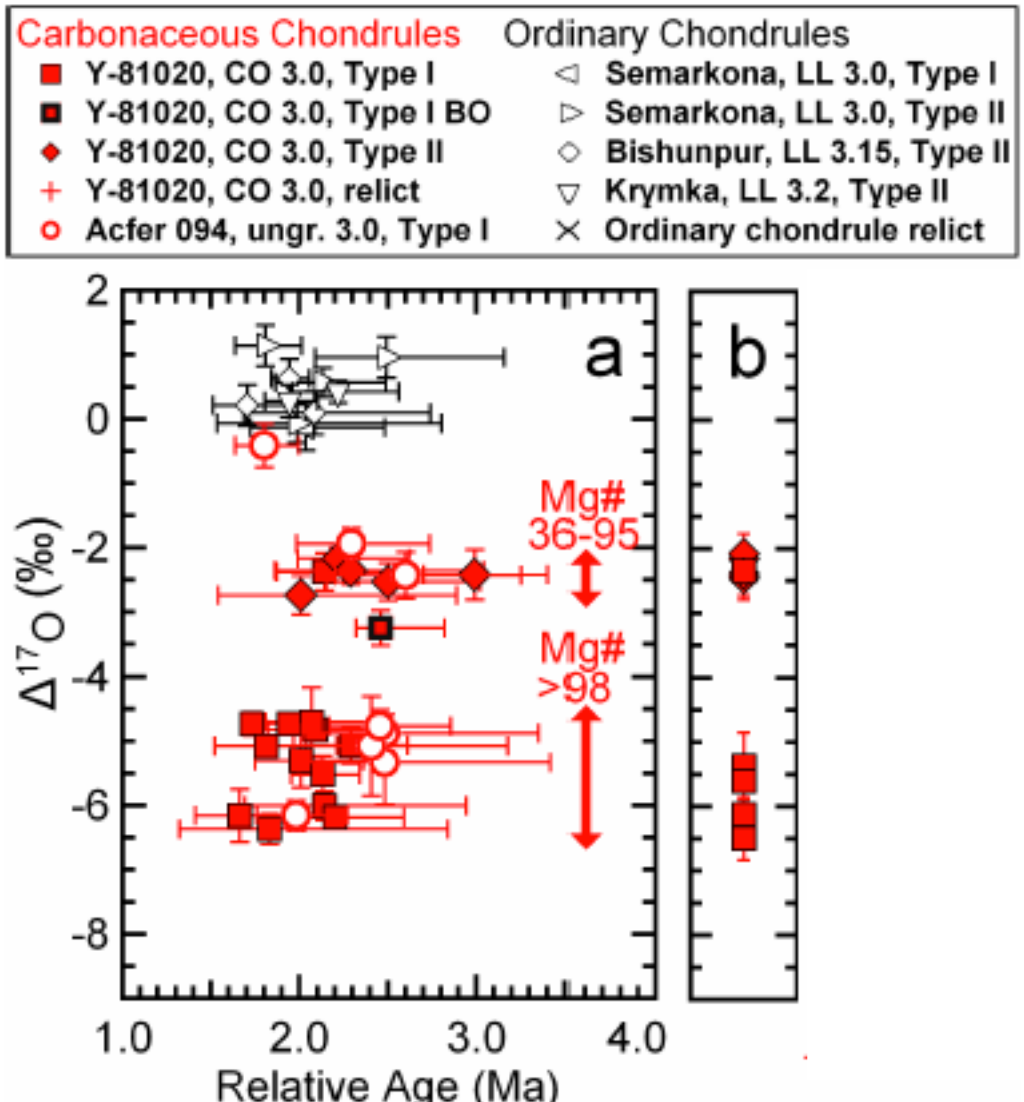

Fig. 3: a) $\Delta^{17}O$ versus the ^{26}Al age relative to CAI. Relative ages are from [2, 4, 5]. Chondrules from Y-81020 form 2

Plan

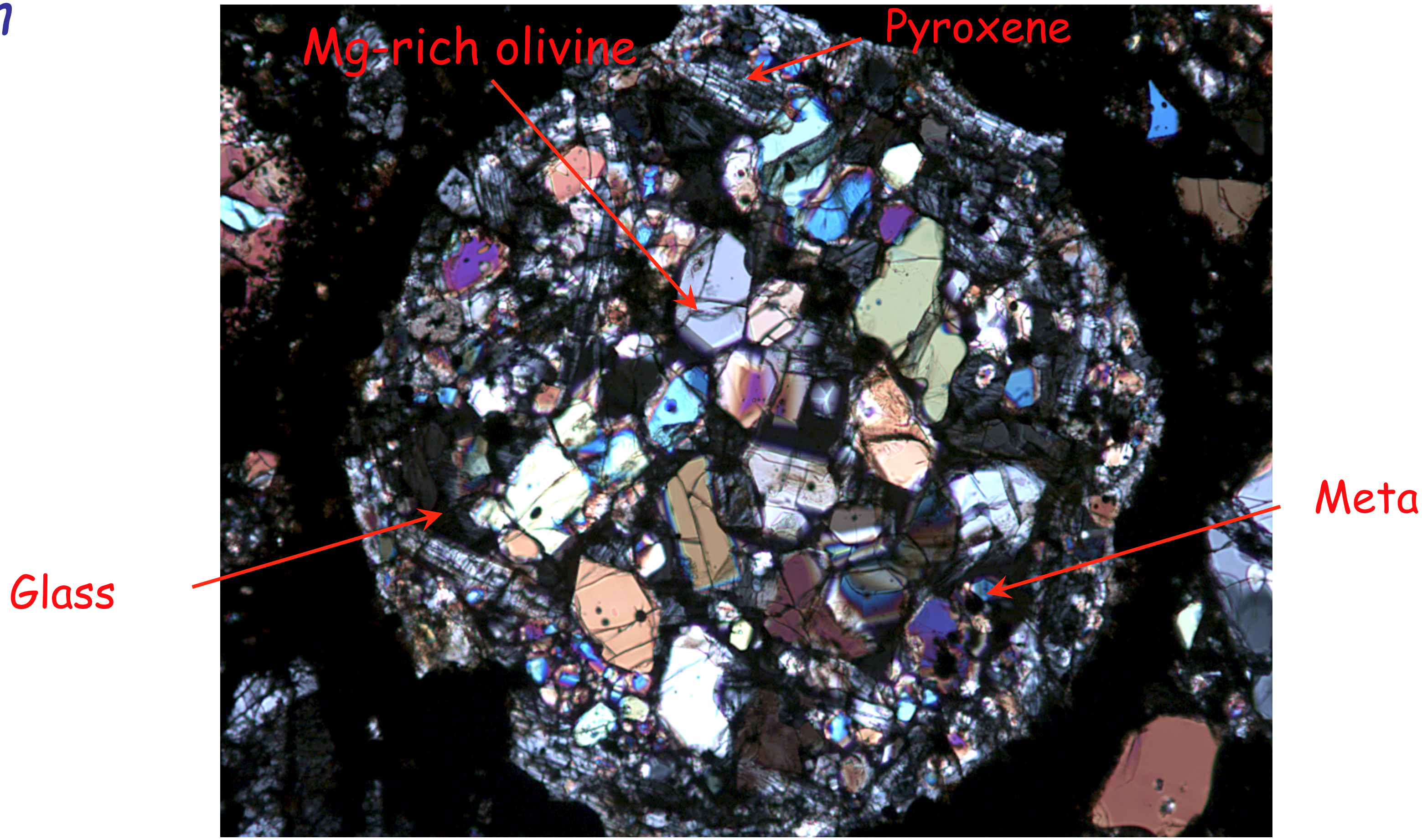

- *Evidence for interaction with gas phase*

- *Mg-rich olivines from differentiated planetesimals?*

- *Constraints on the formation of chondrules*

- Type I and type II chondrules seem contemporaneous from ^{26}Al chronology
- Type I and type II chondrules are both chondritic in bulk composition
- Type I-relict phases (forsterite, metal) are often occurring in type II chondrules

\+ Relict olivine abundance -

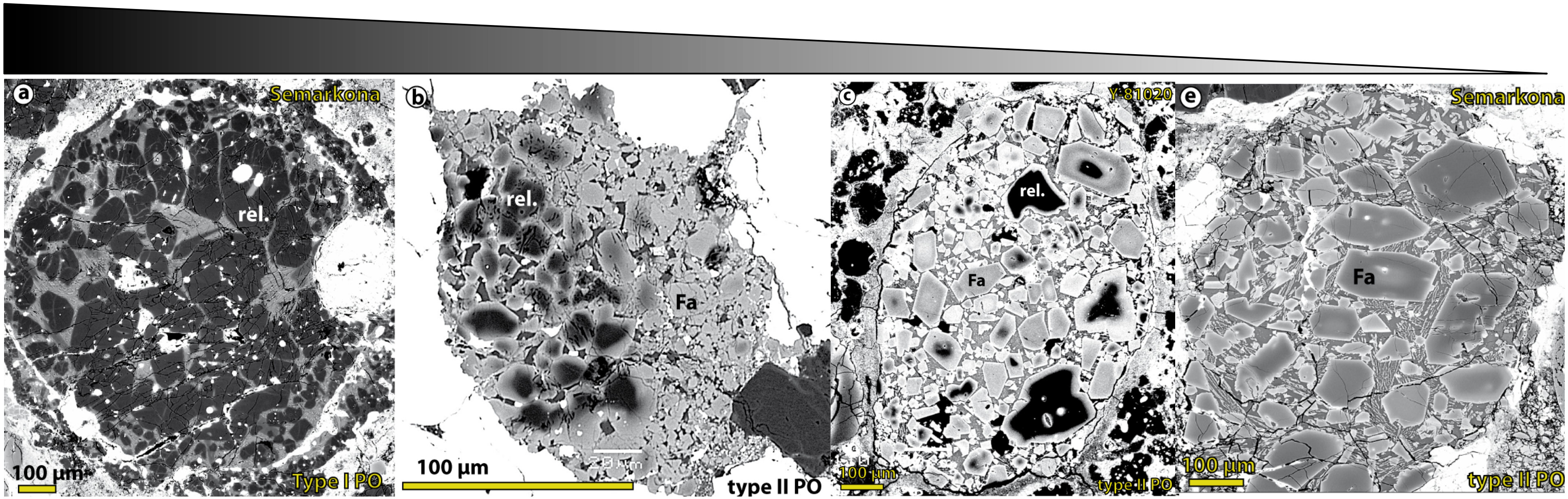

Type I ← Type II →

Can PO type I be transformed into type II by oxidation ?

(an alternative to classical dichotomy)

YES

(Villeneuve 2010)

Isothermal oxidation experiments

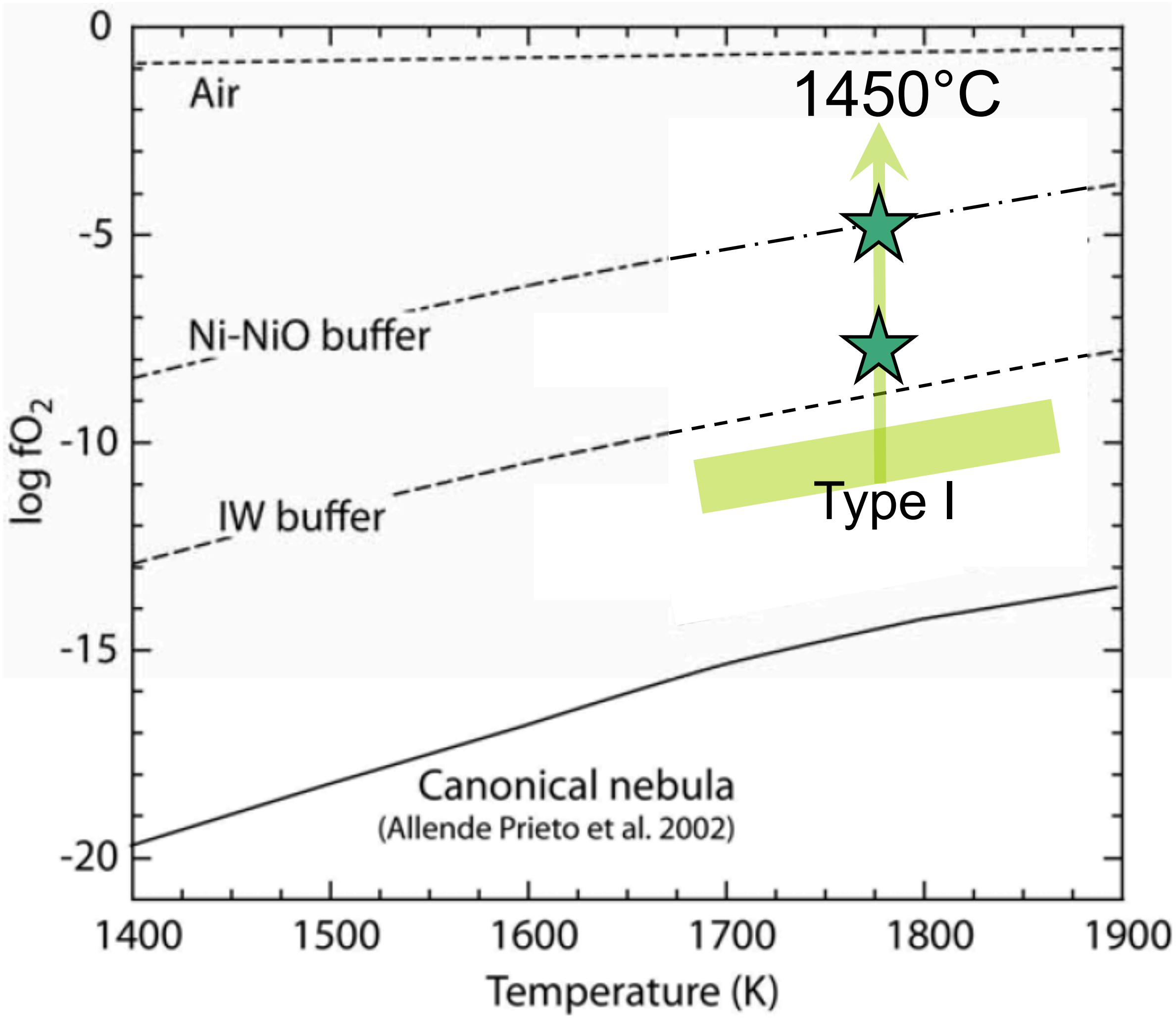

Type I proxy

Starting Composition: Forsterite + Ca, Al-rich glass + **0, 5, 10, 15, 20 wt% Fe metal**

Isothermal oxidation experiments

IW+1 (1450°C)

Start. Comp. 55 wt% Forsterite + 25 wt% Ca, Al-rich glass + **20 wt% Fe metal**

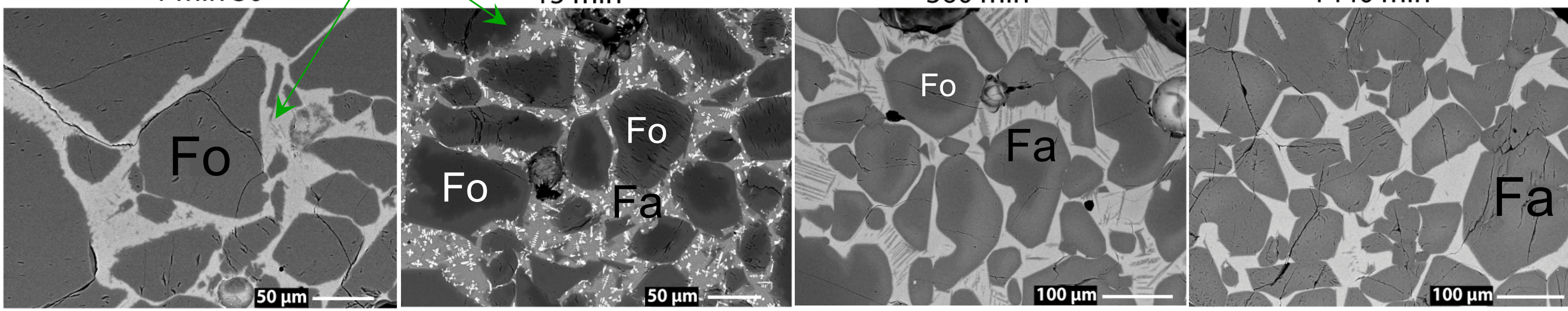

Type I | Type II + relics | Type II + relics | Type II

Olivine up to Fa_{40}

Relict olivine abundance

$$v = d\xi/dt = dFeO/dt = d(Fe, Mg)_2SiO_4/dt$$

$$\text{Fe (metal)} + \tfrac{1}{2}\,O_2 \longrightarrow \text{FeO (liq)}$$

$$\text{FeO (liq)} + \text{MgO (liq)} + SiO_2\ \text{(liq)} \longrightarrow (Fe, Mg)_2SiO_4\ \text{(olivine)}$$

Fe-rich olivine

Chemical evolution of olivines

1450°C, IW +1, 24 hours

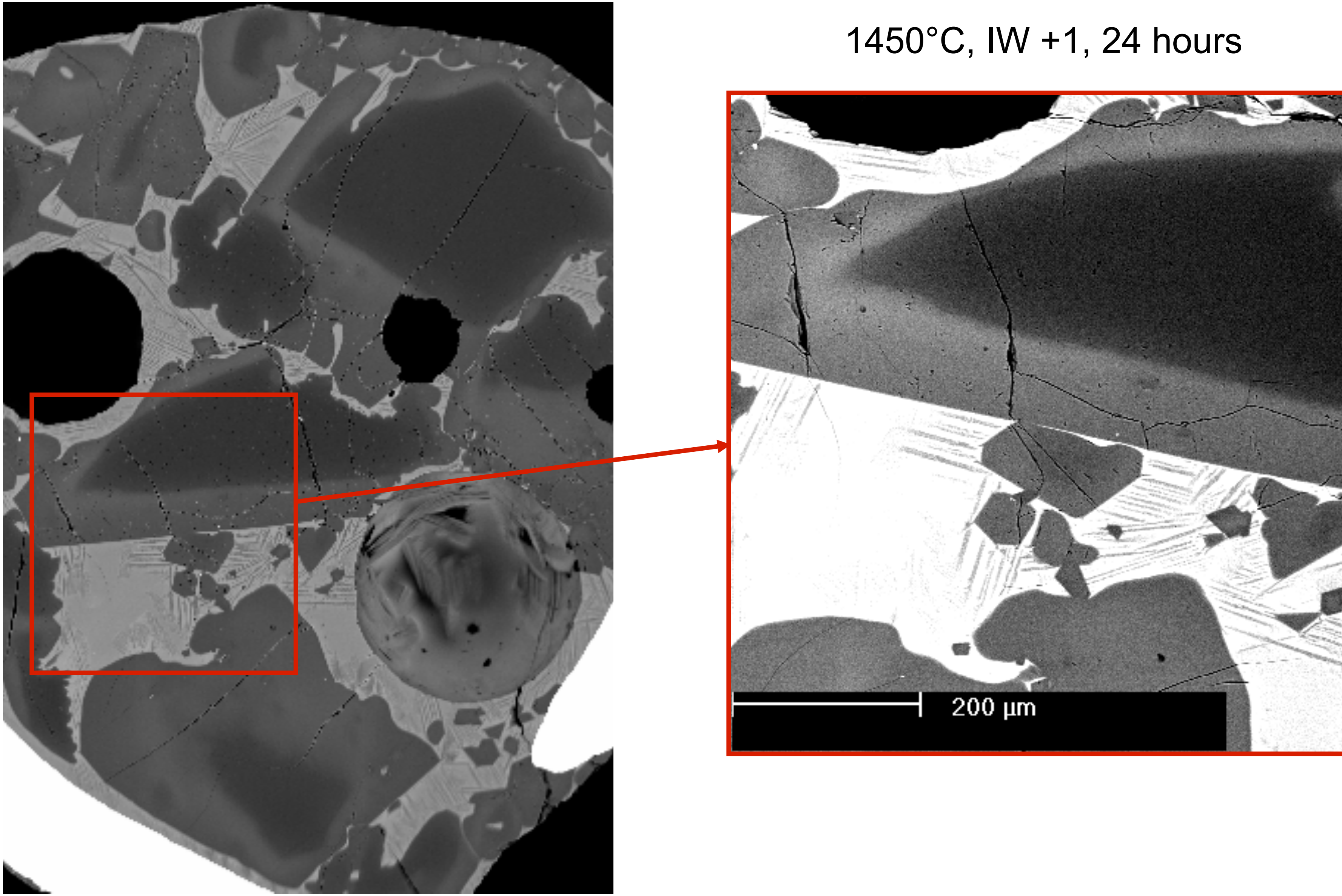

Chemical evolution of olivines

1450°C, IW +1, 24 hours

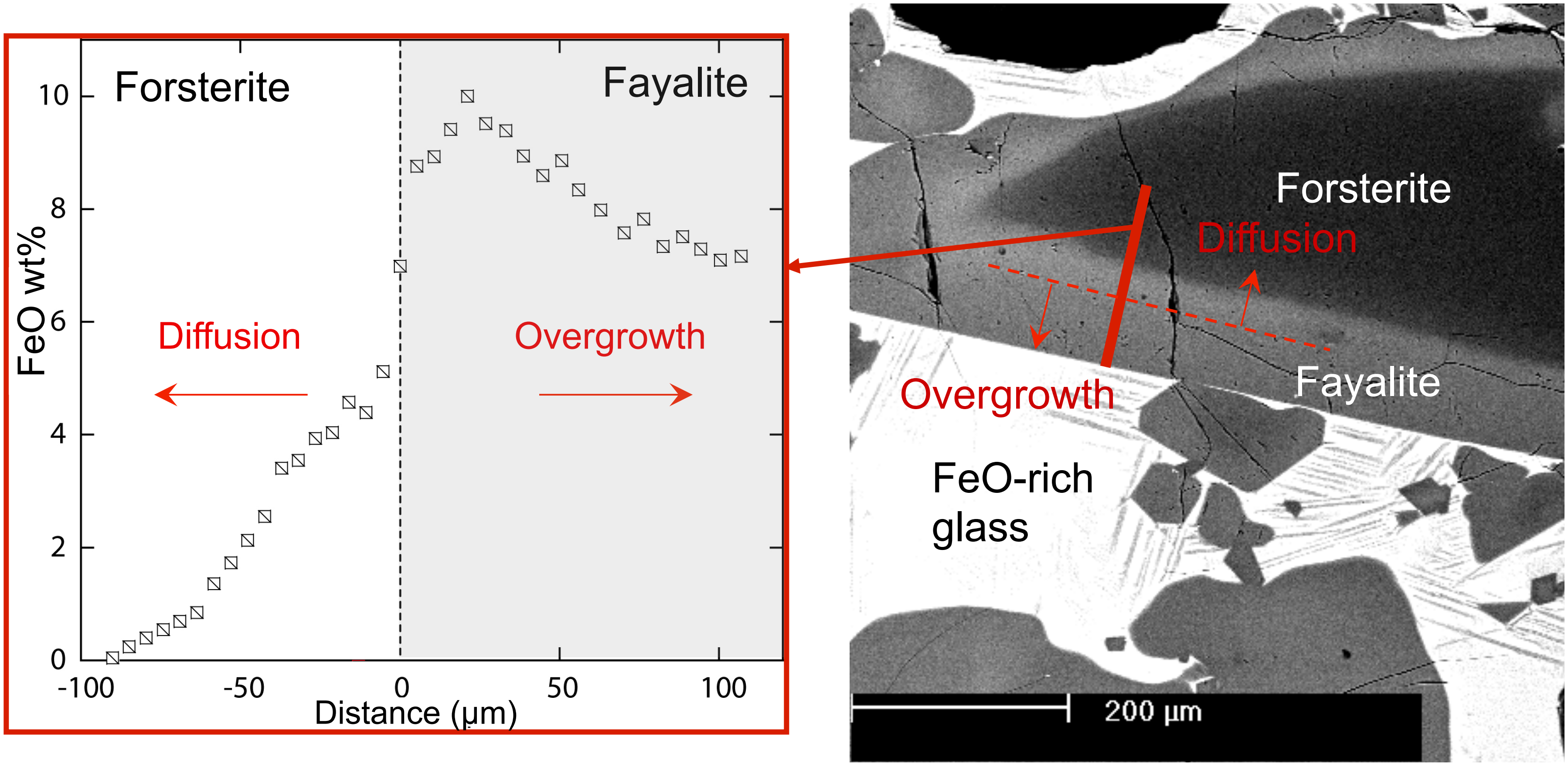

Driving force for overgrowth and diffusion = **ΔC** (and <u>not</u> ΔT)

Chemical evolution of olivines

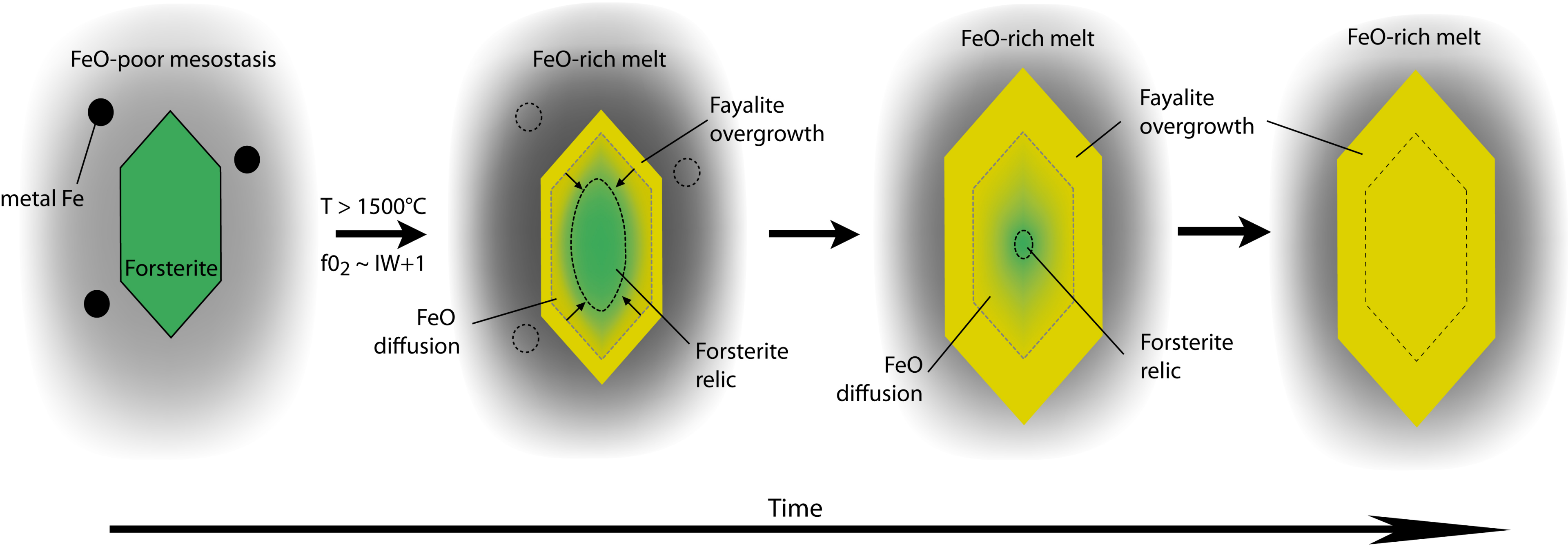

Fe-rich olivine crystallization

$$Fe\ (metal) + \tfrac{1}{2} O_2 \longrightarrow FeO\ (liq)$$

$$FeO\ (liq) + MgO\ (liq) + SiO_2\ (liq) \longrightarrow (Fe, Mg)_2SiO_4\ (olivine)$$

Semarkona Type II PO chondrule

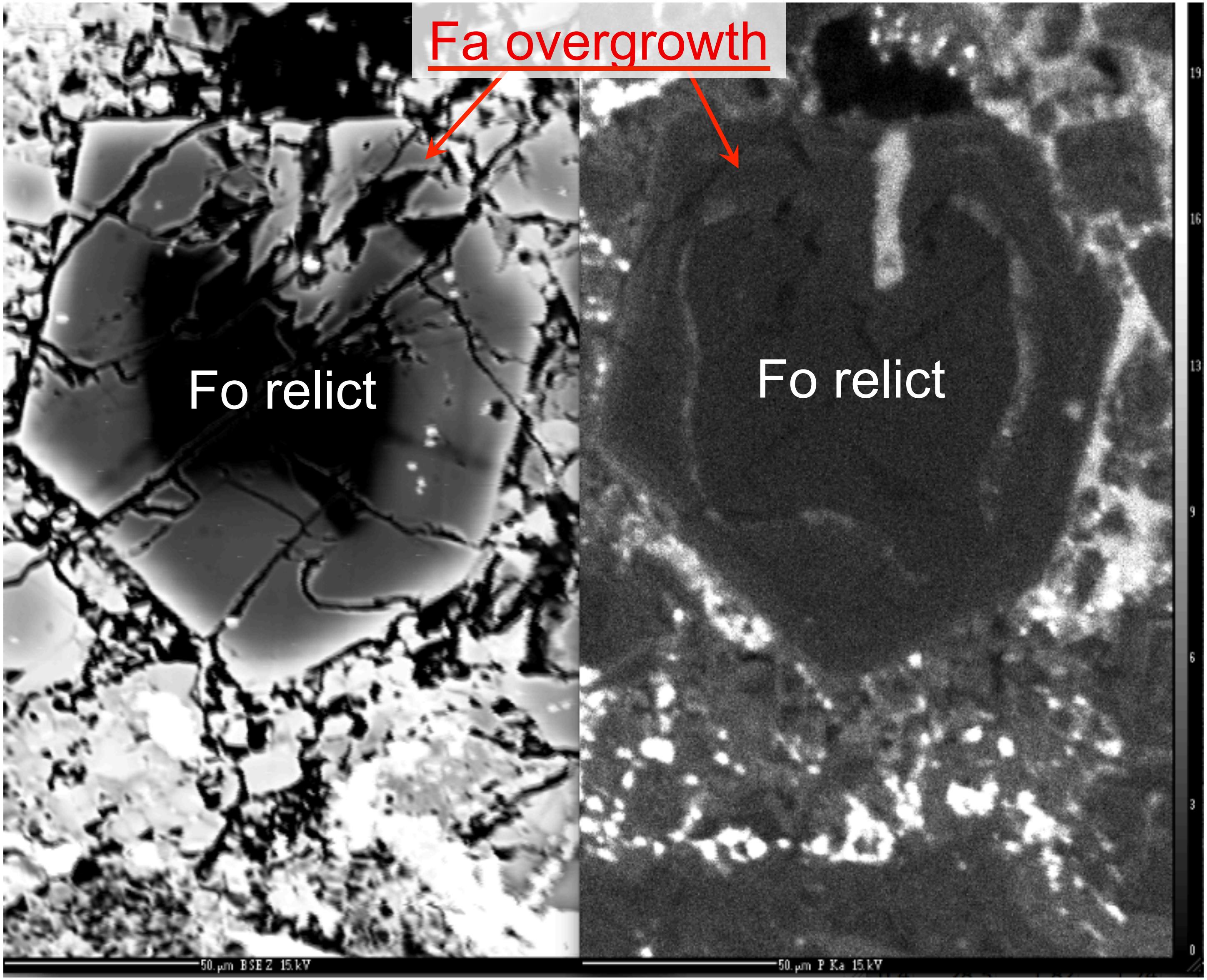

BSE　　　　Phosphorus Xray map

Semarkona Type II PO chondrule

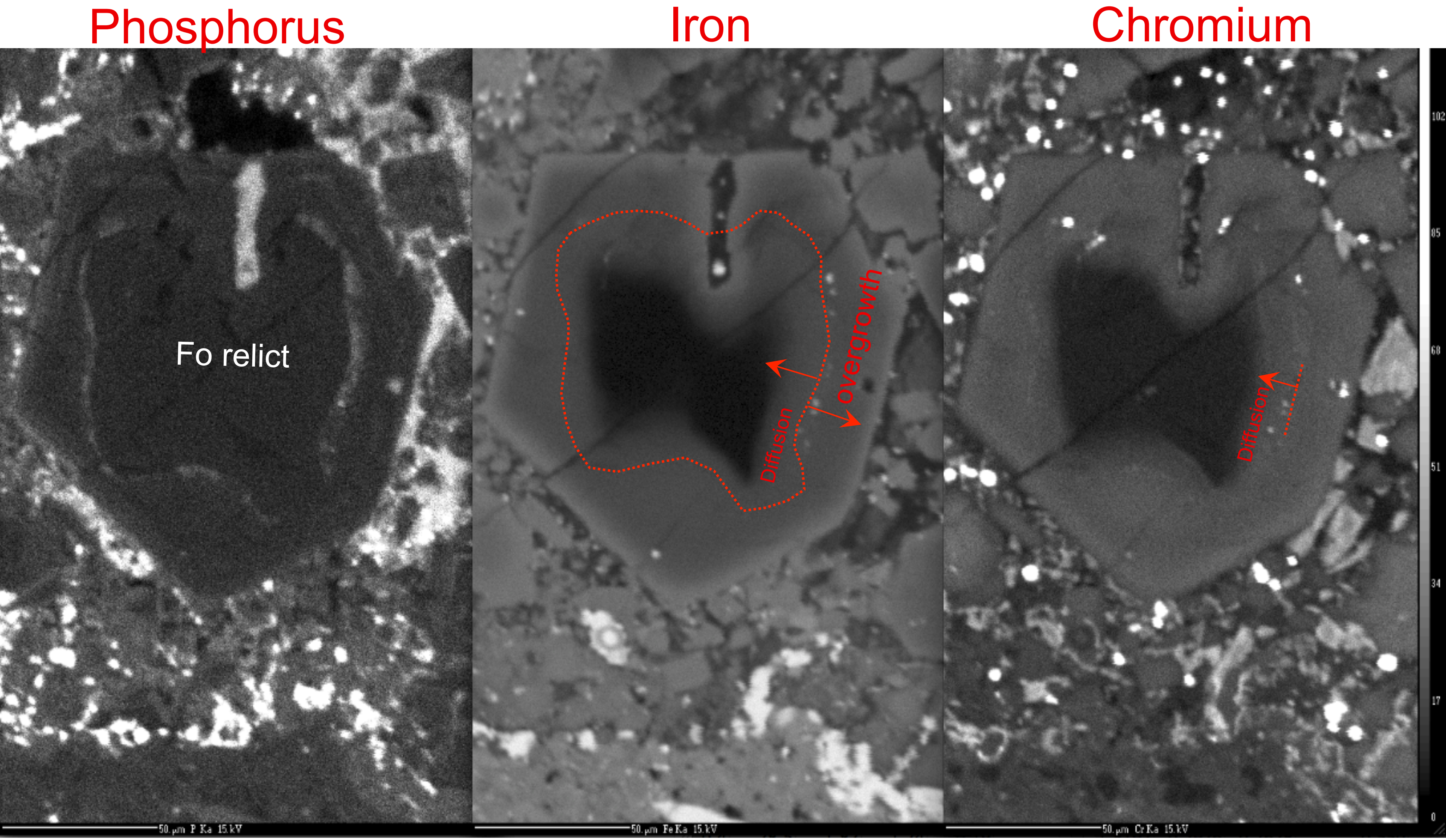

- Enrichment of Fe, Ni, Co, Cr, P siderophile elements
- Oxidation and dissolution of Fe, Ni metal blebs in mesostasis

Application to the thermal history of chondrules

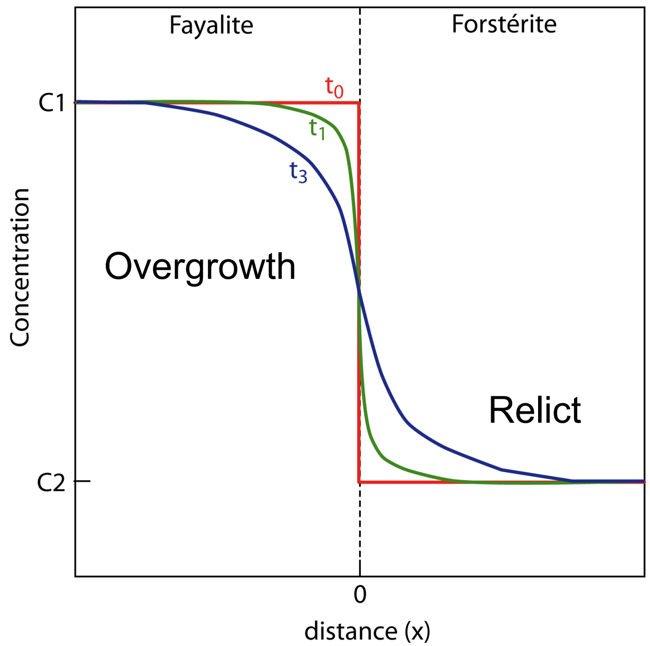

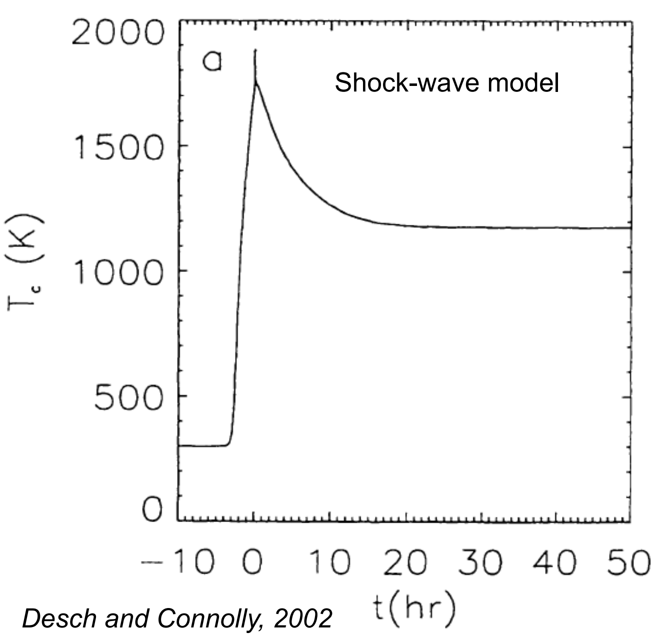

Desch and Connolly, 2002

- ΔT is the driving force for Fe-rich olivine crystallization (and relict olivine resorption).
- As a consequence, diffusion profiles provide information on chondrule thermal history.

$$D(T(t)) = D_0 \times \exp\left(\frac{-E}{RT(t)}\right)$$

<u>Cooling laws (S = cooling rate)</u>

- Linear :
  $T(t) = T_0 - St$ *(Lasaga, 1983)*
- Asymptotic :
  $1/T(t) = 1/T_0 + \eta t$ with $S = \eta T^2$ *(Ganguly et al., 1994)*
- Exponential :
  $T(t) = T_0 \times e^{-\alpha t}$ with $S = \alpha T$

Driving force for diffusion = Δ**C** (and not ΔT)

Caution on the use of diffusion profile to obtain cooling rate of chondrules !!

Application to the thermal history of chondrules

Semarkona 13-66A

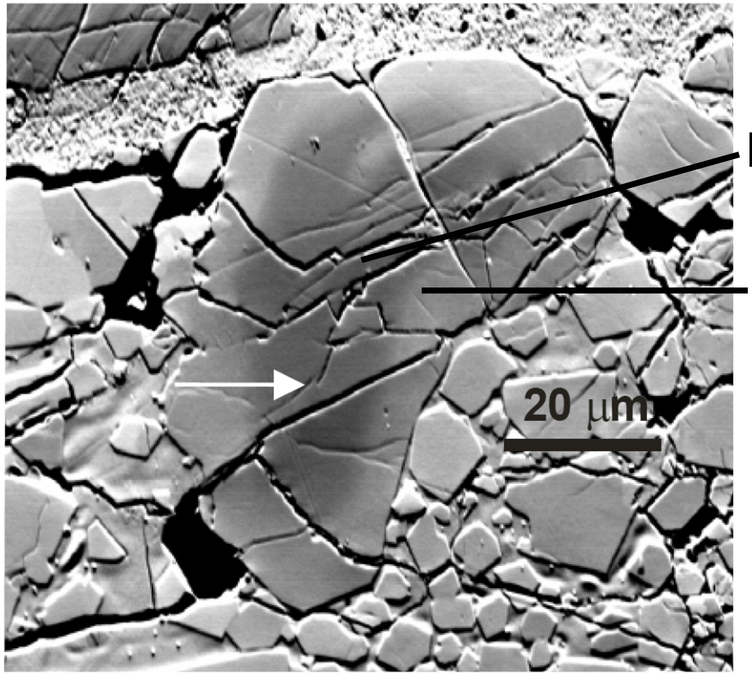

Hewins et al., 2010

- ΔT
- ΔC

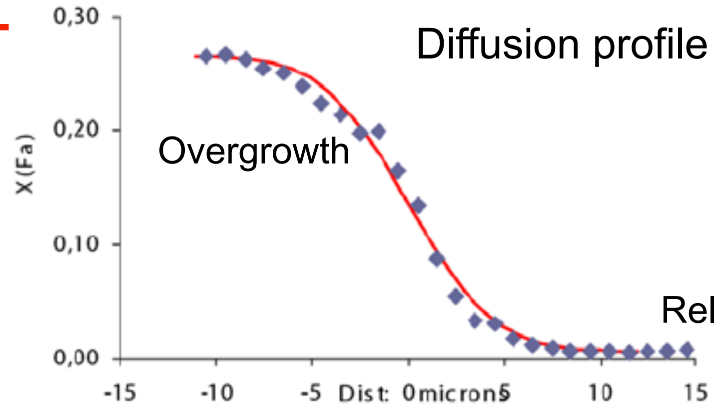

1634°C

S= 400 K/h, t≈ 1080

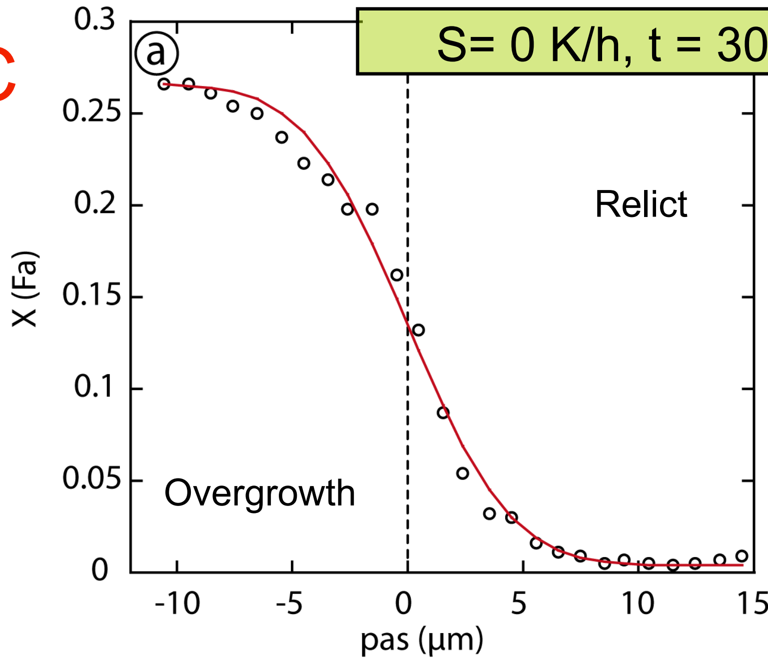

(D_0, E) *Dohmen and Chakraborty (2007)*

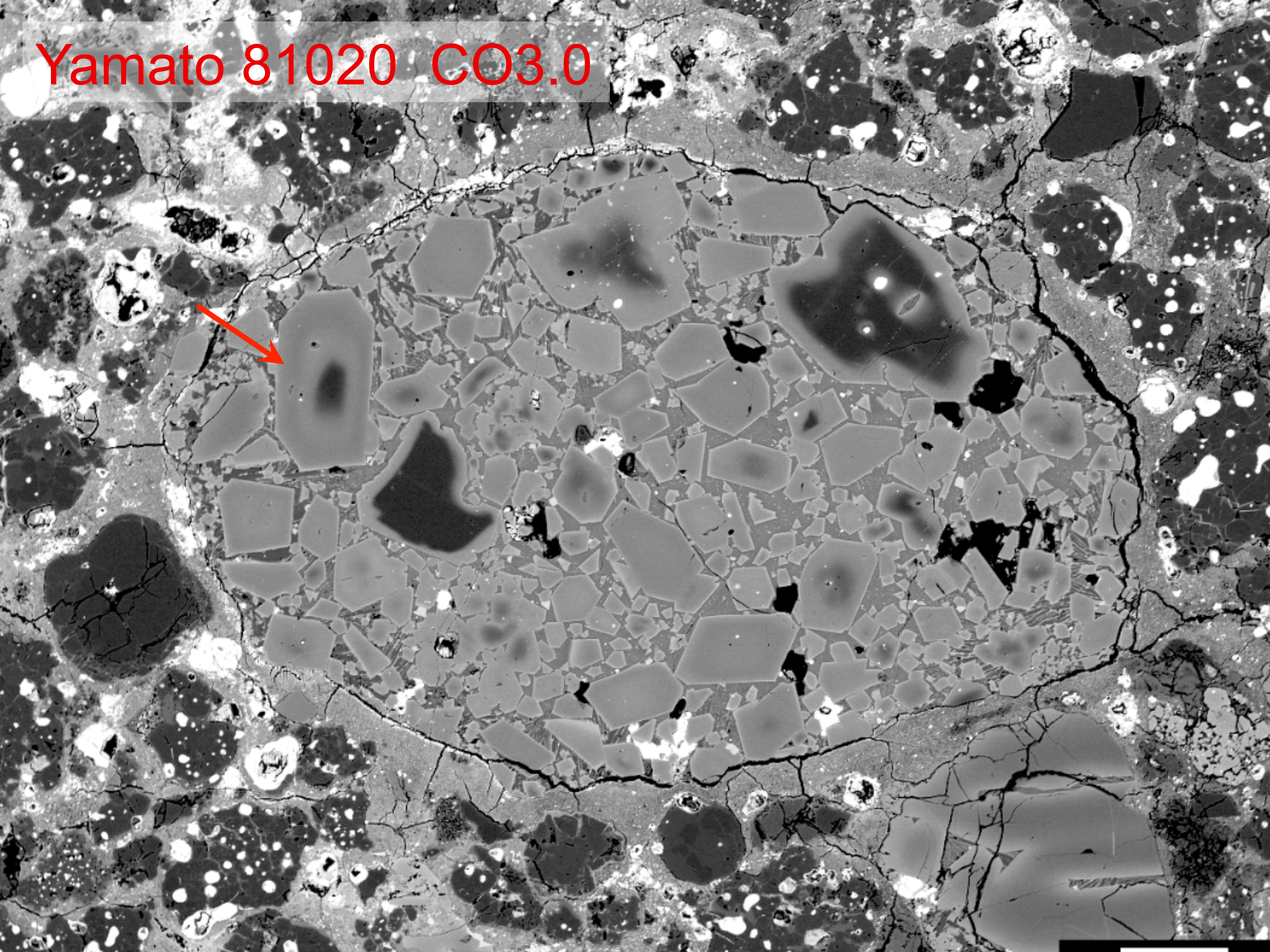
Yamato 81020 CO3.0

BSE map

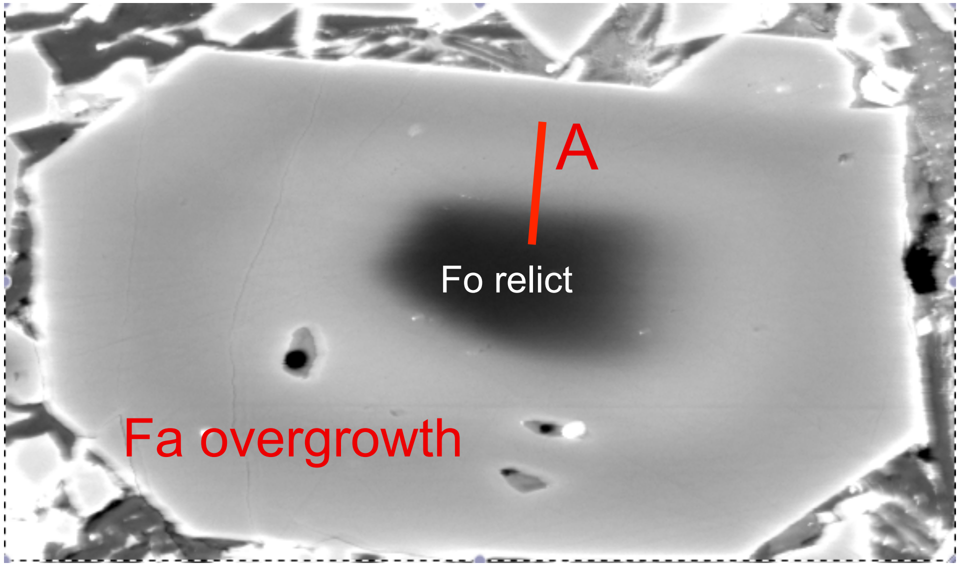

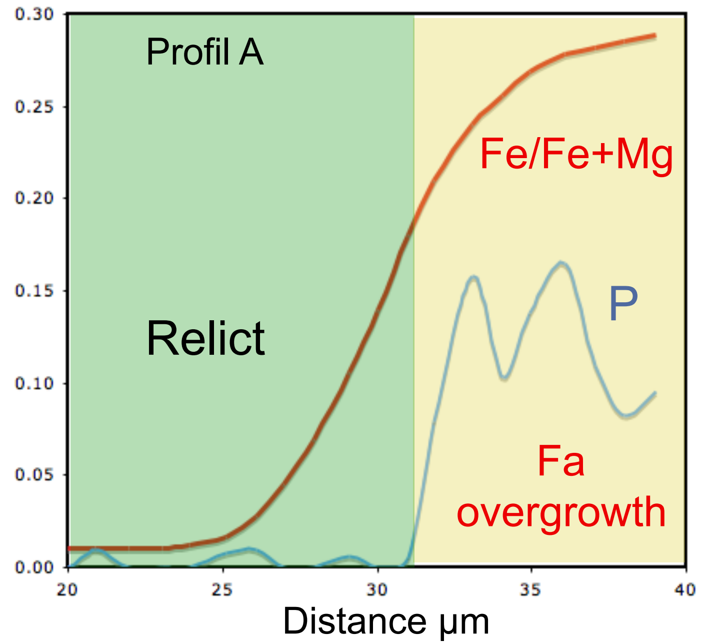

Yamato 81020 CO3.0

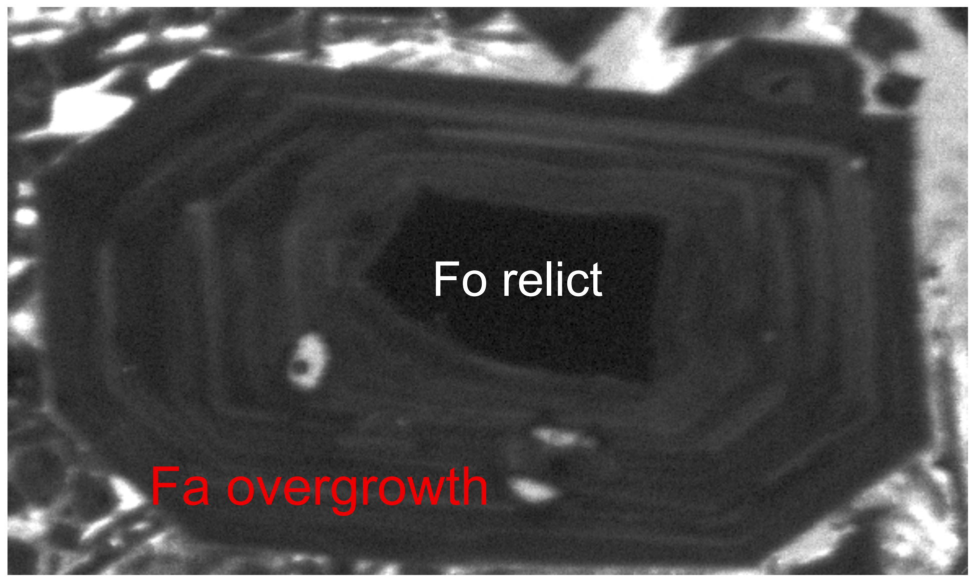

Phosphorus Xray map

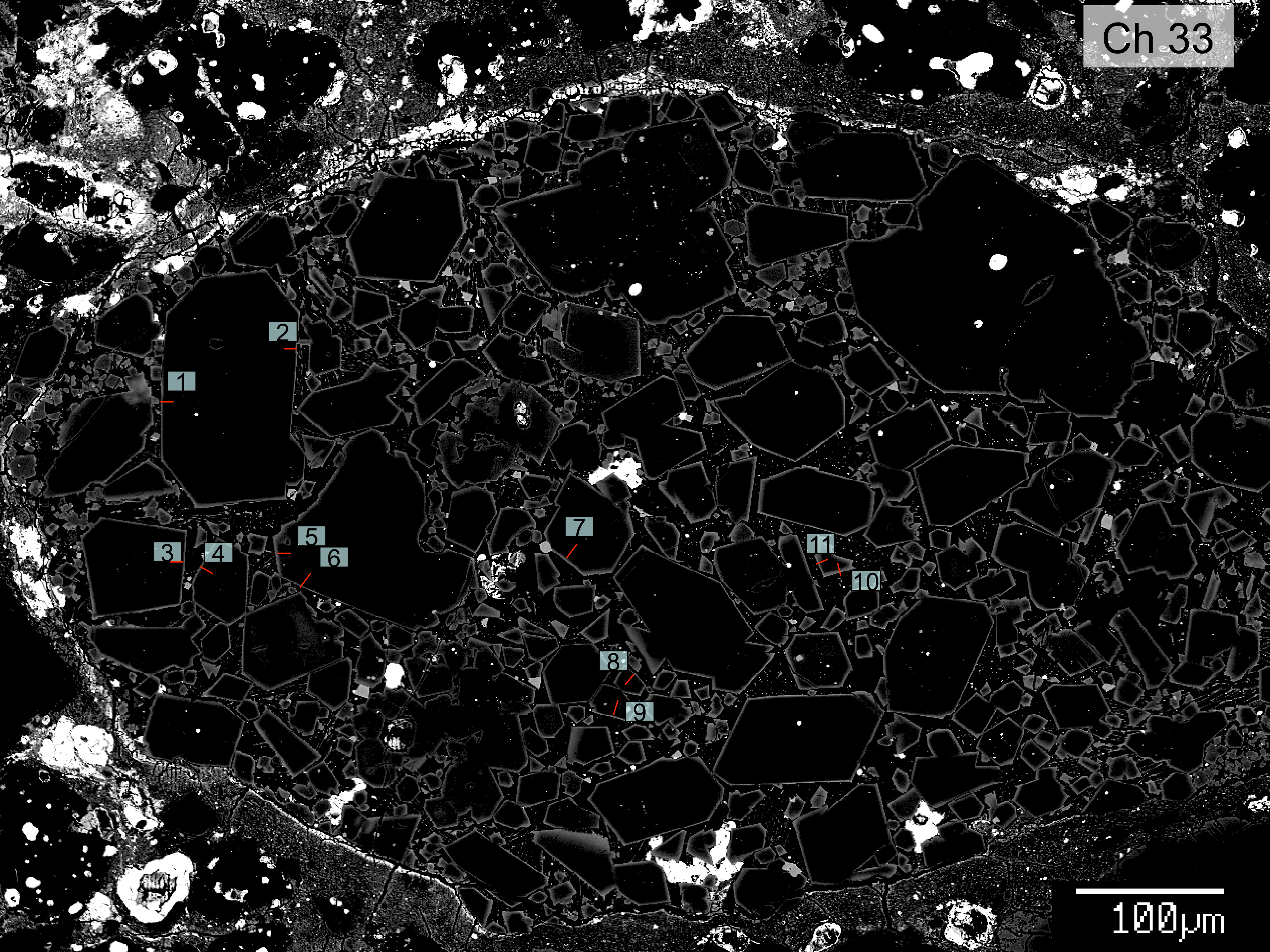
Ch 33
1
2
3
4
5
6
7
8
9
10
11
100μm

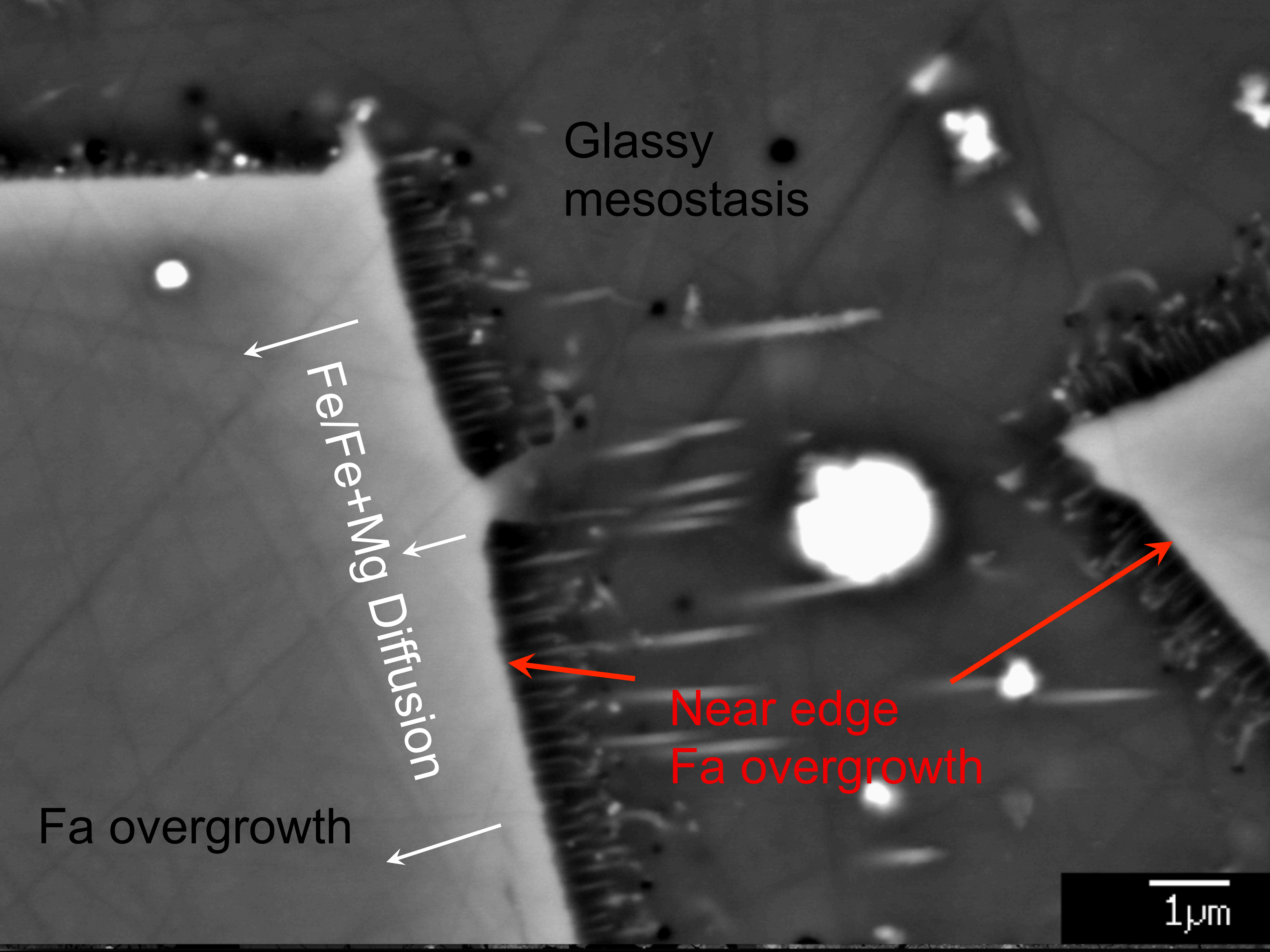
Glassy mesostasis
Fe/Fe+Mg Diffusion
Near edge Fa overgrowth
Fa overgrowth
1μm

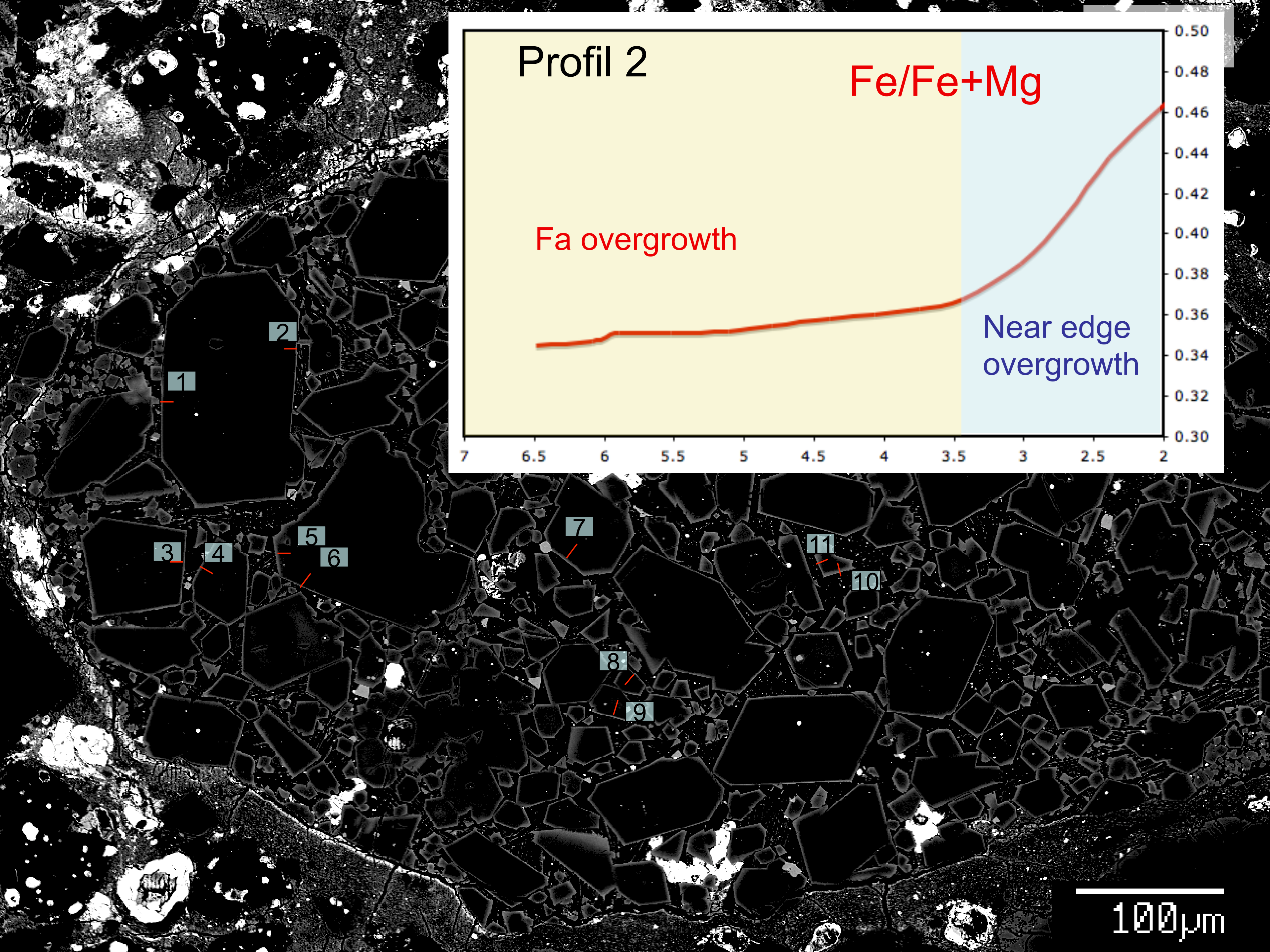

Profil 2
Fe/Fe+Mg
Fa overgrowth
Near edge overgrowth
0.50
0.48
0.46
0.44
0.42
0.40
0.38
0.36
0.34
0.32
0.30
7
6.5
6
5.5
5
4.5
4
3.5
3
2.5
2
1
2
3
4
5
6
7
8
9
10
11
100µm

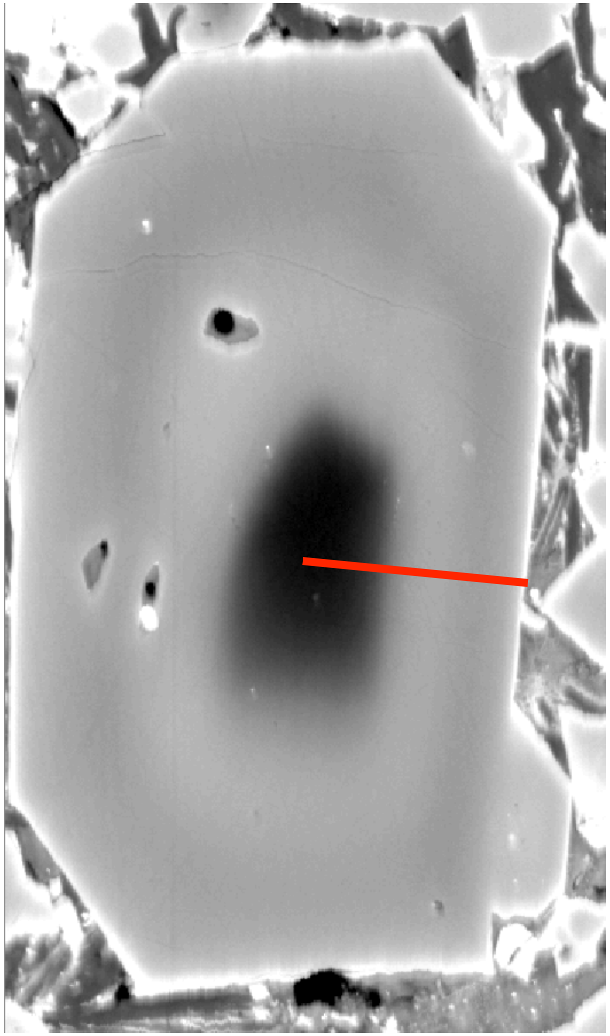

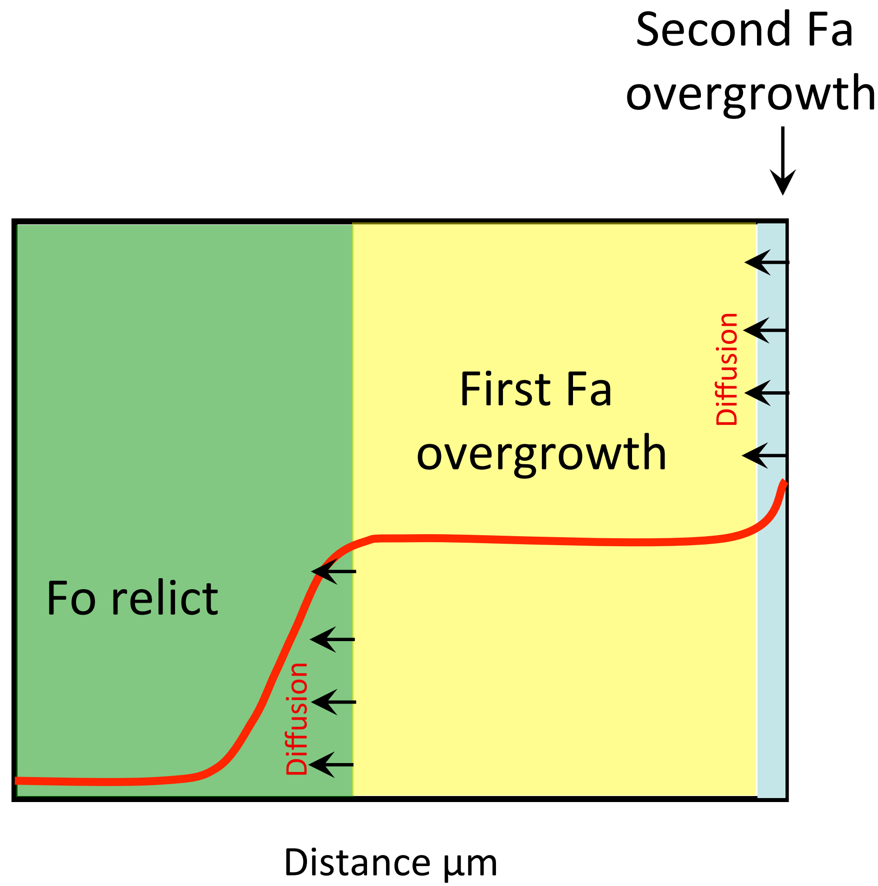

- First fayalitic overgrowth
  - Sub isothermal oxidation
- Second fayalitic overgrowth
  - Rapid cooling (glass)

First Fa overgrowth

$\Delta x = 2.\sqrt{(T \times t)}$

$$D_{(T)} = D_0 \times \exp\left(\frac{-E}{R\ T}\right)$$

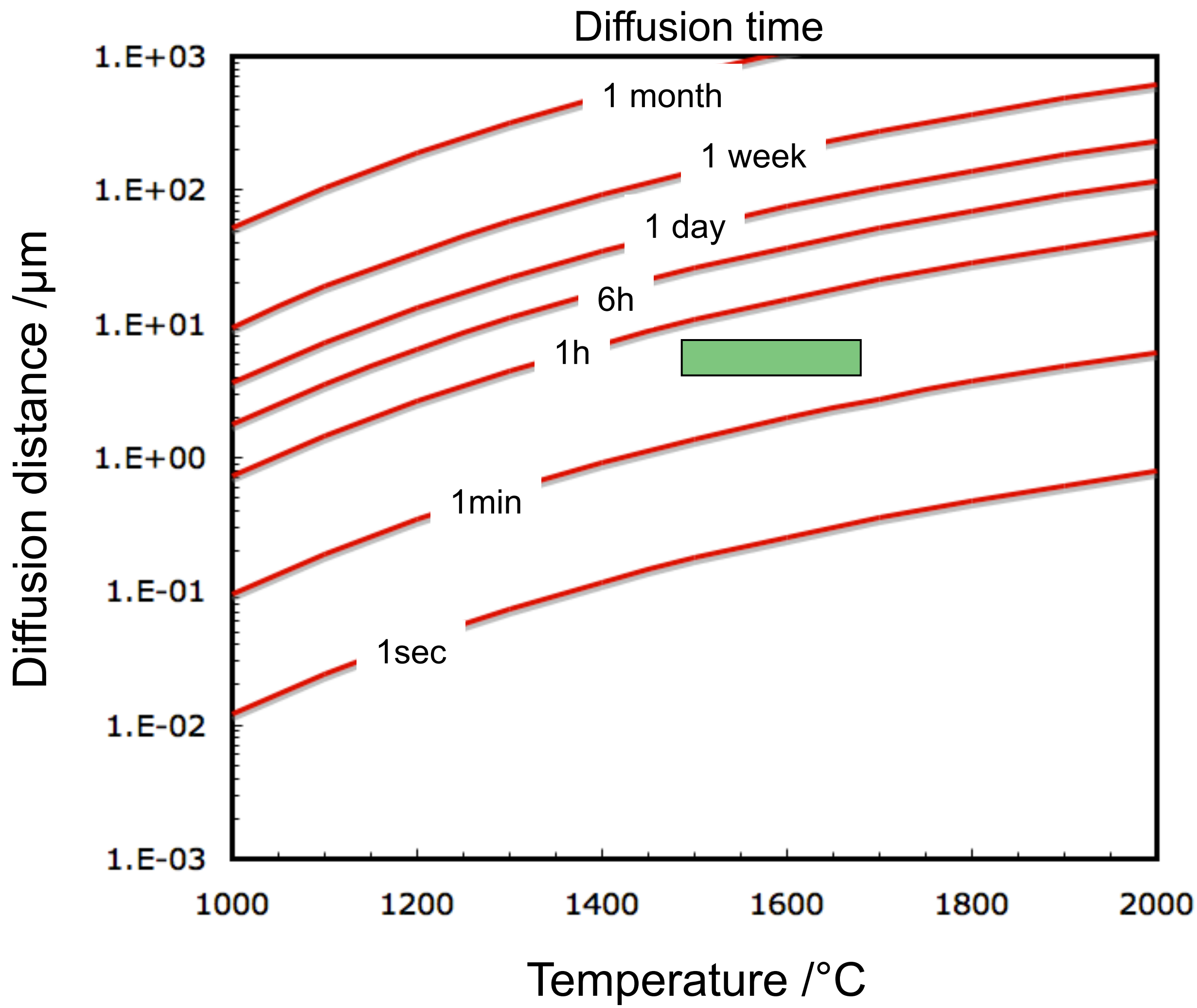

Second Fa overgrowth

$$D(T(t)) = D_0 \times \exp\left(\frac{-E}{RT(t)}\right) \qquad T(t) = T_0 - St \text{ (Lasaga, 1983)}$$

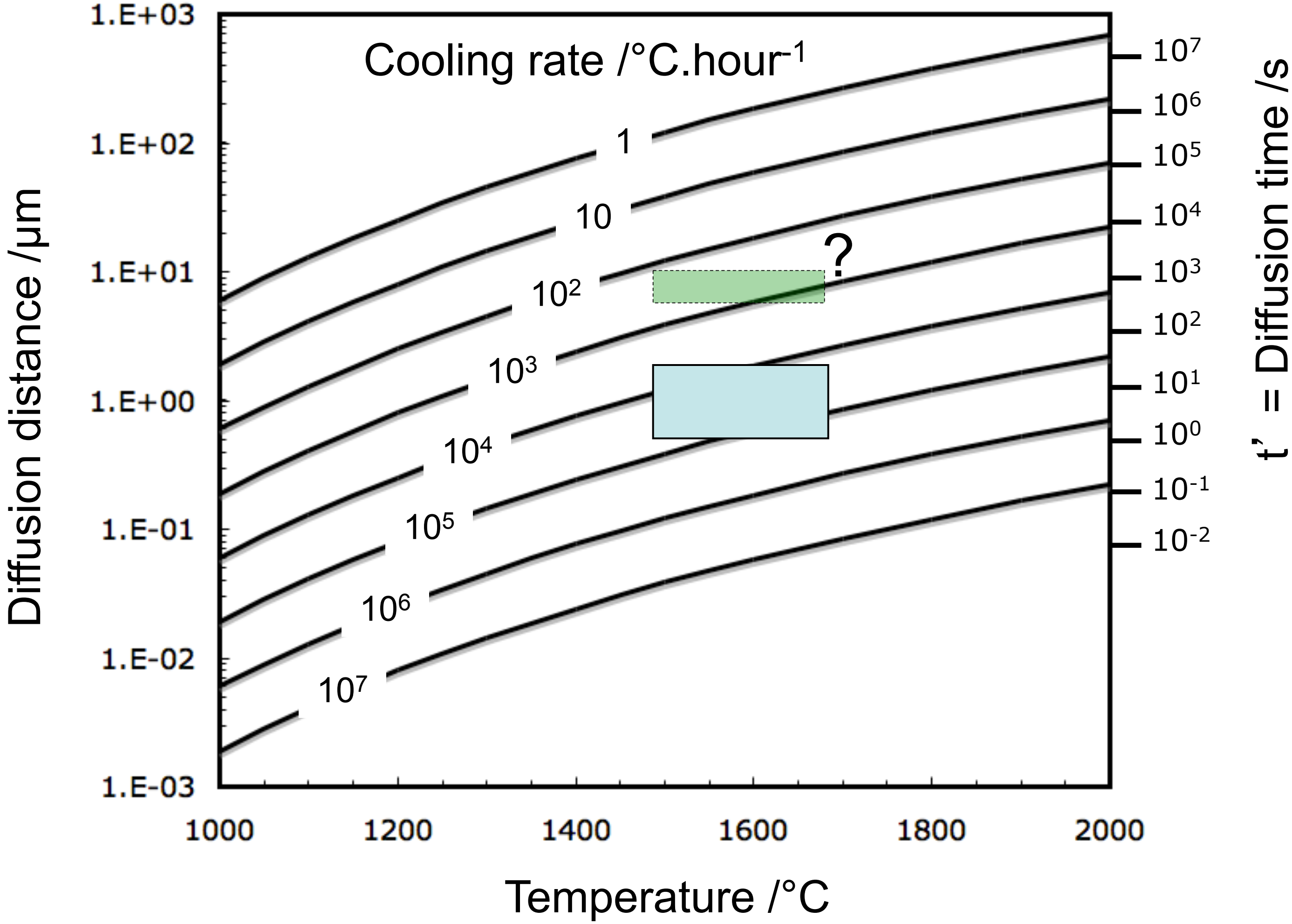

Thermal histories for type I and type II PO chondrule formation

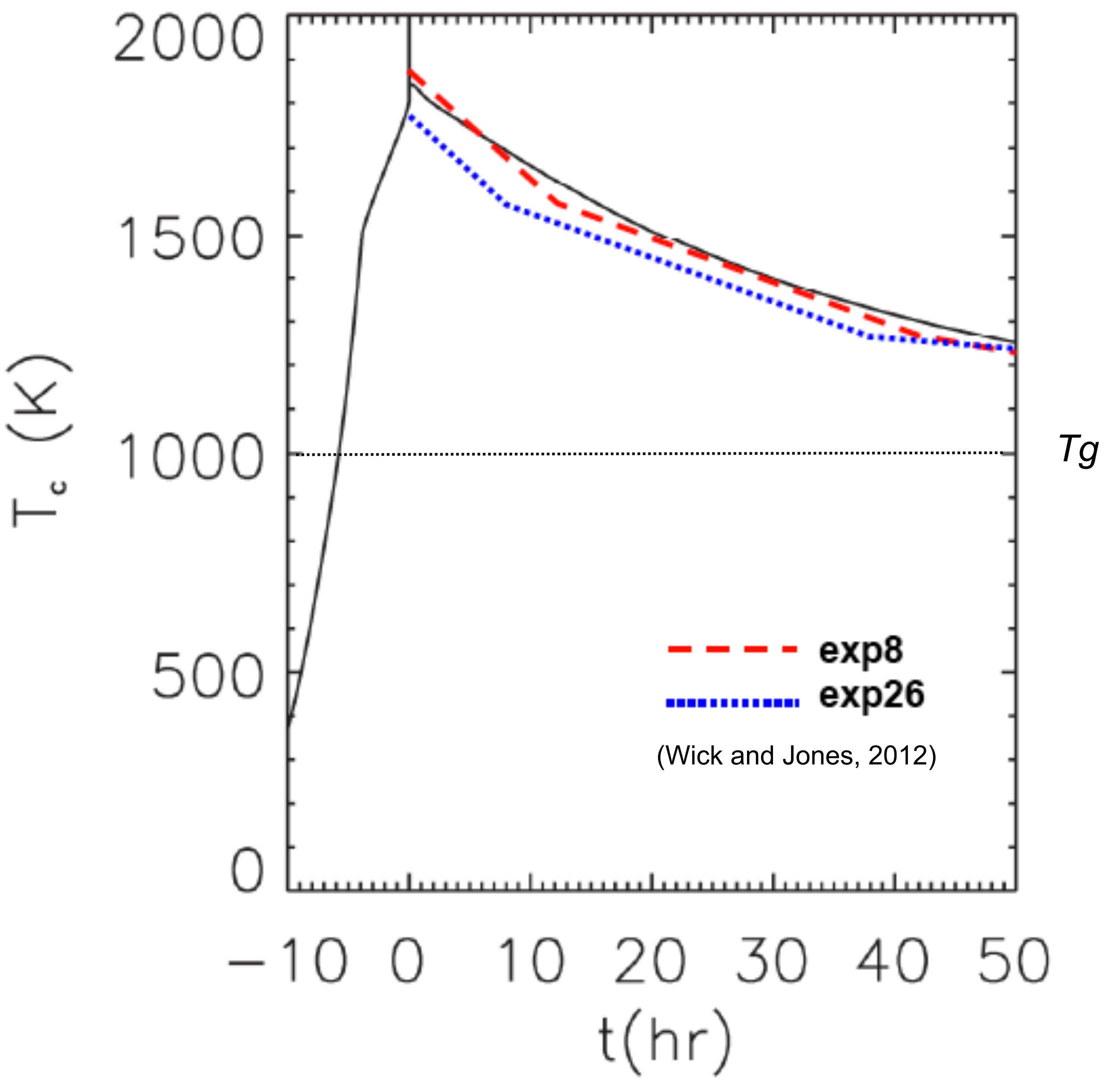

Shock wave model

(Morris and Desch, 2010)

$S = 10 - 10^3$ K/h

$$x = 2.\ (D_0 . t')^{-1/2}$$

t' = diffusion time

$$t' = R \cdot T_0^{\,2} \cdot (E \cdot s)^{-1}$$

$t' > 50 - 100$ h

t' is well too long to match:

- Elements with fast and slow diffusion
- occurrence of glass

Thermal histories for type I and type II PO chondrule formation

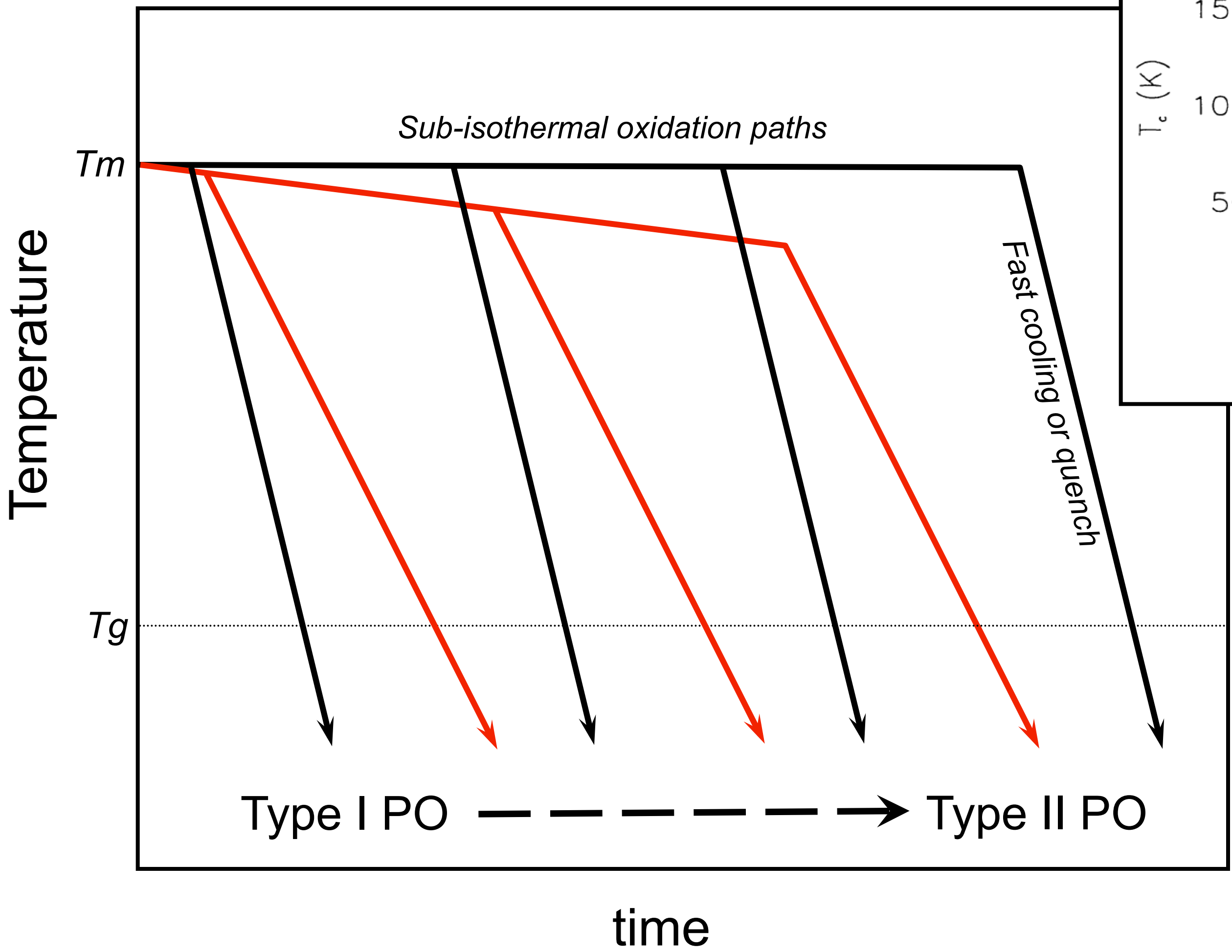

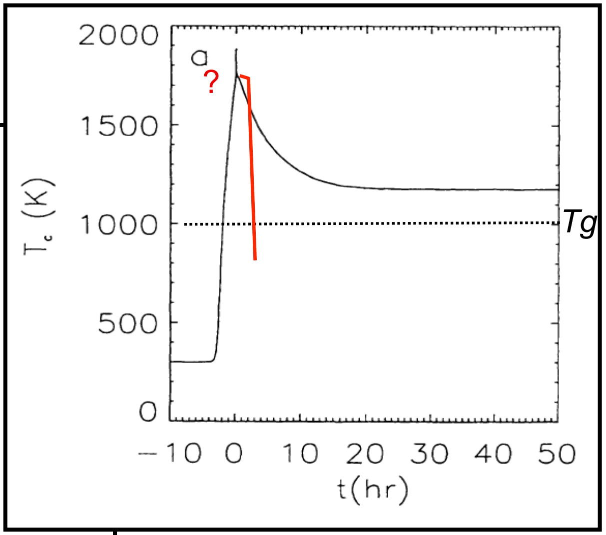

5-10 min < t’ < 5 h

S > 10^4 K/h

Chondrule formation:
Quicker and faster

Strategy: closed system experiments

Sample

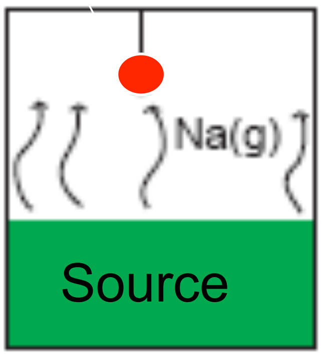

Source (evaporation)

$$Na_2O^{(source)} \leftrightarrow 2Na_{(g)} + 1/2\ O_{2(g)}$$

Sample (condensation)

$$2Na_{(g)} + 1/2\ O_{2\ (g)} \leftrightarrow Na_2O^{(sample)}$$

$$K_{eq(T,P)} = (P_{Na})^2 \cdot (P_{O2})^{1/2} / (X_{Na2O}^{(sample)} \cdot \gamma_{Na2O}^{(sample)})$$

At equilibrium $a_{Na2O}^{(source)} = a_{Na2O}^{(sample)}$

Mathieu et al. 2008, 2010

Model of Na solubility

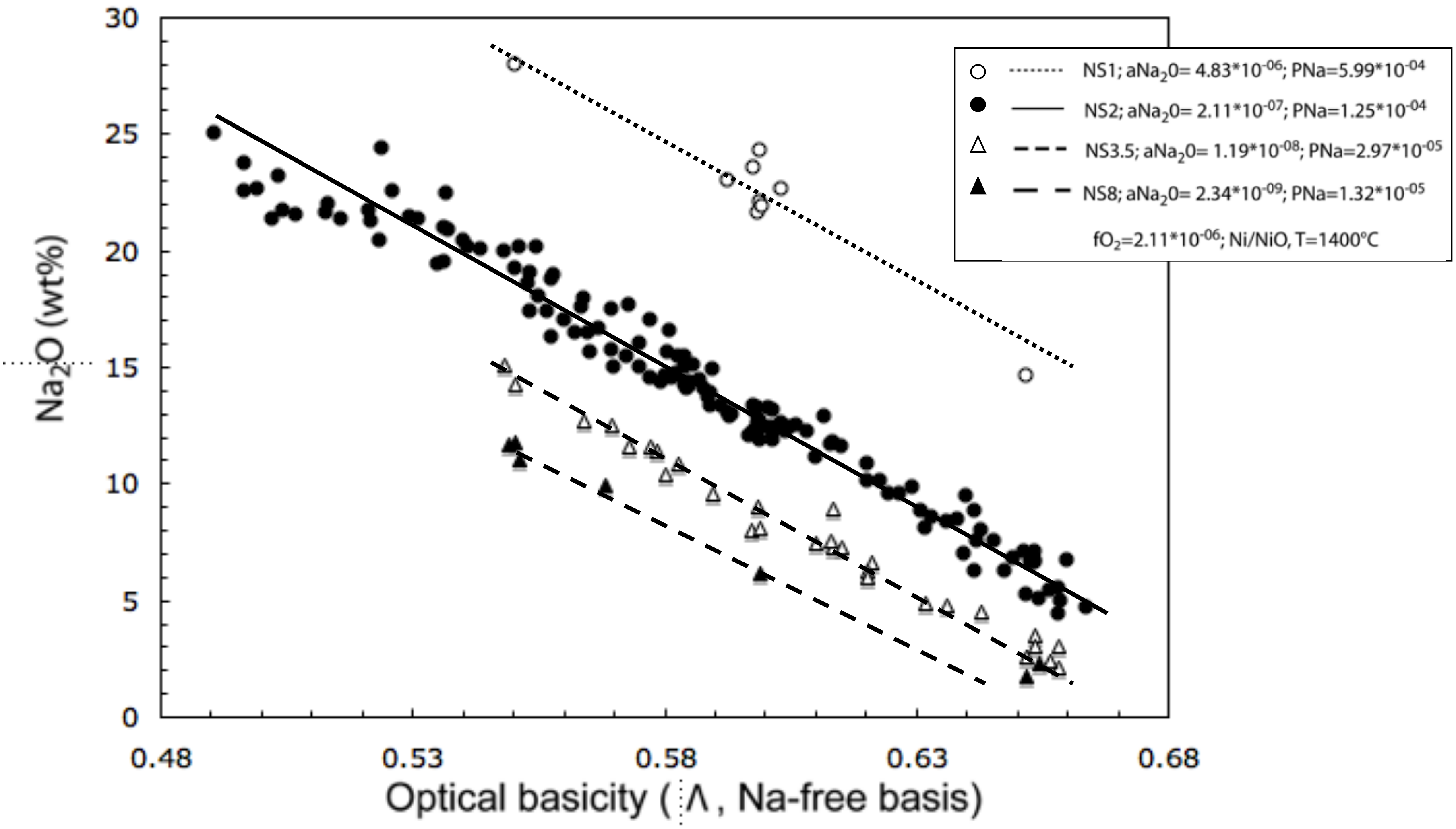

$$Na_2O\ (wt\%) = 106.84 - 110.87*\Lambda + 4.06*\log(aNa_2O) \qquad (R^2=0.88)$$

Model of Na solubility

$$Na_2O_{(liq)} \leftrightarrow 2Na_{(g)} + 1/2\ O_{2(g)}$$

$$K_{eq(T)} = (P_{Na})^2 \cdot (P_{O2})^{1/2} / a_{Na2O}^{(liq)}$$

$$Log\ K_{eq(T)} = -2.6717 * 10000 / T^{(K)} + 12.522$$

$$Na_2O\ (wt\%) = 106.84 - 110.87 * \Lambda + 4.06 * \log(aNa_2O) \quad (R^2 = 0.88)$$

Alkalis in chondrules

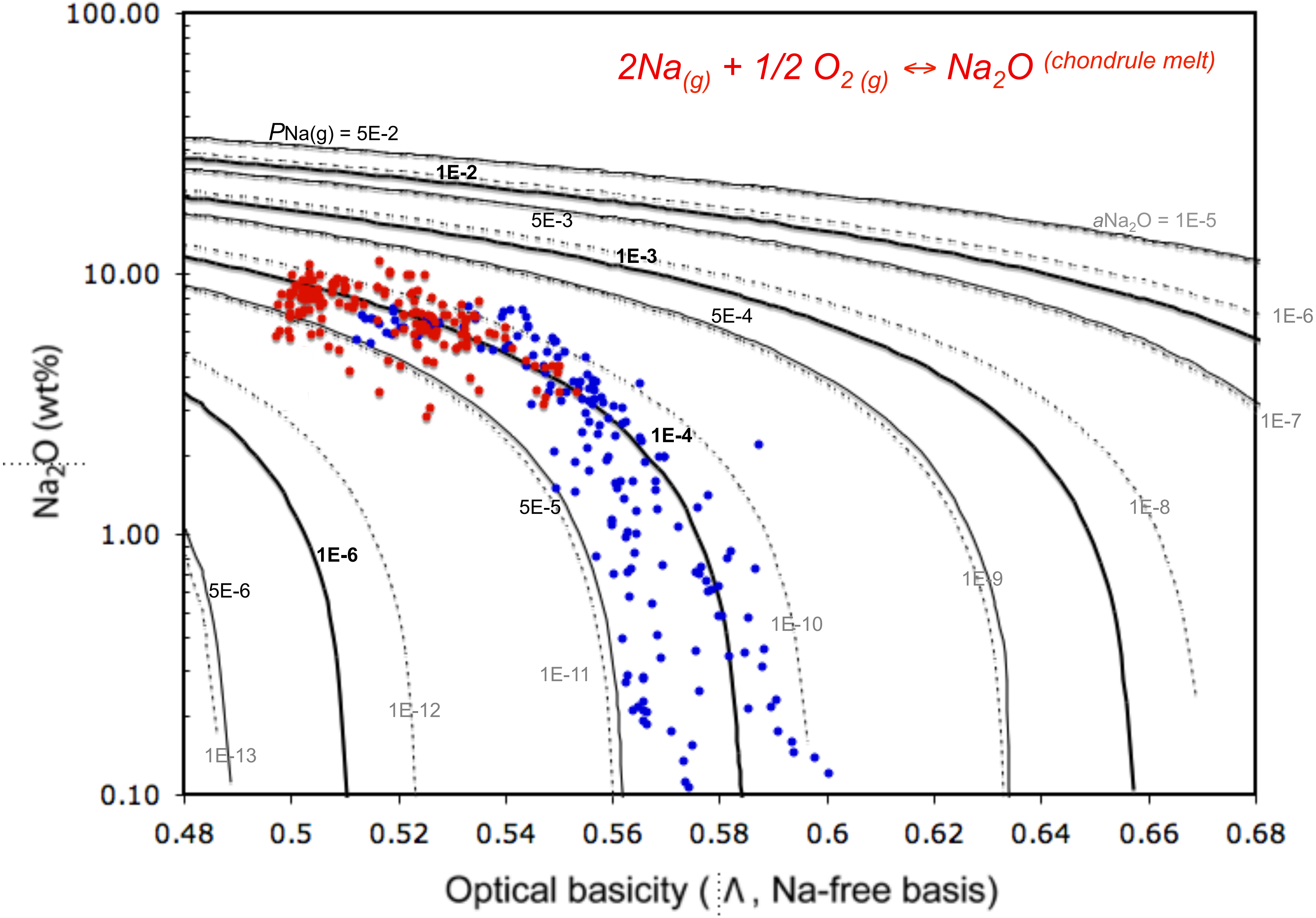

Chondrule formation process

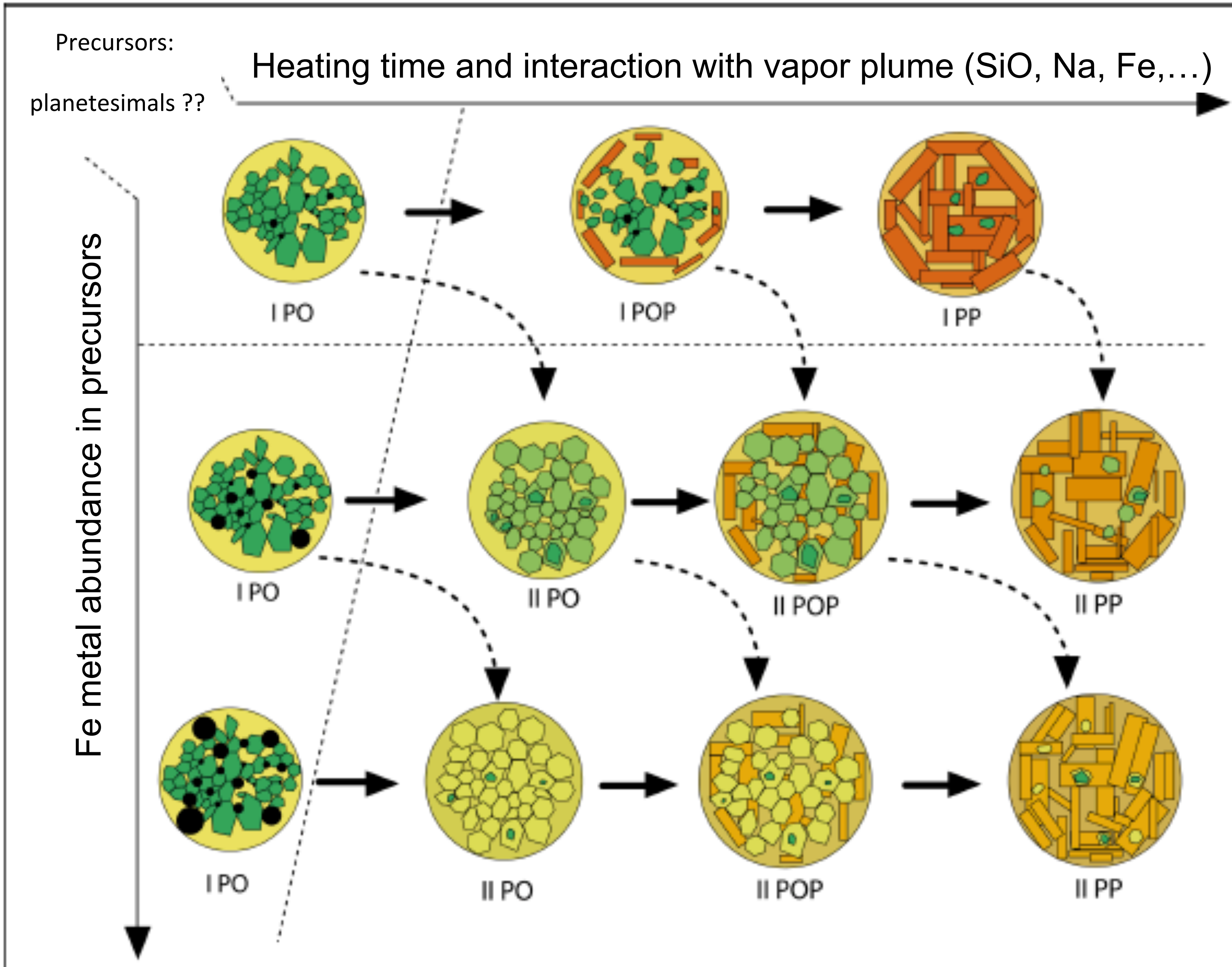

Constraints from short-lived radionuclides on the timing of chondrule formation and primary accretion

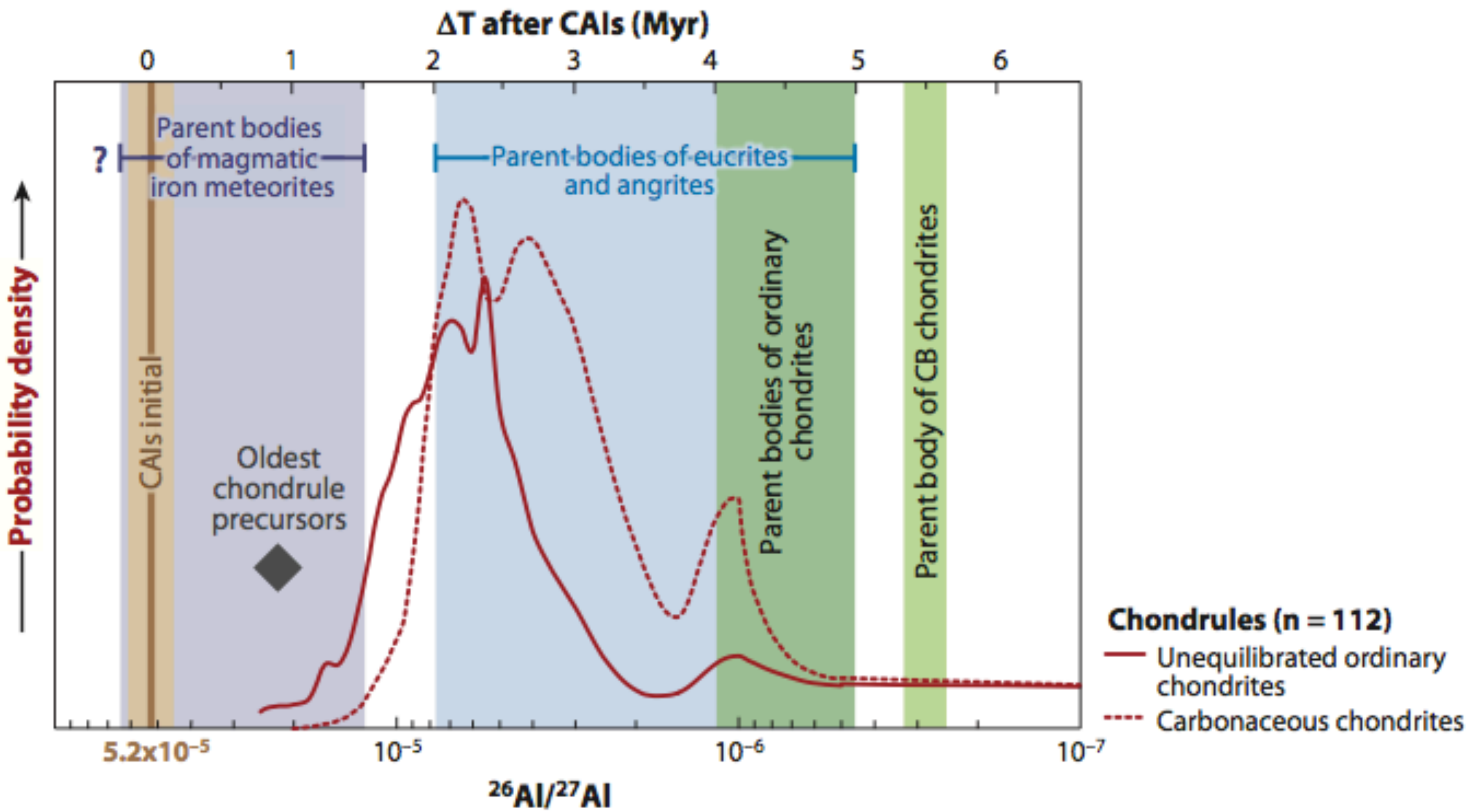

Villeneuve et al. 2009

Dauphas and Chaussidon, 2011

Chondrule formation process

1. The chemistry and the oxygen isotopic compositions indicate that Mg-rich olivines are unlikely to be of nebular origin (i.e., solar nebula condensates) but are more likely debris of broken differentiated planetesimals (each of them being characterized by a given $\Delta^{17}O$).

2. Considering the very old age of chondrules, Mg-rich olivine grains or aggregates might be considered as millimeter-sized fragments from disrupted first-generation differentiated planetesimals.

3. The finding of only a small number of discrete $\Delta^{17}O$ modes for Mg-rich olivines grains or aggregates in a given chondrite suggests that these shattered fragments have not been efficiently mixed in the disk and/or that chondrite formation occurred in the first vicinity of the breakup of these planetary bodies.

Chondrule formation process

4. Type I chondrules or their fragments are very likely the main precursor material involved in the formation of Type II chondrules.

5. Chondrule formation must be preferentially the result of processes generating crystal growth by chemical disequilibrium at high temperature, i.e., dC/dt as in our sub-isothermal open system behavior experiments, rather than processes generating crystallization by cooling rates, i.e., dT/dt as in dynamical cooling rate experiments, <u>questioning</u> the reliability of cooling rate values hitherto inferred for producing porphyritic textures.

6. Last, PO chondrule formation is a very fast process. After periods of sub-isothermal heating as short as several tenths of minutes and no longer than few hundreds of minutes in the range of 1500 -1800°C, PO chondrules terminates their formation by a very fast cooling (>> 10^4 K/h).

Chondrule formation: quicker and faster

Chondrules are interpreted as resulting from various degrees of interaction of the ejected fragments of the collisions with the gas during their ballistic trajectory through the impact vapor plume;

-The most reducing conditions recorded by type I PO chondrules are interpreted as remnant of the conditions of their parental planetimals from which they were ejected during the impact

- The most oxidizing conditions recorded in type II PO chondrules being very likely the closest to those imposed by the impact vapor plume.

High velocity impacts (>> 1km.s^{-1})

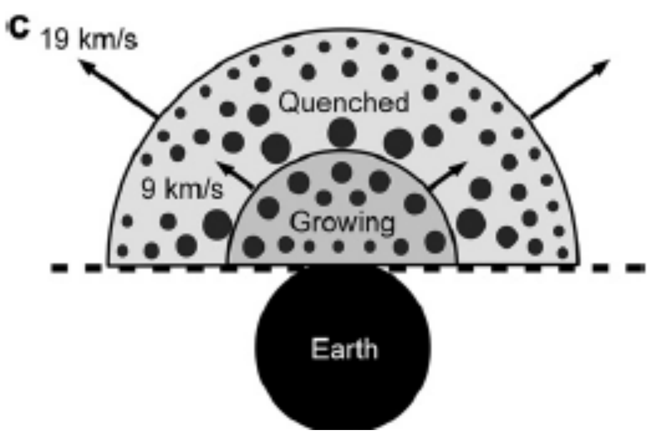

Johnson and Melosh, 2012

?

Low velocity impacts (< 1km.s^{-1})

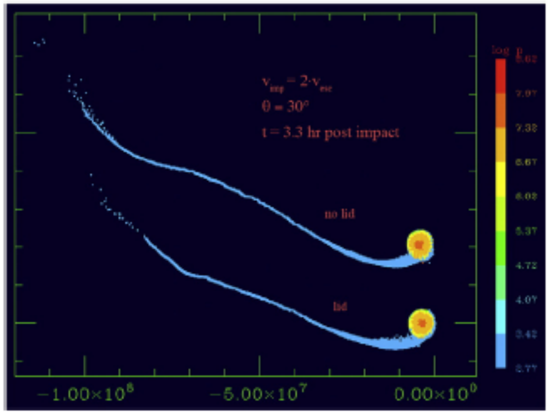

Asphaug et al., 2011

Semarkona PO chondrule

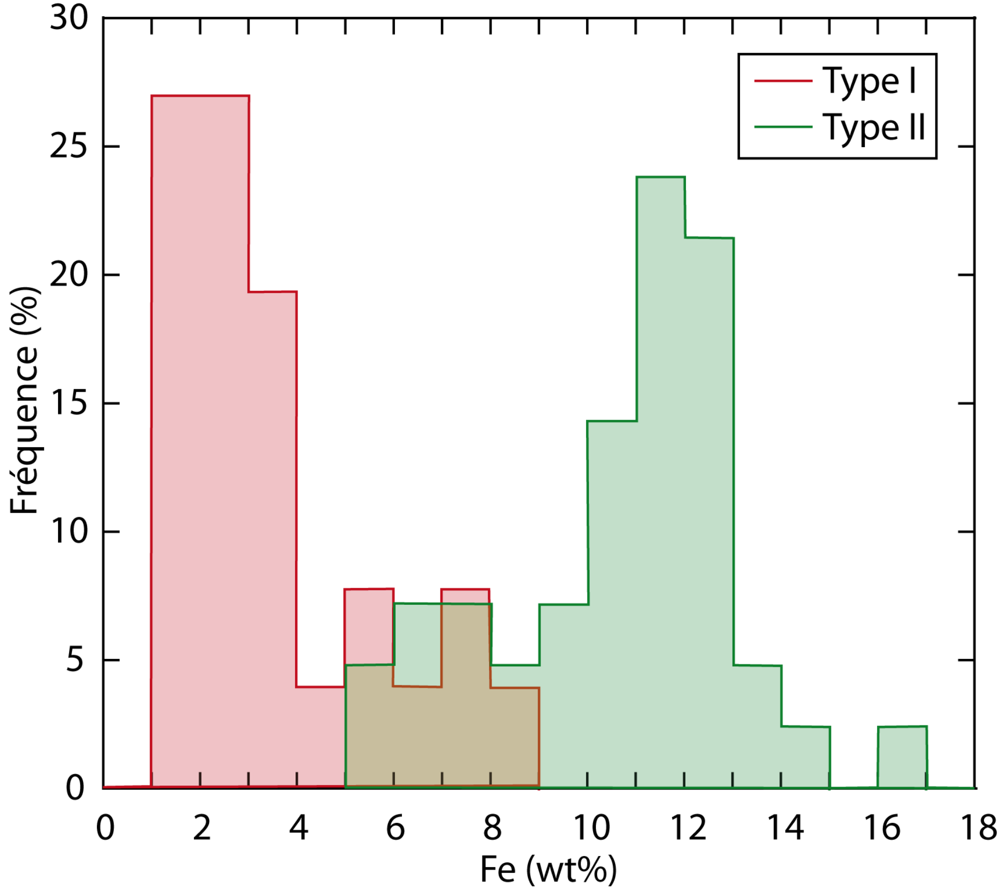

Fe (metal) + ½ O_2 ⟶ FeO (liq)

Fe (gas) + ½ O_2 ⟶ FeO (liq)

FeO (liq) + MgO (liq) + SiO_2 (liq) ⟶ $(Fe, Mg)_2SiO_4$ (olivine)

Thermal model for type I and type II PO chondrules formation